The role of Hepatic 11-β hydroxysteroid dehydrogenase Type 1 in Uraemia-induced Insulin Resistance.

A thesis submitted to Queen Mary University of London for the degree of

DOCTOR OF PHILOSOPHY

Ananda Chapagain

Translational Medicine and Therapeutics,

William Harvey Research Institute,

Queen Mary University of London.

TABLE OF CONTENTS

Acknowledgements

I would like to thank Drs Steve Harwood, P Caton, J Kieswich,P Androkopoulous, A Findlay, W White, K MCafferty, C Byrne for their invaluable help. Furthermore, I would like to thank Kenta, Yashinori and Scott from Prof Suzuki's Lab for help with mRNA isolation, stabilisation and qRT-PCR. I would also like to thank N. Khan, N Nayuni and J Long for help with HPLC.

List of Figures

.

List of Tables

Acknowledgements

I would like to thank Drs Steve Harwood, P Caton, J Kieswich,P Androkopoulous, A Findlay, W White, K MCafferty, C Byrne for their invaluable help. Furthermore, I would like to thank Kenta, Yashinori and Scott from Prof Suzuki's Lab for help with mRNA isolation, stabilisation and qRT-PCR. I would also like to thank N. Khan, N Nayuni and J Long for help with HPLC.

Abstract

Insulin resistance and associated metabolic sequelae are common in Chronic Kidney Disease (CKD) and are positively and independently associated with increased cardiovascular mortality. However, the pathogenesis has yet to be fully elucidated. 11β-Hydroxysteroid Dehydrogenase type 1 (11β-HSD1) catalyses intracellular regeneration of active glucocorticoids, promoting insulin resistance in liver and other metabolic tissues. Using data from two experimental rat models of CKD (subtotal nephrectomy and adenine diet) which show early insulin resistance, we found that 11β-HSD1 mRNA and protein increase in hepatic and adipose tissue, together with increased hepatic 11β-HSD1 activity. This was associated with intrahepatic but not circulating glucocorticoid excess, and increased hepatic gluconeogenesis and lipogenesis. Oral administration of the 11β-HSD inhibitor carbenoxolone to uraemic rats for 2 weeks improved glucose tolerance and insulin sensitivity, improved insulin signalling, and reduced hepatic expression of gluconeogenic and lipogenic genes.

Furthermore, 11β-HSD1−/− mice and rats treated with a specific 11β-HSD1 inhibitor (UE2316) were protected from metabolic disturbances despite similar renal dysfunction following adenine-induced experimental uraemia. Therefore, we demonstrate that elevated hepatic 11β-HSD1 is an important contributor to early insulin resistance and dyslipidaemia in uraemia. Specific 11β-HSD1 inhibitors potentially represent a novel therapeutic approach for management of insulin resistance in patients with CKD.

Abbreviations

11β-HSD1	11beta-hydroxysteroid dehydrogenase type 1
11β-HSD2	11beta-hydroxysteroid dehydrogenase type 2
11DHC	11-dehydrocortocosterone
ACC	Acetyl-CoA carboxylase
ACTH	Adrenocorticotropic hormone
AD	Adenine diet uraemic model
ADP	Adenosine diphosphate
Akt	Protein kinase B
AME	Apparent mineralocorticoid excess syndrome
AMP	Adenosine monophosphate
AMPK	AMP-dependent protein kinase
AS160	Akt substrate of 160 kDa
AU	Arbitrary units
ATF	Activating transcription factor
ATGL	Adipose triglyceride lipase
ATP	Adenosine triphosphate
AUC	Area under curve
BSA	Bovine serum albumin
BMI	Body mass index
cAMP	Cyclic adenosine monophosphate
CREBP	cAMP response element-binding protein
CBP	CREB binding protein
cDNA	Complementary deoxyribonucleic acid

CKD	chronic kidney disease
CORT	Corticosterone
CPM	Counts per minute
CPT	Carnitine palmitoyltransferase
CRH	Corticotropin-releasing hormone
Ct	Cycle threshold
CV	cardiovascular
Cyclo B	Cyclophilin B
D50	50% Dextrose
DAG	Diacylglycerol
DEX	Dexamethasone
DGAT	Diacylglycerol acyltransferase
DGK-δ	Diacylglycerol kinase-delta
DHEA	Dehydroepiandrosterone
DIO	Diet-induced obese
DMEM	Dulbecco's modified eagle medium
DNA	Deoxyribonucleic acid
DPM	Disintegrations per minute
E	Cortisone
ECL	Enhanced chemiluminescence
eGFR	estimated glomerular filtration rate
ER	Endoplasmic reticulum
ERK	Extracellular signal-regulated kinase
FABP	Fatty acid binding protein
FGF	Fibroblast growth factor

eIF2B	Eukaryotic initiation factor 2B
F	Cortisol
FAS	Fatty acid synthase
FAT/CD36	Long-chain fatty acid transporter
FCS	Foetal calf serum
FFA	Free fatty acids
FOXO	Forkhead transcription factors
GABA	γ-Aminobutyric acid
G3PDH	Glyceraldehyde-3-phosphate dehydrogenase
G6P	Glucose-6-phosphate
G6Pase	Glucose-6-phosphatase
GC	Glucocorticoid
GE	Glycyrrhetinic acid
Glu	Glucose
GLUT	Glucose transporter
GR	Glucocorticoid receptor
GRE	Glucocorticoid response element
GS	Glycogen synthase
GSK	Glycogen synthase kinase
GTP	Guanosine triphosphate
GTT	Glucose tolerance test
H6PDH	Hexose-6-phosphate dehydrogenase
HOMA	Homeostasis model assessment
HPA	Hypothalamic-pituitary-adrenal axis
HRP	Horse radish peroxidase

HS	Horse serum
HSL	Hormone sensitive lipase
HSP	Heat shock protein
IGF	Insulin-like growth factor
IKKB	Inhibitor of NF-κB kinase
IL-6	Interleukin-6
IMTG	Intramyocellular triglyceride
Ins	Insulin
InsR	Insulin receptor
IRS	Insulin receptor substrate
IP	Intraperitoneal
JNK	Jun N-terminal kinase
KRB	Kreb's ringer buffer
LDL	Low-density lipoprotein
LPL	Lipoprotein lipase
MAG	Monoacylglycerol
MAPK	Mitogen-activated protein kinase
MC4R	Melanocortin-4 receptor
MHC	Myosin heavy chain
MODY	Maturity onset diabetes of the young
MR	Mineralocorticoid
MRF	Myogenic regulatory factors
mRNA	Messenger RNA
mTOR	Mammalian target of rapamycin
MuRF	Muscle specific ring finger protein

MyoG	myogenin
NAD	Nicotinamide adenine dinucleotide
NADP	Nicotinamide adenine dinucleotide phosphate
p70S6K	Ribosomal protein S6 kinase
PAGE	Polyacrylamide gel electrophoresis
PAI-1	Plasminogen activator inhibitor-1
PBS	Phosphate buffered saline
PCR	Polymerase chain reaction
PDE3B	Phosphodiesterase-3B
PDK	Pyruvate dehydrogenase kinase
PEPCK	Phosphoenolpyruvatecarboxy kinase
PH	Pleckstrin homology domain
PHLPP	PH-domain leucine-rich repeat protein phosphatase
PI3K	Phosphoinositide 3-kinase
PIP2	Phosphatidylinositol-4,5-bisphosphate
PIP3	Phosphatidylinositol-3,4,5-triphosphate
PKA	Protein kinase A
PKB	Protein kinase B
PKC	Protein kinase C
PMA	Phorbol 12-myristate 13-acetate
PP2A	Protein phosphatase-2A
PPAR	Peroxisome proliferator-activated receptor
PTB	Phosphotyrosine binding domain
PTEN	Phosphatase and tensin homolog
RNA	Ribonucleic acid

rRNA	Ribosomal ribonucleic acid
RT-PCR	Real-time polymerase chain reaction
SCD	Stearoyl-CoA desaturase
SDS	Sodium dodecyl sulphate
SH2	Src homology 2 domain
SH3	Src homology 3 domain
SiRNA	Small interfering ribonucleic acid
SNX	Sub-total nephrectomy uraemic model
SOCS	Suppressor of cytokine signalling
SPT	Serine palmitoyl-CoA transferase
SRC1	Steroid receptor coactivator-1
SREBP1	Sterol regulatory element-binding protein-1
StAR	Steroidogenic acute regulatory protein
T2D	Type 2 diabetes
TAG	Triacylglycerol
TC	Tissue culture
THE	Tetrahydrocortisone
THF	Tetrahydrocortisol
TNFα	Tumour necrosis factor-alpha
TRB3	Tribbles homolog-3
TSC	Tuberous sclerosis complex
TZD	Thiazolidinedione
VLDL	Very low-density lipoprotein
WAT	White adipose tissue
WHO	World health organization

Hypothesis:

Hepatic 11-βhydroxysteroid dehydrogenase Type 1 activation in uraemia induces hepatic gluconeogenesis, contributing to insulin resistance in uraemia.

Contributions:

Julius Kieswich helped with animal husbandry, implanted the osmotic mini-pump and bred HSD1-/- mice. I performed in vivo experiments with Julius and performed all gavages.

Dr Nanda Nayuni and Dr J Long developed optimized tissue steroid extraction protocols. I performed the optimisation steps and performed the steroid extraction.

Dr Steve Harwood optimized HPLC, and performed the HPLC.I analysed data from HPLC.

Dr Scott Broulette optimized tissue mRNA extraction and PCR methodology. I performed all PCRs independently.

Dr Paul Caton helped in study design, Western blots on SNX hepatic tissue, and Western blots on adipocytes and muscle from SNX animals. He performed the tissue lipid assay.

Prof R Corder, Prof C Thiermermann provided key contributions to study design and analysis

Prof J Seckl Dr N Morton provided transgenic mice, UE236 and helped in analysis of transgenic mice.

Prof M M Yaqoob conceived of the project and guided it through.

Chapter 1- General Introduction

Introduction

1.1. Chronic kidney disease

Chronic Kidney Disease (CKD) is a term used to describe abnormal kidney function and/or structure. It is common, frequently unrecognised and often exists together with other conditions (for example, cardiovascular disease and diabetes). CKD is defined as impaired kidney function or raised proteinuria that are confirmed on two or more occasions at least 3 months apart (1).

The United Kingdom 'National Service Framework for Renal Services' adopted the US 'National Kidney Foundation Kidney Disease Outcomes Quality Initiative' (NKF-KDOQI) classification of CKD. This classification divides CKD into five stages. Stages 3–5 may be defined by Glomerular Filtration Rate (GFR) alone, whereas stages 1 and 2 also require the presence of persistent proteinuria, albuminuria or haematuria, or structural abnormalities. The National Institute for Clinical Excellence (NICE) has produced guidance on early detection and management of CKD (1).

1.2. CKD and cardiovascular (CV) mortality risk

Insulin resistance and associated hyperinsulinaemia are common complications in patients with CKD (2, 3), with an insulin resistance-like syndrome occurring even in the earliest stage of renal dysfunction, irrespective of the primary aetiology of the renal failure(4). CKD-induced insulin resistance is positively and independently associated with increased CV mortality (5, 6). Furthermore, mortality among haemodialysis patients is higher in those with more severe insulin resistance (7). Despite this, the mechanisms responsible for the onset of insulin resistance in CKD have yet to be fully elucidated.

1. 2.1. Historical perspective

Richard Bright (1789 –1858) was an English physician generally considered now to be the father of modern nephrology. He noted in 1836, *"The obvious structural changes in the*

heart have consisted chiefly of hypertrophy...and what is most striking, out of fifty-two cases…no valvular disease could be detected in thirty-four…This naturally leads us to look for some less local cause", and "It is observable, that the hypertrophy of the heart seems, in some degree, to have kept pace with the advance of disease in the kidneys; for in by far the majority of cases, when the heart was increased, the hardness and contraction of the kidney bespoke the probability of long continuance of the disease." Indeed, Bright was the first to report the association between CKD and CV abnormalities. He suggested that the altered quality of the blood in patients with renal disease affected the peripheral vasculature, particularly the capillaries, in a way that required increased force to propel the blood around the body (8, 9). By taking the view that renal disease is the primary disorder and CV changes are secondary, Bright established the concept of the renal origin of CV disease. Many studies have since confirmed and extended these findings, and various mechanisms have been proposed for CV risk and disease in CKD.

1. 2.2. Epidemiology of CV disease risk in CKD

The association of eGFR and raised albuminuria with CV disease has been established over various studies in a variety of populations. Only a handful of studies have, however, simultaneously assessed these two measures of chronic kidney damage in this context.

A meta-analysis with a total patient cohort of 1.4 million (10,11,12) revealed, after adjustment for traditional cardiovascular risk factors (for example hypercholesterolemia, hypertension and smoking) and albuminuria, the risk gradient for cardiovascular mortality changed little when the estimated glomerular filtration rate by modification of diet in renal disease formula (MDRD eGFR, or eGFR) was higher than 75 mL/min per 1·73 m^2 and linearly increased with decreasing eGFR below this threshold (Figure 1) (10,11,12). CV mortality was about twice as high in patients with stage 3 CKD (eGFR 30–59 mL/min per 1·73 m^2) and three times higher at stage 4 (15–29 mL/min per 1·73 m^2) than that in individuals with normal kidney

function. In contrast to the non-linear risk relationship for eGFR, the association of albuminuria with CV risk has no threshold effect, even after adjustment for traditional cardiovascular risk factors and eGFR, Figure 1). The adjusted risk of CV mortality is more than doubled at the upper end of the microalbuminuria category (30–299 mg of albumin per g creatinine compared with the risk in individuals with normal albuminuria. This lack of a threshold effect indicates that albuminuria even at the upper end of the normal range (threshold 30 mg/g) is associated with CV risk.

A wide variety of specific CV diseases (CVD) have been associated with impaired kidney function. Heart failure risk is roughly doubled in patients with eGFR lower than 60 mL/min per 1·73 m² compared to people with preserved eGFR. The risk is similarly increased for stroke, peripheral artery disease, coronary heart disease and atrial fibrillation (10, 11, and 12). The associations between CKD and CVD are largely irrespective of age, sex, and ethnic origin; data have been reported for US, European, Taiwanese, and South Korean general-population cohorts (12).

1.4. Metabolic syndrome, glucose intolerance and insulin resistance.

The metabolic syndrome describes the clustering of dyslipidaemia, hypertension, glucose intolerance and central adiposity. It was first described by Reaven in 1988 (13) who postulated that insulin resistance was the cause of glucose intolerance, hyperinsulinaemia, increased VLDL, decreased HDL and hypertension. A body of work, with the concurrent observation that certain metabolic and biological characteristics, associated with an increased risk of diabetes and atherosclerotic disease, tend to cluster (occur together greater than predicted by chance) within individuals, led to the definition of metabolic syndrome. The evidence and research on metabolic syndrome is broadly:

1. Based on the epidemiological studies established to identify risk factors for CVD.

2. Clinical and experimental studies concerning the pathogenesis of diabetes and atherosclerosis.

There have been four main criteria published for the diagnosis of the metabolic syndrome. The most widely used is the World Health Organization (WHO) criteria . A brief summary of each is given overleaf.

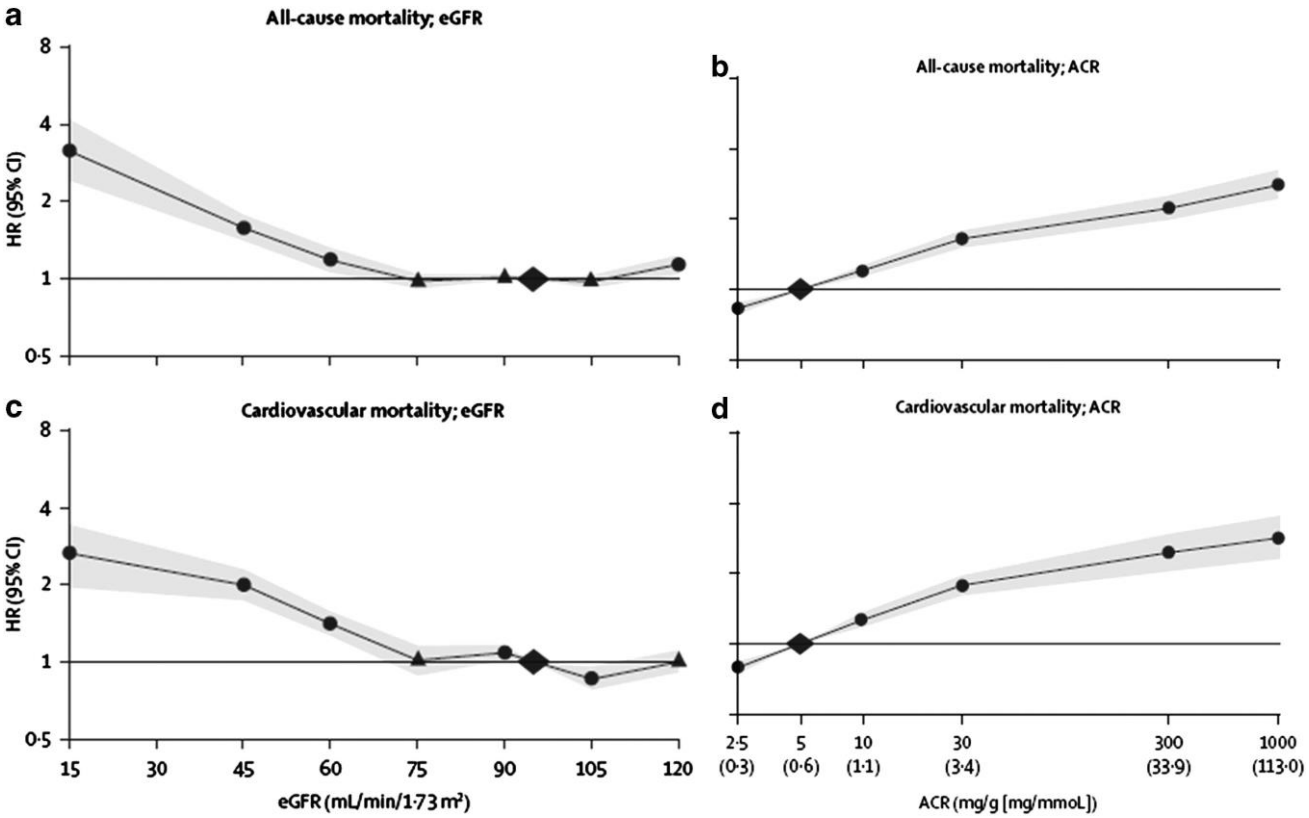

Figure 1.1: Independent associations of kidney function and proteinuria with CV mortality.
Relationship of eGFR with mortality. HRs and 95% CIs for all-cause (a) and cardiovascular mortality (c) according and to eGFR and HRs and 95% CIs for all-cause (b) and cardiovascular mortality (d) according to ACR. HRs and 95% CIs (shaded areas) are adjusted for ACR, age, sex, ethnic origin, history of CVD, systolic BP, diabetes, smoking, and total cholesterol. The reference (diamond) was eGFR 95 ml/min/1.73 m2 and ACR 5 mg/g (0.6 mg/mmol), respectively. Circles represent statistically significant and triangles represent not significant. **(16)**

Reaven,1988	ATPIII,2002	AACE, 2003	WHO,1999
•Glucose intolerance, hypertension, •Low (HDL) cholesterol and raised triglycerides, •Hyperinsulinaemia	• Abdominal obesity, given as waist circumference* • Triglycerides** • HDLcholesterol*** • Blood pressure**** • Fasting glucose******	• Overweight/obesity BMI ≥25 kg/m2 • Elevated triglycerides ≥150 mg/dL (1.69 mmol/L) • Low HDL cholesterol • Men <40 mg/dL (1.04 mmol/L) • Women<50 mg/dL (1.29 mmol/L) • Elevated blood pressure ≥130/85 mm Hg • 2-Hour postglucose challenge >140 mg/dL(7.8 mmol/L) • Fasting glucose Between 110 and 126 mg/dL • Other risk factors Family history of DM2, HTN, • or CVD ○ Polycystic ovary syndrome ○ Sedentary lifestyle ○ Advancing age ○ Ethnic groups having high risk for DM2 or CVD	• Glucose intolerence, • Impaired glucose tolerance (IGT) or diabetes mellitus (DM), • and/or insulin resistance with two of: 1)Raised BP i.e., ≥140/90 mm of Hg 2)Raised plasma triglyceride and/or low HDL-C 3)Central obesity and/or body mass index (BMI) >30 kg/m^2 4)Microalbuminuria,

Table 1.1 Four chief definitions of the metabolic syndrome *Men>102 cm (>40 in) Women >88 cm (>35 in), **TG ≥150 mg/dL ***HDL Men<40 mg/dLWomen<50 mg/dL ****BP ≥130/≥85 mm Hg *****Fasting glucose ≥110 mg/dL, 6.1 mmol/L. **(16-19).**

i. *Reaven's original description*: In the 1988 Banting Lecture (14), Reaven used the term syndrome X to refer to the tendency of glucose intolerance, hypertension, low high density lipoprotein (HDL) cholesterol and raised triglycerides, and hyperinsulinaemia to occur in the same individual (Table 1). He proposed that the common feature of the syndrome is insulin resistance and that '... all other changes are likely to be secondary to this basic abnormality'. Neither obesity nor abdominal obesity was included in Reaven's original description although secondary sources often state that they were included. However, Reaven did suggest that avoiding obesity and remaining physically active were measures that would protect against insulin resistance.

ii. ATP III: The National Cholesterol Education Program's Adult Treatment Panel III report (ATP III) identified the metabolic syndrome as a multiplex risk factor for CVD (15). ATP III viewed CVD as the primary clinical outcome of metabolic syndrome.

   a. *Atherogenic dyslipidaemia* manifests in routine lipoprotein analysis by raised triglycerides and low concentrations of HDL cholesterol. A more detailed analysis usually reveals other lipoprotein abnormalities such as increased remnant lipoproteins, elevated apolipoprotein B, small LDL particles, and small HDL particles. All of these abnormalities have been implicated as being independently atherogenic.

   b. *Elevated blood pressure* strongly associates with obesity and commonly occurs in insulin-resistant persons. Hypertension thus commonly is listed among metabolic risk factors. However, some investigators believe that hypertension is less "metabolic" than other metabolic-syndrome components. Certainly,

hypertension is multifactorial in origin. For example, increasing arterial stiffness contributes significantly to systolic hypertension in the elderly

c. *Insulin resistance* is present in the majority of people with the metabolic syndrome. It strongly associates with other metabolic risk factors and correlates univariately with CVD risk. These associations, combined with belief in its priority, account for the term *insulin resistance syndrome*. Even so, mechanisms underlying the link to CVD risk factors are uncertain, hence the ATP III's classification of insulin resistance as an emerging risk factor. Patients with longstanding insulin resistance frequently manifest *glucose intolerance*, another emerging risk factor. When glucose intolerance evolves into diabetes and prevalent hyperglycaemia, elevated glucose constitutes a major, independent risk factor for CVD.

d. A *proinflammatory state*, recognized clinically by elevations of C-reactive protein (CRP), is commonly present in persons with metabolic syndrome. Multiple mechanisms seemingly underlie elevations of CRP. One cause is obesity because excess adipose tissue causes the release of inflammatory cytokines that may elicit higher CRP levels.

e. A *prothrombotic state*, characterized by increased plasma plasminogen activator inhibitor (PAI)-1 and fibrinogen, also associates with the metabolic syndrome. Fibrinogen, an acute-phase reactant like CRP, rises in response to a high-cytokine state. Thus, prothrombotic and proinflammatory states may be metabolically interconnected.

iii. *American Association of Clinical Endocrinologists (AACE definition):* These criteria (14) appear to be a hybrid of those of ATP III and WHO metabolic

syndrome. However, no defined number of risk factors is specified; diagnosis is left to clinical judgment.

iv. *World Health Organization (WHO) definition:* WHO, in 1999, suggested a working definition of metabolic syndrome (MS), which was improved in due course of time (18). WHO defined MS as glucose intolerance, impaired glucose tolerance (IGT) or diabetes mellitus (DM), and/or insulin resistance, together with two or more of the components listed below:

1) Raised arterial pressure, defined as ≥140/90 mm of Hg
2) Raised plasma triglyceride (≥ 150 mg/dl) and/or low HDL-C (<35 mg/dl in men and <39 mg/dl in women)
3) Central obesity, i.e., waist/hip ratio (WHR) >0.9 in men and >0.85 in women and/or body mass index (BMI) >30 kg/m^2
4) Microalbuminuria, urinary albumin excretion rate ≥ 20 μg/min or albumin/creatine ratio ≥ 30 μg/mg.

This definition further insisted on a need for a clear description of the essential components of the syndrome, along with data to support the relative importance of each component. These conditions seem to be highly technical and the definition is rather impractical.

v. *The European Group for Study of Insulin Resistance (EGIR) definition:* This (19) is a modification of the WHO definition (18), focusing more on abdominal obesity but excludes diabetes mellitus from the definition. Metabolic syndrome was diagnosed as insulin resistance with two of the following:

1. Abdominal obesity: waist circumference (WC) ≥94 cm in men and ≥80 cm in women
2. Hypertension: ≥140/90 mm of Hg or on anti-hypertensive treatment

3. Elevated triglycerides (≥150 mg/dL) and/or reduced HDL-C (<39 mg/dL for both men and women)
4. Elevated plasma glucose: impaired fasting glucose (IFG) or IGT, but no diabetes.

1. 4. Insulin

Insulin is a peptide hormone synthesised by the pancreatic β-cells. High blood glucose stimulates its release into the blood where it acts on peripheral tissues to increase glucose uptake, suppress hepatic glucose production and prevent lipolysis (20).

Insulin production involves intermediate steps. Initially, preproinsulin is the single polypeptide inactive precursor, which is secreted into the endoplasmic reticulum. Post-translational processing clips the N-terminal signal sequence and forms the disulphide bridges. Cleavage of the signal peptide releases proinsulin into the ER lumen where it is transported to the golgi complex, and subsequent cleavage of the C-peptide yields the mature 5808 kDa dipeptide hormone (21, 22). Insulin is then transported out of the golgi and accumulates in secretary granules in the cytoplasm.

1.4.1. Insulin: Structure

Insulin gene transcription is normally restricted to the pancreatic β-cells within the islets of Langerhans. Insulin mRNA is translated on ribosomes attached to the endoplasmic reticulum (ER) as preproinsulin (Figure 1.2.). Structurally, preproinsulin consists of four domains: a C-terminal A-chain; an N-terminal B-chain; a connecting region known as the C-peptide; and an N-terminal signal peptide (20). The signal peptide anchors preproinsulin to the membrane of the ER (21). The ER lumen is a highly oxidising environment which facilitates the formation of two disulphide bridges between the A and B chains of preproinsulin.

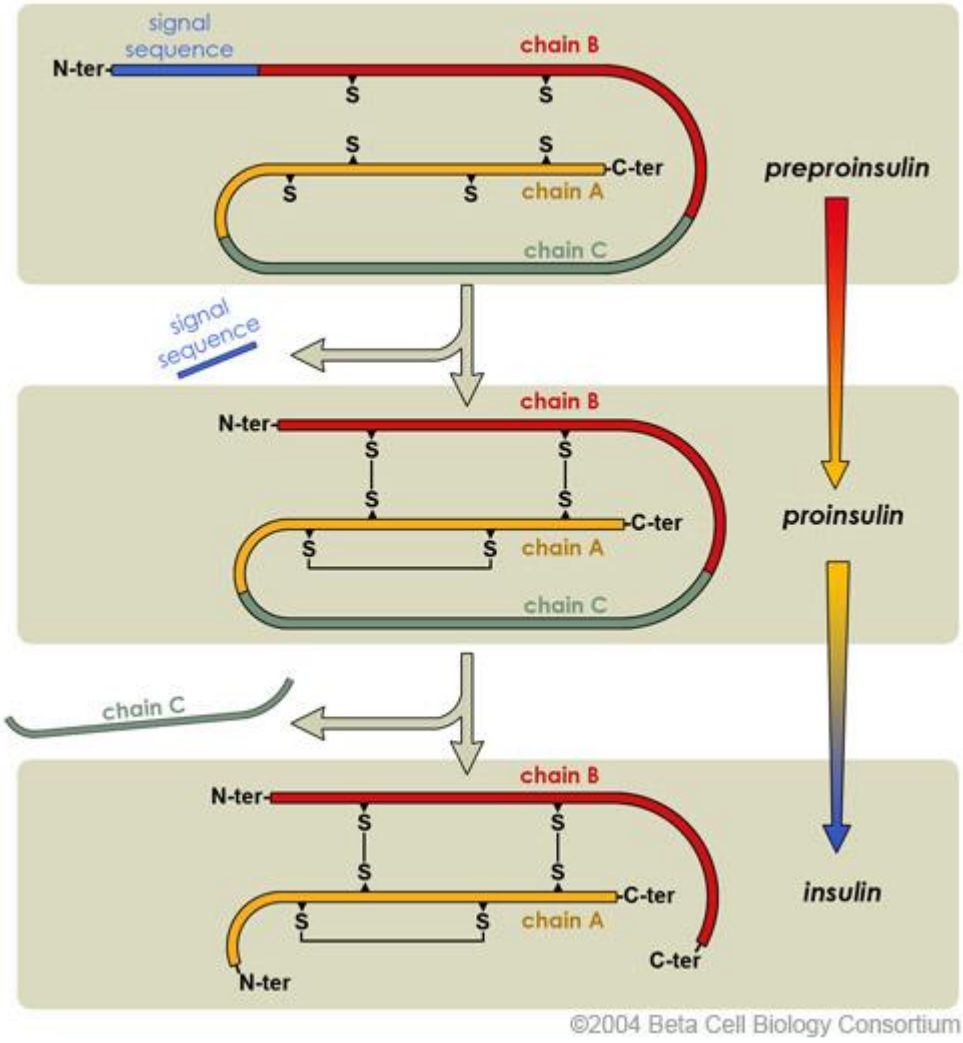

Fig 1.2. The major steps of insulin secretion in pancreatic β-cells. (http://www.betacell.org/content/articlepanelview/article_id/1/panel_id/1)

1. 4.2. Insulin: Secretion

Insulin secretion is enhanced by a number of stimuli including: glucose (23), amino acids (24) and gastrointestinal hormones such as secretin and glucagon-like peptide-1 (GLP-1) (25). Since the primary role of insulin is to control glucose homeostasis, glucose is the most important of these stimuli. Glucose induces a bi-phasic pattern of insulin release from the β-cells. Shortly following glucose stimulation, a transient spike in insulin secretion is observed, this is followed by a more enduring phase of insulin release (26). The mechanism by which glucose stimulates insulin secretion is as follows: glucose, when circulating at high concentrations, is able to diffuse into the β-cells through GLUT2 transporters (Figure 1-3) (27). Within the cytosol, glucose is metabolised through glycolysis generating pyruvate which is further metabolised in the mitochondria generating ATP. The elevated ATP/ADP ratio induces closure of cell-surface ATP-sensitive K^+ channels - preventing K^+ from leaving the cell, leading to cell membrane depolarization (28). This in turn leads to an opening of membrane bound voltage-gated Ca^{2+} channels, resulting in an influx of Ca^{2+} into the cytosol (28). The increased cytosolic Ca^{2+} signals exocytosis of storage vesicles containing insulin (Figure 1.3) (29). During stress (defined as trauma, sepsis, emotion, starvation) adrenal secretion of GCs and adrenaline increases, which inhibits insulin secretion from pancreatic β-cells (30).

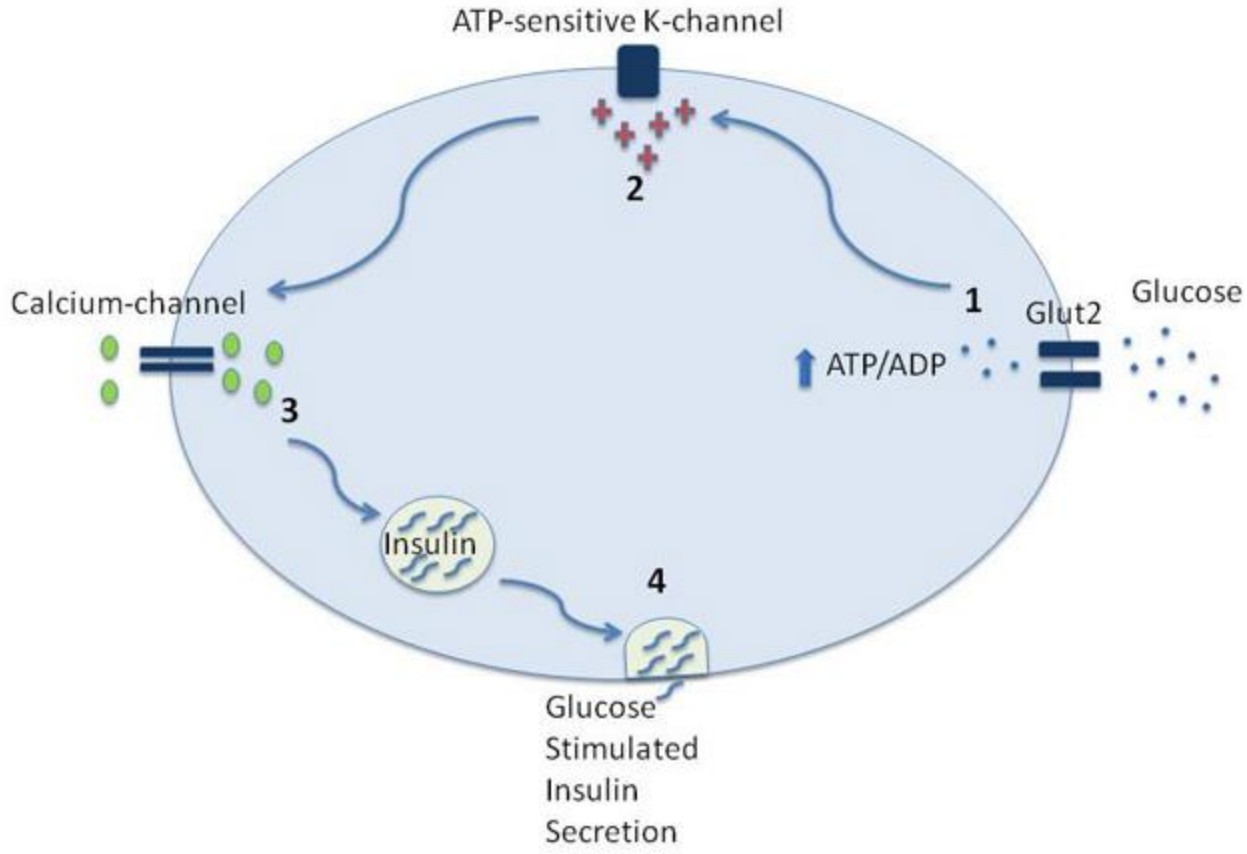

Fig. 1.3. Schematic of processes leading to insulin secretion in pancreatic β-cell. (27). Increased levels of glucose in the circulation lead to increased glucose uptake into pancreatic beta cells through GLUT2, a glucose transporter. Increased intracellular glucose then leads to increased production of ATP, and an increase in the ATP/ADP ratio (1); the increased ATP/ADP ratio leads to closing of the potassium channel and depolarization of the cell (2); and cell depolarization opens a calcium channel (3) which leads to insulin secretion (4).

1. 4.3. Insulin: Metabolic actions

Insulin is an anabolic hormone, important during times of nutrient excess; promoting energy storage and decreasing energy release (in the form of glucose from the liver and fatty acids and glycerol from adipose tissue).

1. 4.3.1. Carbohydrate metabolism

The most important insulin target tissues are liver, adipose tissue and skeletal muscle. In the fed state when circulating glucose levels are elevated, insulin enhances glucose uptake by the adipose tissue and skeletal muscle (31). Insulin also upregulates glucose storage by increasing glycogen synthesis in these three tissues (32). In the fasted state, the liver synthesizes glucose via gluconeogenesis from precursors such as glycerol, lactate and amino acids. Glucose is also liberated by hydrolysis of hepatic glycogen stores. During the transition to the fed state insulin effectively inhibits both hepatic gluconeogenesis and glycogenolysis, consistent with its role as an anabolic effector (33).

1. 4.3.2. Protein metabolism

In addition to insulin's signalling role when energy is abundant, with regards to protein metabolism it acts to increase amino acid uptake from the circulation (34), and incorporation into proteins (35), whilst inhibiting protein breakdown (36). This occurs most notably in tissues where protein content is high such as in skeletal muscle.

1. 4.3.3. Lipid metabolism

Insulin promotes lipid storage by increasing lipogenesis - the *de novo* synthesis of fatty acids (37). *De novo* lipogenesis occurs predominantly in adipose tissue, liver and to a lesser extent in the skeletal muscle. Insulin also enhances uptake of fatty acid (38) and their

esterification with glycerol generating triacylglycrides (TAG) (39). During fasting (in the presence of low insulin), TAG stores are broken down by lipolysis, and the resultant free fatty acids are oxidised in the mitochondria yielding ATP. In addition, some of these TAG derived fatty acids (particularly from liver) are released into the circulation as lipoproteins which are utilised as an energy source by other tissues, including the skeletal muscle. During the fed state, insulin inhibits lipolysis and fatty acid oxidation (40), instead promoting the use of carbohydrates as a source of energy.

1. 4.4. Insulin Signalling

1. 4.4.1. Insulin Receptor

The actions of insulin are mediated through activation of cell surface receptors, in particular the insulin receptor (InsR), but also the closely related insulin-like growth factor receptor (IGF-IR) (Figure 1.4). InsR mediates metabolic regulation whereas IGF-IR is involved in normal growth and development. Both receptors can bind insulin, however, the binding affinity of IGF-IR for insulin is ~100-fold lower than for its cognate ligand, IGF-I (41). InsR is a disulphide-linked heterotetrameric structure, composed of two identical extracellular α-subunits, and two identical transmembrane β-subunits that have tyrosine kinase activity (42). Upon binding of insulin to the α-subunits, the receptor undergoes a conformational change leading to activation of the kinase domain resulting in auto-phosphorylation of specific tyrosine residues on the β-subunit (43).

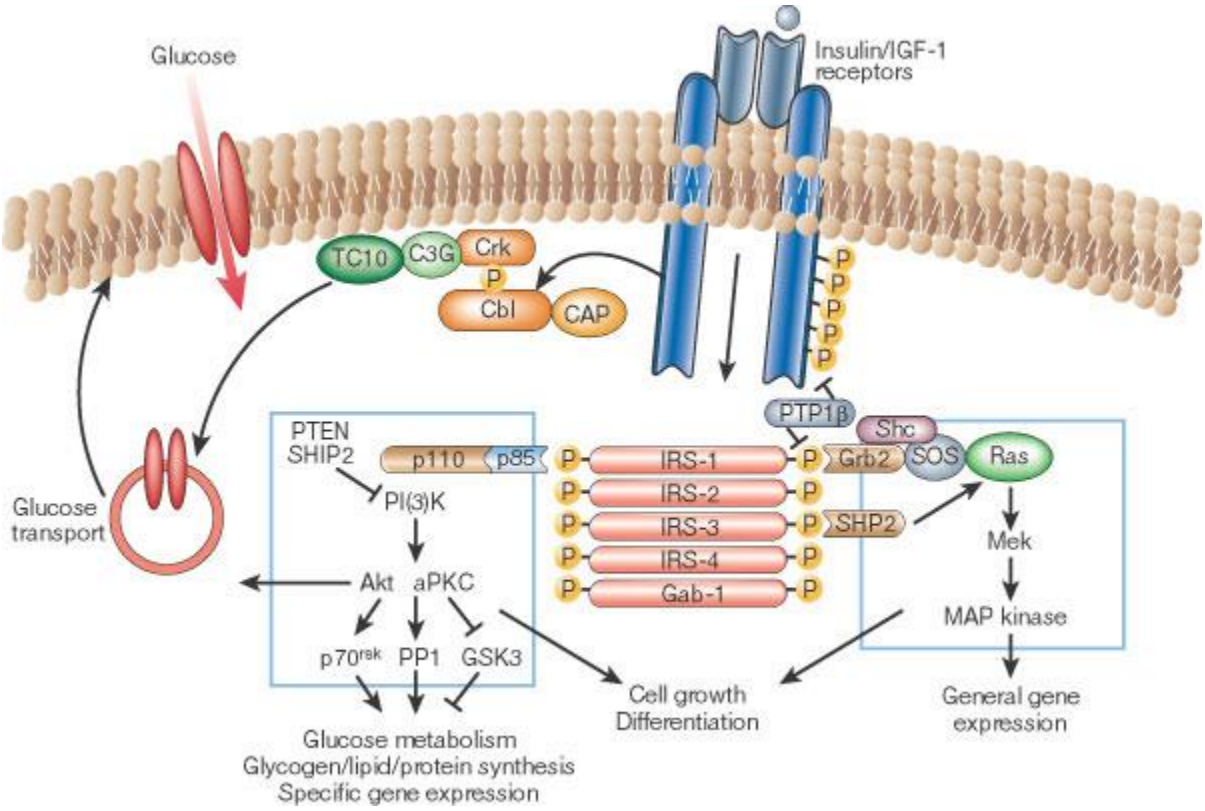

Fig. 1.4. The insulin signalling cascade. The insulin receptor is a tyrosine kinase that undergoes autophosphorylation, and catalyses the phosphorylation of cellular proteins such as members of the IRS family, Shc and Cbl. Upon tyrosine phosphorylation, these proteins interact with signalling molecules through their SH2 domains, resulting in a diverse series of signalling pathways, including activation of PI(3)K and downstream PtdIns(3,4,5)P_3-dependent protein kinases, ras and the MAP kinase cascade, and Cbl/CAP and the activation of TC10. These pathways act in a concerted fashion to coordinate the regulation of vesicle trafficking, protein synthesis, enzyme activation and inactivation, and gene expression, which results in the regulation of glucose, lipid and protein metabolism. (49).

1. 4.4.2. Insulin receptor substrates

Upon activation by insulin, the auto-phosphorylated tyrosine residues on InsR act as docking sites for numerous proteins including the family of insulin receptor substrate (IRS) proteins (Figure 1. 5). To date, six IRS isoforms have been identified (IRS1-6). IRS1 and IRS2 are ubiquitously expressed, and are most important in mediating metabolic signal transduction (44), whereas the expression of IRS3 is limited to brain and adipocytes and IRS4 is expressed primarily in embryonic tissue, IRS5 and IRS6 have limited expression and function in signal transduction (45). Structurally, IRS proteins share a high degree of homology; each containing an N-terminal pleckstrin-homology (PH) domain for phospholipid binding; a phosphotyrosine-binding (PTB) domain for docking with phospho-tyrosine sites on activated InsR; and a variable C-terminal region containing numerous tyrosine, threonine and serine phosphorylation sites which confers IRS activity (46). The association between IRS1 and 2 and the activated InsR allows the kinase domain of the receptor to phosphorylate various tyrosine residues within the C-terminal of these proteins (47). This allows IRS1/2 to act as an adaptor; linking InsR to various Src-Homology 2 (SH2) domain containing proteins. For example, phosphorylation of IRS1 at tyrosine-612 and 632 (corresponding to 608 and 628 in rodents) is required for full activation of phosphoinositide-3 kinase (PI3K) (48). IRS activating tyrosine phosphorylation is negatively regulated by the phosphatase SHP2; attenuating the metabolic actions of insulin (49) (Figure 1.4).

In addition to tyrosine phosphorylation, IRS proteins also undergo serine phosphorylation (Figure 1.5). With over 70 putative serine phosphorylation sites, IRS1 is by far the most characterised isoform. As a general rule, serine phosphorylation inhibits IRS1 function, with increased serine phosphorylation seen in various insulin resistant states. These post-translational modifications could be a major contributor to the pathogenesis of insulin resistance (50). Probably the most characterised of these residues is serine-307 (corresponding

to serine 312 in humans), which is located adjacent to the PTB-domain (Figure 1.5). From work using yeast tri-hybrid assays it was found that phosphorylation at this site inhibits the InsR / IRS1 interaction thereby attenuating signal transduction. Other residues associated with inhibiting IRS1 function include serine-612 and serine-632 (corresponding to human serine 616 and serine 636), which are located proximal to the PI3K binding site (Figure 1.5). It is thought that phosphorylation here can preclude the association between PI3K and IRS1, preventing the former from becoming activated (50).

Numerous kinases have been implicated in mediating inhibitory serine phosphorylation of IRS proteins, and their dysregulation has been implicated in the pathogenesis of insulin resistance (50). These include Jun kinase (JNK), inhibitor of nuclear factor κB (NF-κB) and kinase-β (IKKβ), p70S6K (S6K1), the mammalian target of rapamycin (mTOR), extracellular signal-regulated kinase (ERK) and certain protein kinase C (PKC) isoforms.

1.5.1. Hepatic glucose metabolism under normal physiological conditions

1.5.1.1. Hepatic Glucose uptake

In health the portal venous glucose concentration after a meal may approach 10 mmol/L, much higher than is ideal in the systemic circulation. Hepatocytes take up glucose independently of insulin via the low affinity GLUT-2 transporter, which facilitates glucose entry into cells in the presence of high sinusoidal glucose concentrations. Hence, hepatocytes are in a key position to buffer the hyperglycaemic effects of a high carbohydrate meal. It has been proposed that hepatic injury in critical illness leads to hyperglycaemia because of unregulated glucose uptake by the liver. Hepatocytes are not able to rapidly down regulate glucose uptake to protect vital intracellular metabolic functions. Strict control of blood glucose concentration during critical illness protects from hepatic mitochondrial injury and may therefore contribute to improved outcomes clinically (51).

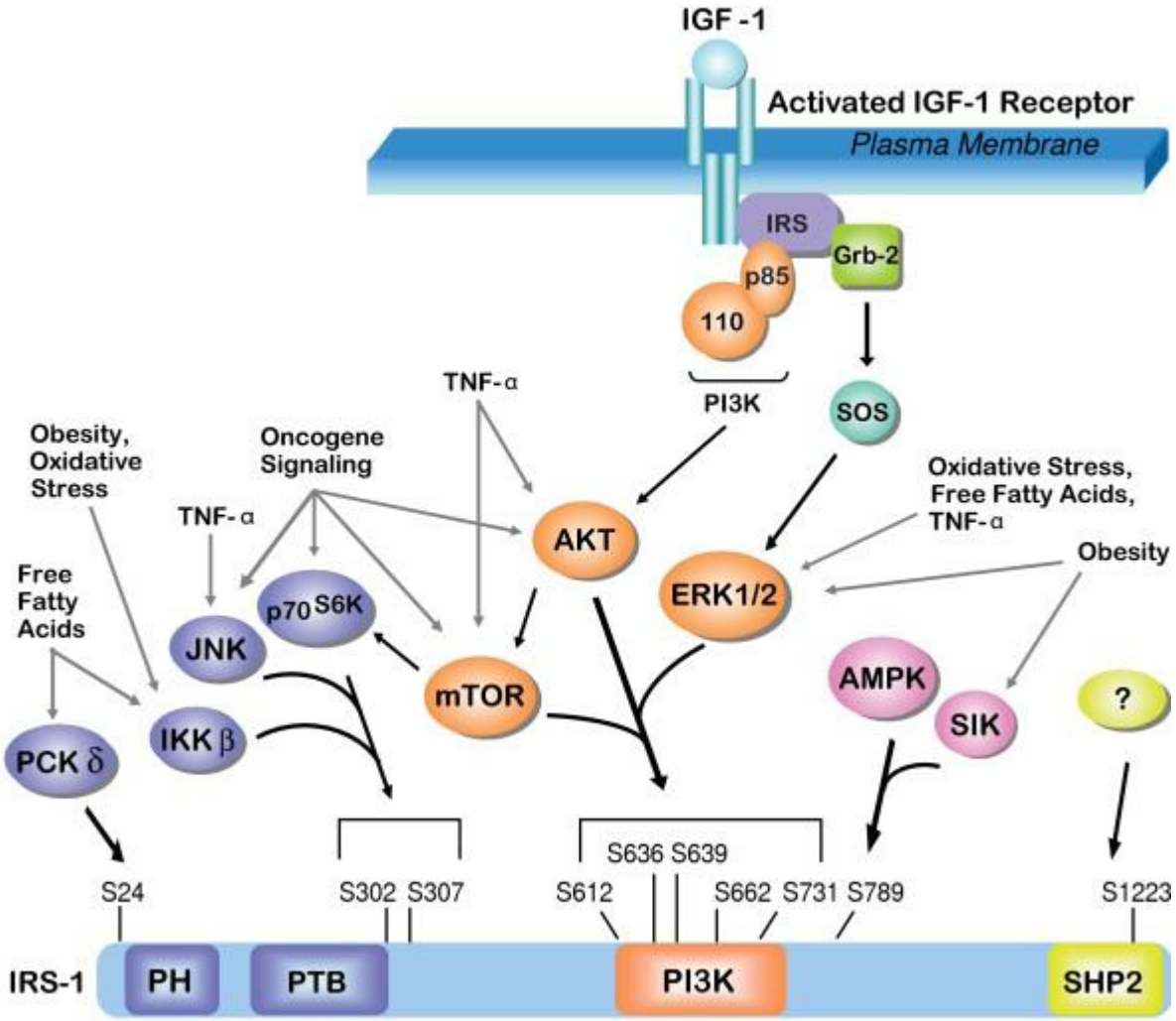

Figure 1.5. The structure of IRS1, highlighting some of the serine phosphorylation residues known to negatively regulate its function. Kinases shown in purple mediate signaling events that impede IRS-1 localization to the membrane or upstream receptors by disrupting PH and/or PTB domain function. Kinases shown in orange mediate signaling events that interfere with PI3K recruitment and activation. Kinases shown in pink mediate signaling events that result in phosphorylation of S789. Kinases that initiate signaling events that result in phosphorylation of S1223 and interfere with SHP-2 binding are unknown (yellow). Exogenous stimuli that have been implicated in cancer and inflammation and that can activate kinases to regulate IRS-1 serine phosphorylation are indicated. (50).

Once taken up by the liver, glucose is rapidly phosphorylated to glucose-6-phosphate (G6P), by the hepatic specific hexokinase isoform, glucokinase. This reaction is the prelude to glycolysis (resulting in the production of 3-carbon compounds such as lactate and pyruvate). Alternatively the glucose flux can be directed towards the direct pathway of glycogen synthesis via uridine diphosphate (UDP) - glucose, or the pentose phosphate shunt.

1.5.1.2. Glycolytic flux and gluconeogenesis

Carbon-3 compounds can enter the tricarboxlylic acid (TCA) cycle and undergo further oxidation or serve as substrates for *de novo* synthesis of glucose and glycogen (G6Pneogenesis and the indirect/gluconeogenic pathway of glycogen synthesis) (52). These processes form substrate cycles, a system which allows fine regulation of the direction and rates of flux, by changes in concentration, gene expression and covalent modification (phosphorylation) of effector enzymes (53). Gluconeogenesis substrate cycles are controlled by the enzymes phosphoenolpyruvate carboxykinase (PEPCK) and fructose 1,6 biphosphatase, while glycolytic substrate cycles are regulated by pyruvate kinase and phosphofructo-1-kinase.

1.5.1.3. Glycogen synthesis and glycogenolysis

Glycogen synthase and glycogen phosphorylase are involved in another substrate cycle that can be active simultaneously, resulting in glycogen cycling. The effect of this is negligible in the non-diabetic fasting state. Both enzymes are regulated by phosphatases, kinases and allosteric effectors which are dependent on the nutrient and hormonal microenvironment (53). Glycogenolysis requires the action of glycogen phosphorylase and a debranching enzyme to release glucose-1-phosphate which is in equilibrium with G6P (Figure.1.6).

1.5.1.4. Glucose-6-phosphatase and glucose release

Glucose-6-phosphatase (G6Pase) catalyses the "terminal step" resulting in the release of free glucose into the hepatic veins, from either gluconeogenesis or glycogenolysis (Figure.1.6). G6Pase catalyses the dephosphorylation of G6P to glucose and is expressed in liver and kidney, G6P neogenesis can result in glucose release from these tissues only. In contrast, skeletal muscle is devoid of G6Pase and therefore cannot release glucose from glycogen despite muscle glycogen depots being four to five fold greater than in liver. Instead lactate is released from skeletal muscle which is shuttled back to the liver via the Cori cycle. G6Pase activity is deficient in patients with glycogen storage disease Type 1a which is usually diagnosed by the detection of profound hypoglycaemia in infancy.

1.5.1.5. Insulin and glucagon, and endogenous glucose production (EGP).

Insulin, glucagon and hyperglycaemia primarily regulate endogenous glucose production (EGP). The cephalic phase of insulin secretion primes the liver to rapidly facilitate the hormonal responses to eating before there is any carbohydrate induced hyperglycaemia. This, coupled with the direct delivery of pancreatic hormones to the liver sinusoids, allows rapid control and response to nutritional stimuli. The ingestion of a mixed meal also results in an increase in plasma glucagon concentration, although a pure glucose load can result in it being unchanged or even decreased. In both situations however, the plasma insulin/glucagon ratio rises due to the more marked rise in plasma insulin (54).

Under postprandial conditions, the portal vein insulin concentration is around 180 pmol/L, which is almost 3-fold higher than in the systemic circulation. This concentration of insulin is necessary to half maximally stimulate hepatic glycogen production (HGP) and suppress HGP during periods of hyperglycaemia, much higher than the concentration required in the periphery to stimulate the uptake of glucose by cells (55).

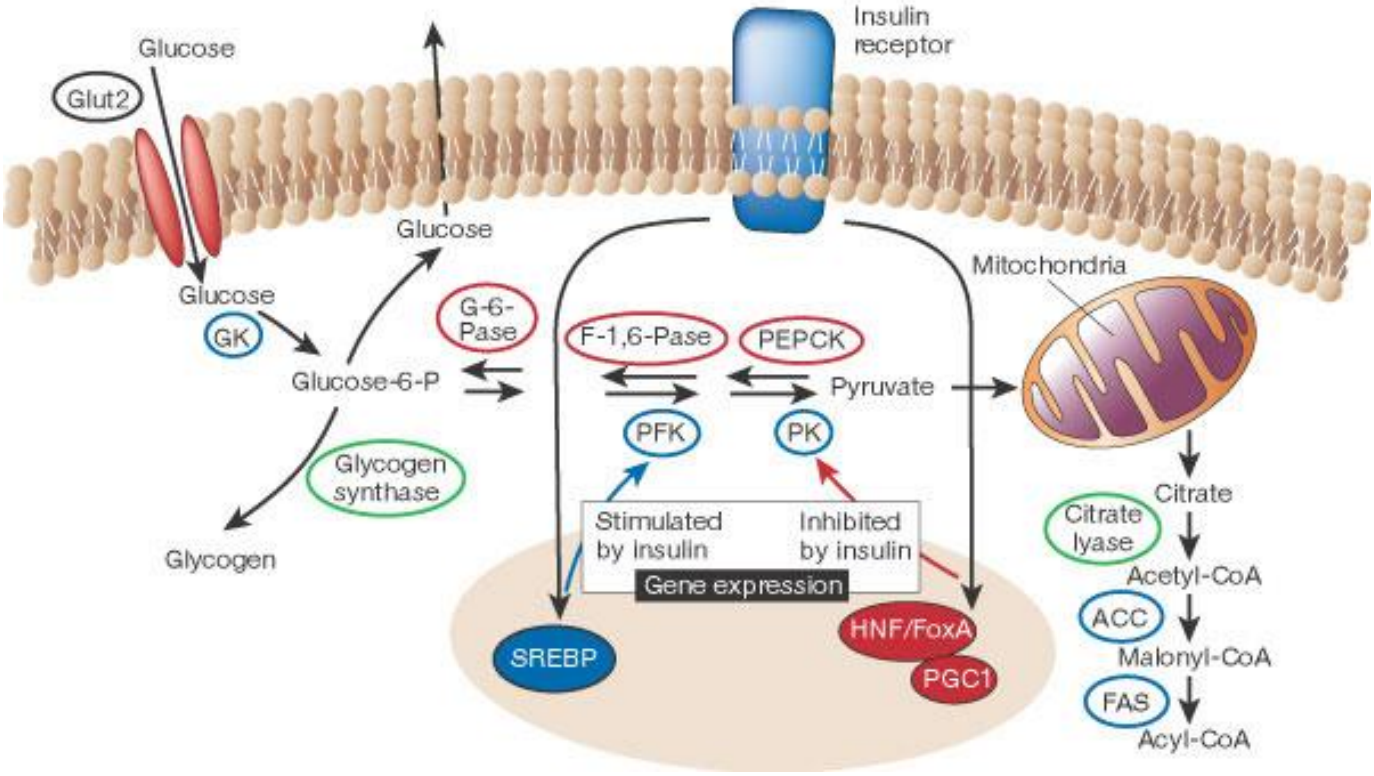

Figure 1.6. The fate of glucose in the hepatocyte.
In the hepatocyte, insulin stimulates the utilization and storage of glucose as lipid and glycogen, while repressing glucose synthesis and release. This is accomplished through a coordinated regulation of enzyme synthesis and activity. Insulin stimulates the expression of genes encoding glycolytic and fatty-acid synthetic enzymes (in blue), while inhibiting the expression of those encoding gluconeogenic enzymes (in red). These effects are mediated by a series of transcription factors and co-factors, including sterol regulatory element-binding protein (SREBP)-1, hepatic nuclear factor (HNF)-4, the forkhead protein family (Fox) and PPARγ co-activator 1 (PGC1). The hormone also regulates the activities of some enzymes, such as glycogen synthase and citrate lyase (in green), through changes in phosphorylation state. (Ref 53).

During periods of hypoglycaemia, plasma glucagon concentrations rise causing an immediate rise in plasma glucose. Studies using continuous glycogen infusions have shown that the immediate rise in EGP is accounted for by hepatic glycogenolysis. Following this there is a decline in EGP that is explained by a decrease in glycogenolysis due to decreased glycogen stores, and an increase in gluconeogenesis (56). Glycogen stimulates PEPCK expression and pyruvate carboxykinase activity as well as inhibiting pyruvate kinase and phophofructo-1-kinase (57). Even small changes in the portal vein insulin and glucagon concentration affect hepatic glycogen synthesis and glycogenolysis, exerting a fine control on glucose homeostasis.

1.5.1.6. Hepatic amino acid, carbohydrate, and lipid metabolism.

A high protein intake in humans can induce glucose intolerance as well as increasing EGP in the fasting state (58). Transamination of unbranched amino acids has also been linked to carbohydrate and lipid metabolism. Branched chain amino acids and alanine are often elevated in patients with obesity and insulin resistance. This may result from a change in the secretion of regulatory hormones and the stimulation of gluconeogenesis by amino acids (59). Metabolic studies have shown that the rise in EGP as a result of the gluconeogenic effect of post prandial amino acid concentrations and this is only unmasked when insulin secretion is impaired. Hence in subjects with normal glucose tolerance, the stimulatory effect of post prandial amino acid concentrations on the secretion of insulin and glucagon balances the increase in gluconeogenesis with no significant effect on glycaemia (60).

Hepatic carbohydrate metabolism is closely linked to lipid metabolism. In the fasting state, plasma free fatty acid (FFA) concentrations increase and energy is derived from fat oxidation. In insulin resistant states, plasma FFA concentrations correlate with the extent of hyperglycaemia and EGP (61). The liver is able to synthesise and oxidize fatty acids, but lacks the enzymes necessary to complete the metabolism of the ketone bodies resulting from mitochondrial beta-oxidation. The balance between glucose and lipid oxidation is coordinated

by the enzyme malonyl-coenzyme A through its ability to inhibit the entry of acetylated fatty acid derivatives into the mitochondria. Fatty acid synthesis is promoted by insulin. Insulin deficiency, with the presence of elevated glucagon levels drives ketogenesis by promoting beta-oxidation (Figure 1.7). This is the mechanism that drives ketogenesis from fatty acids.

Adipocytes act in conjunction with the liver to convert excess glucose to triglyceride for storage. In the liver, triglycerides are formed from glycerol-3-phosphate (from triose phosphate) and fatty acids (from acyl CoA), and are incorporated in very low density lipoproteins (VLDL) where they are hydrolysed by lipoprotein lipase. The released FFA are re-esterified with glycerol-3-phosphate derived from glucose that has entered the tissue under the influence of insulin. The resulting triglyceride is stored in adipose tissue.

1.5.2. The liver in diabetes mellitus

Insulinopaenia in type 1 diabetes results in increased hepatic glucose production that correlates with the degree of fasting hyperglycaemia.

In type 2 diabetes, there is evidence for a reduction in glycogen synthesis, implying that the increase in hepatic glucose output is mainly a result of increased gluconeogenesis. Isotopic tracer dilution studies have shown that there is a loss of auto-regulation in patients with fasting hyperglycaemia, as hepatic glucose output rates are either inappropriately normal or elevated by 10-25%.

The increase in hepatic gluconeogenesis is further fuelled by increased rates of lipolysis in adipose tissue, due to impaired insulin action, releasing FFA and glycerol which are subsequently delivered to the liver. Increased hepatic uptake of non-esterified fatty acids also promotes hepatic lipid synthesis as well as increased hepatic secretion of VLDL, resulting in the typical type 2 diabetic dyslipidaemic phenotype.

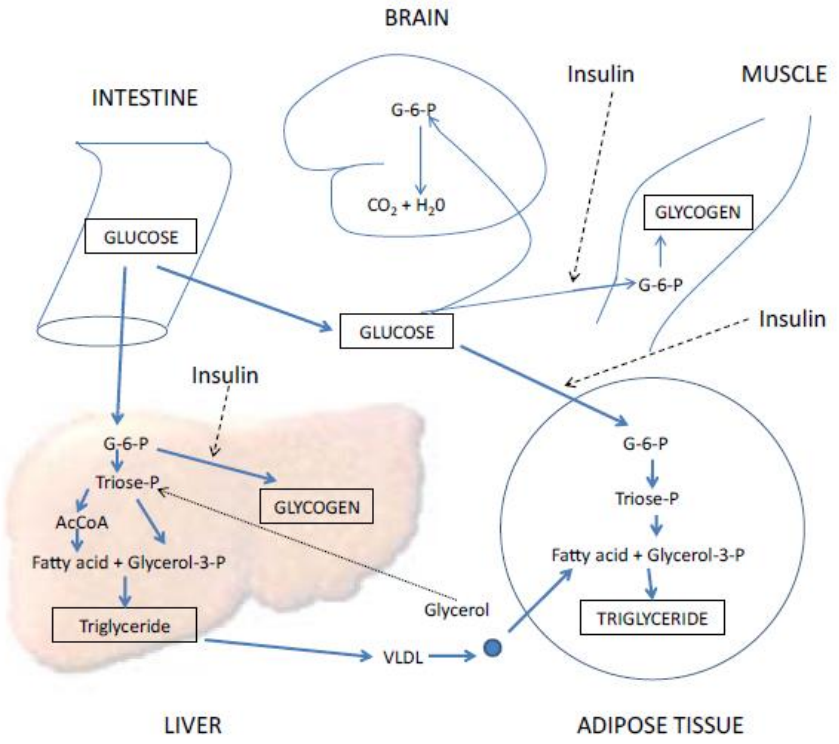

A.

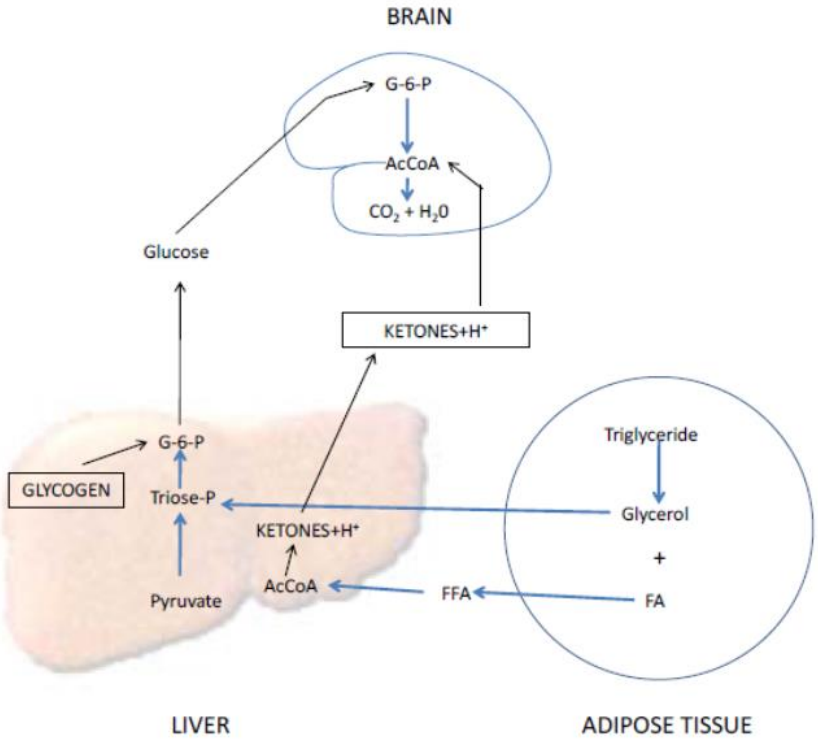

B.

Figure 1.7 A. Brief overview of postprandial metabolism of glucose, and, B. Brief overview of intermediary metabolism during fasting (61).

1. 6. Glucocorticoids, obesity and metabolic disease

1.6.1. Glucocorticoids

Glucocorticoids are well characterized ubiquitous hormones that play a key role in modulating immune and inflammatory responses, regulating energy metabolism and cardiovascular homeostasis and in the body's responses to stress. Opposing the action of insulin, glucocorticoids stimulate production of glucose, switching the homeostatic balance towards catabolism. Thus, glucocorticoids promote gluconeogenesis but inhibit beta-cell insulin secretion and peripheral glucose uptake (62). They also increase protein breakdown and lipolysis with consequent fatty acid mobilization. Patients with endogenous or exogenous glucocorticoid excess (Cushing's syndrome) develop visceral obesity, insulin resistance, diabetes type 2, dyslipidaemia, hypertension and increased CV mortality.

The striking similarity of phenotype between the rare Cushing's syndrome and the common metabolic syndrome/idiopathic obesity spectrum has spurred the search for a common underlying mechanism. However, plasma cortisol levels are not notably elevated in simple obesity or in metabolic syndrome, at least in the absence of marked complications. It has been hypothesised that tissue-specific differences in glucocorticoid metabolism and hence increased local cellular corticosteroid exposure may explain this apparent paradox. Since most of the features of Cushing's syndrome are reversible by removal of glucocorticoid excess, manipulations reducing cortisol action at a local cellular or tissue level might provide a novel therapeutic strategy for the metabolic syndrome.

1.6.1.1 Mechanism of action of corticosteroids

The conventional view is that corticosteroids (cortisol and aldosterone) exert their actions through specific intracellular receptors, glucocorticoid and mineralocorticoid receptors (GR and MR) respectively. More recently, evidence has been presented for the existence of cell surface steroid receptors, and second messengers inside cells that may result in steroid

induced non-genomic actions (63).While there is molecular evidence of the existence of these cell surface receptors, detailed information about them is lacking. Steroids are also able to facilitate the action of GABA receptors by binding to $GABA_A$ receptors. The traditional view that steroid receptors exert similar responses for all ligands has also been put into question by studies that demonstrate that the oestrogen receptor is able to exert a range of actions, often opposing, when activated by molecules with very similar structures (64). These observations have led to the awareness that a key component of steroid hormone action involves interaction of the ligand with a coactivator known collectively as corepressor molecules.

1.6.1.2. Corticosteroid receptors

Historically, glucocorticoids were thought to bind exclusively to GR and aldosterone to MR, and regulate carbohydrate and sodium homeostasis respectively. However, following *in vitro* observations that both receptors bind to glucocorticoids with high affinity, they were classified as Type 1 'high affinity' GR (corresponding to the MR) and Type 2 'low affinity' GR (corresponding to GR). In this discussion, the traditional MR and GR classification will be used. Separate receptors for glucocorticoids and mineralocorticoids appear to have occurred via gene duplication late in evolution, explaining why they behave in a similar fashion in some circumstances. This may also reflect the utility of pre receptor mechanisms in some tissues to confer further specificity to these receptors. Both receptors have similar ligand binding properties. The MR binds cortisol with an equal affinity to that of aldosterone (K_d for both ~ 1nM) (65), while the GR binds cortisol and corticosterone with a K_d between 20 and 40 nM and aldosterone with a K_d of 25 to 65 nM (66).

The MR is expressed in target tissues such as the epithelia of renal distal tubules, salivary glands and distal colon, as well as within the central nervous system (CNS), in the placenta and foetal tissues, and in bone cells. The GR is widely expressed in tissues involved

in glucose homeostasis, such as liver, adipose tissue and muscle, as well as bone cells and cells in the immune system.

1.6.1.3 Steroid hormone receptor structure

The typical domains common to steroid hormone receptors are illustrated in Figure 1.8 along with the corresponding domains in the hGR, hMR and other steroid hormones. The DNA binding domain is a critical component responsible for binding to the double helix. The N-terminal region mediates transactivation functions, and the C-terminal is the ligand binding domain. In reality this model is rather simplistic and activation functions can also be mediated by sequences located throughout the receptor, including NLSs and sequences mediating receptor dimerisation. These features are displayed in GR and MR. The cDNAs encoding the proteins for human GR and MR are highly homologous and share a conserved DNA binding domain with 94% homology and a 57% homology across the ligand binding domain (67) .This reflects the promiscuity of ligand binding of aldosterone to the GR and cortisol to the MR. The parts of the complex that are responsible for transrepression of genes are currently unclear. Specificity upon the MR is conferred by the process of pre receptor metabolism of cortisol by 11β-hydroxysteroid dehydrogenase type 2 (11β-HSD2), which inactivates cortisol and corticosterone to inactive 11-keto metabolites, allowing aldosterone to bind to the MR (68).

1.6.1.4 Transactivation of genes by corticosteroid receptors

Transactivation of genes occur when the GR or MR bind to glucocorticoid response elements (GREs) – specific regulatory sequences of DNA which are usually located near the promoter region of target genes (69). The classic GRE sequence for GR binding is a partially palindromic structure with the sequence GGTACAnnnTGTTCT (where n is any nucleotide). The consensus sequence for negatively regulated genes is less well conserved. There is a large body of

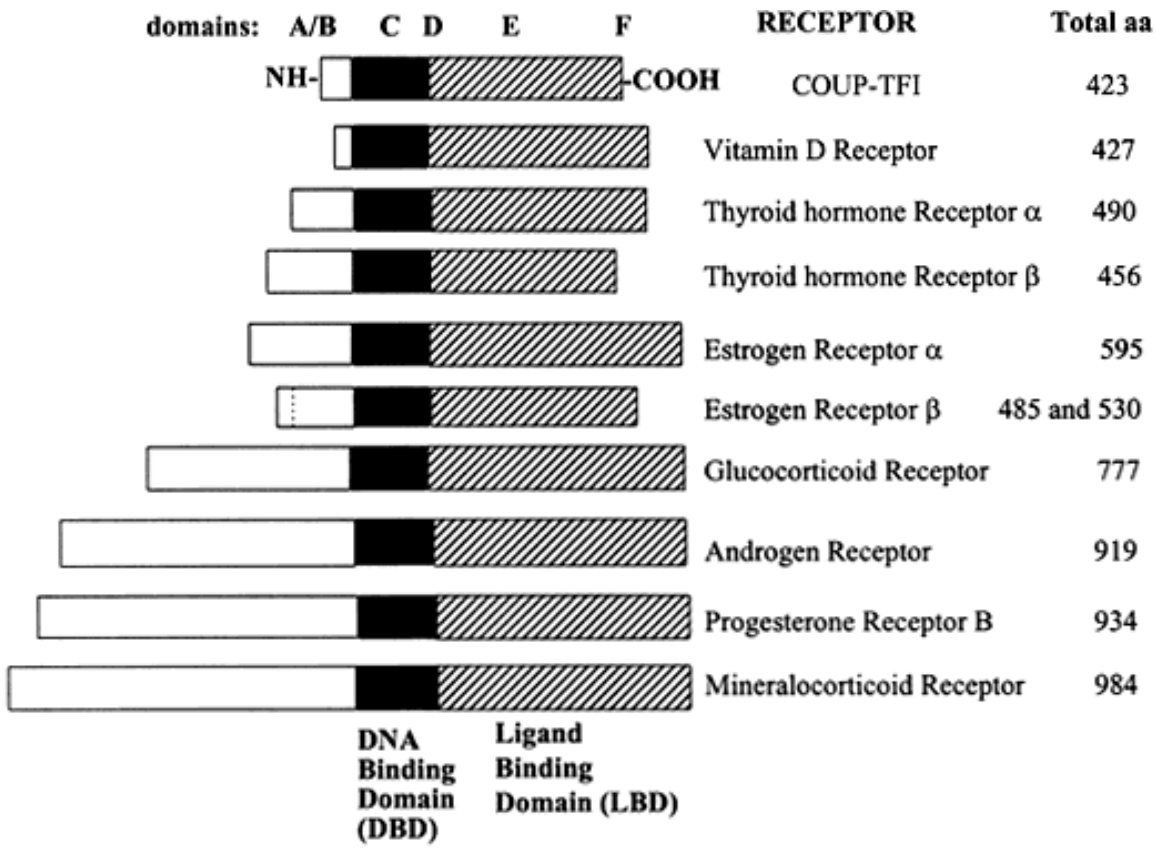

Figure 1.8. Relative lengths of several members of the steroid/nuclear hormone receptor superfamily, shown schematically as linearized proteins with common structural and functional domains. Variability between members of the steroid hormone receptor family is due primarily to differences in the length and amino acid sequence of the amino (N)-terminal domain. Ref.67.

investigation into the exact mechanism of transactivation and how the binding of the complex to GREs affects gene transcription. Dimerisation of the steroid-GR complex is required for transactivation. This has been shown *in vitro* and in transgenic dimerisation deficient transgenic animals (70).

In addition to the interaction of DNA binding and activation domains of the receptor with GREs, gene transcription relies on a number of other vital components. These include general transcription factors and coactivator or corepressors that initiate or repress transcription. Coactivators are thought to be involved in the linking of the hormone receptor to general transcription factors and in chromatin remodelling during assembly of the transcription complex (71).

There is no known classic response element for the MR. However MR is able to bind to the GRE and a number of genes appear to be induced by both MR and GR for example serum and glucocorticoid inducible kinase (Sgk), a key gene of mineralocorticoid hormone action (73). Some genes respond differently depending on whether GR or MR binds to the GRE. These variations are likely to be due to differences in the recruitment of coactivators and corepressors. Studies have also shown that GR and MR are able to heterodimerise with each other. These heterodimers appear to have different effects to GR or MR homodimers at the GREs of several genes.

1.6.1.5. Transrepression of genes by corticosteroid receptors

Transrepression of genes is critical to restrict gene expression so that only a subset of genes are expressed in a particular cell type and to exert a degree of tissue specificity. The process of transrepression occurs via protein-protein interactions. GR associates with other transcription factors via leucine zipper interactions. Binding of a repressor to the activator can mask its transactivational ability. This type of repression is called quenching, an example of

which is the interaction of the GR with members of the bZIP FOS and JUN family of transcription factors, constituting the AP-1 complex.

GR acts as a repressor by adjacent binding to the AP-1 factors or tethering to AP-1 factors bound to the composite element, quenching activation by AP-1(74). This process is of particular importance to the anti-inflammatory effects of glucocorticoids, by negative regulation of the expression of several genes involved in the inflammatory cascade, by interaction with AP-1 and NF-κB. NF-κB is a key regulator of several inflammatory processes and can act as an amplifier of inflammatory pathways, and interaction of GR with NF-κB effects a significant anti-inflammatory action. MR is also able to interact with AP-1 and NF-κB, although the relevance of this finding is unclear but has been implicated in the pathogenesis of cardiovascular disease via MR activation (75).

1.6.1.6. Effects of glucocorticoids on carbohydrate, protein and lipid metabolism

The inability of adrenalectomized animals to maintain hepatic glycogen stores was noted in 1927 by Cori (76). Replacement of adrenocortical steroids returned hepatic glycogen stores to normal and reversed hypoglycaemia.

Glucocorticoids promote glycogen deposition in the liver by activating glycogen synthase (by promoting its dephosphorylation) and inactivating glycogen phosphorylase (involved in glycogen mobilisation) (77).

Glucocorticoids are directly able to increase hepatic glucose production. This occurs by activation of key hepatic gluconeogenic enzymes such as glucose-6-phosphatase and PEPCK. Interaction of the glucocorticoid receptor complex with a GRE located in the 5‟ flanking region of the PEPCK gene mediates glucocorticoid induced gene transcription (78). Glucocorticoids also exert a secondary effect by increasing substrate availability to increase hepatic glucose

production by promoting the release of glucogenic amino acids from peripheral tissues such as skeletal muscle.

Additionally, glucocorticoids also promote hepatic glucose production by exerting a permissive effect upon other gluconeogenic hormones such as adrenaline and glucagon, and to increase the sensitivity of target tissues to respond to catecholamines causing an increase in substrate for glucose production such as increasing muscle lipolysis (79). Glycerol and FFA released from lipolysis provides substrate and energy for hepatic glucose production.

Glucocorticoids also increase sensitivity to glucagon action but the mechanism for this has not yet been elucidated (80).

The effects of glucocorticoids on peripheral glucose utilization further promote the hyperglycaemic state that can often result from glucocorticoid administration. Glucose transport into cells and utilisation by peripheral tissues is inhibited. Glucocorticoids affect lipid metabolism by directly activating lipolysis in adipose, increasing serum FFA, and hence FFA delivery into the circulation. In adrenalectomised animals FFA levels and lipolysis are reduced, and return to normal 2 h after glucocorticoid administration. The molecular mechanism for this is not yet known but may occur by a permissive effect upon sensitivity to lipolytic hormones such as catecholamines.

The chronic effects of glucocorticoids on lipid metabolism are well known, with the marked redistribution of body fat. Deposition of fat is seen over the trunk, anterior mediastinum and mesentery, as well as dorsocervical and supraclavicular regions, with sparing fat deposition of the extremities. The mechanism underlying this central predisposition is not understood but may be related to increased lipogenesis from the hypeinsulinaemia that results from the effects of glucocorticoids.

Glucocorticoids stimulate adipocyte differentiation and adipogenesis via key differentiation genes including lipoprotein lipase, glycerol-3-phosphate dehydrogenase and

leptin (80). Centripetal obesity and weight gain are extremely common in patients with Cushing's syndrome. Generalised obesity is more common among the general population than in patients with Cushing's syndrome. This predisposition to visceral obesity may also relate to the increased expression of GR and 11β-HSD type 1 (generating active cortisol from inactive cortisone) in omental compared with subcutaneous tissue (81).

1.6.2.Determinants of tissue sensitivity to glucocorticoids: Pre-receptor metabolism, Glucocorticoid receptor variability and post-receptor variation and effects on steroid action

Studies have failed to show a clear relationship between serum glucocorticoid level and the effect on tissues, suggesting that there are factors intrinsic to tissues that are important in determining tissue sensitivity to glucocorticoids. These differences could occur at a number of levels, including changes in the concentration and affinity of GR or any of the steps involved in the formation of the steroid-receptor complex, to translocation to the nucleus and modulation of transactivation or transrepression of genes. The action of glucocorticoid transporters may also be involved in regulating intracellular glucocorticoid levels. The major part of this thesis relates to the expression and activity of hepatic glucocorticoid metabolising enzymes in chronic uraemia in rodent and murine models, where very little has been published. However, a great deal of mechanistic insight and data are available from work obtained in non-uraemic diabetic subjects, from bench to bedside, which has been discussed and used to inform the current work.

The 11β-Hydroxydehydrogenase (11β-HSD) enzymes are major candidates for determining tissue sensitivity to glucocorticoids. While variation in concentration of glucocorticoid receptors may underlie differences in glucocorticoid sensitivity, data suggest that GR variants are not a major factor.

Mutations in the GR gene have been associated with glucocorticoid resistance. Numerous GR-gene variants have been identified, as well as single nucleotide polymorphisms

(SNP) which are relatively prevalent. In particular, one GRβ-variant has been proposed to influence corticosteroid sensitivity, with evidence derived from the immune system and asthma. Also of relevance are the restriction fragment polymorphism and a substitution of Asp363Ser which have been identified to influence the regulation of the HPA axis and are associated with changes in metabolism and cardiovascular control. These findings further implicate cortisol in the pathophysiology of these disorders.

Post receptor variation most probably does occur but is difficult to analyse due to sparse knowledge of coactivators and corepressors. Of potential importance are post receptor factors such as AP-1 and NF-κB, and other transcription factors that directly interact with the GR. An example would include the increase in GR-mediated transcription by pro-inflammatory cytokines TNFα and IL-1β seen in several cell types (82). Very little is known about the impact of variation in coactivator/corepressors molecules in modulating glucocorticoid action.

1.6.2.2. Pre-receptor metabolism and steroid action

Pre receptor metabolism as a regulator of steroid action has been seen in several tissues, and for several different enzymes. Enzymatic conversion of steroid in the target cell cytoplasm can interconvert hormone between active and inactive forms.

One clinical example where pre-receptor hormone metabolism is crucial relates to androgen action. Androgens are converted to oestrogens by the action of aromatase. Aromatase deficiency has a profound effect on skeletal development, resulting in a eunuchoid habitus with low bone mineral density that is treatable with exogenous oestrogens (83).

Until recently, it was axiomatic that the major determinant of corticosteroid action was the level of free cortisol in the plasma and the densities of GR and MR in target tissues. However, it has recently become apparent that tissue specific metabolism of glucocorticoids, notably by the two isoforms of the enzyme 11β-HSD, 11β-HSD1 and 11β-HSD2, alters tissue

glucocorticoid levels and hence receptor access. 11β-HSD catalyses the interconversion of non-receptor-binding and therefore inert 11-ketosteroids, cortisone and 11-dehydrocorticosterone (11-DHC), and their receptor-binding active 11-hydroxy forms, cortisol and corticosterone. Inactive cortisone circulates unbound at around 100 nM in humans and therefore its concentration is greater than active cortisol, notably during the diurnal nadir. In rats, 11-DHC circulating concentrations are also around a mean of 70 nM, though its concentrations in mice are lower.

1.7. 11β-hydroxysteroid dehydrogenases

Two isoforms of 11β-HSD are known, the products of distinct genes (84). 11β-HSD2, a high affinity NAD-dependent dehydrogenase, is expressed mainly in mineralocorticoid target tissues (kidney, colon, salivary glands). This distribution reflects its role in protecting intrinsically non-selective MR from activation by cortisol and corticosterone and therefore enabling selective aldosterone binding. Additionally, 11β-HSD2 is highly expressed in the placenta and the developing foetus, providing a potent barrier to maternal glucocorticoids.

In contrast 11β-HSD1 is a lower-affinity NADP (H)-dependent enzyme, which though bi-directional in purified preparations and tissue homogenates, acts as a predominant 11-ketoreductase in intact cells and organs.11β-HSD1 is expressed primarily in tissues with high sensitivity to glucocorticoids (liver, adipose tissue, brain and lung). 11β-HSD1 is active as a dimer and exhibits cooperative kinetics with cortisone and 11-DHC as substrates. Thus, 11β-HSD1 dynamically adapts to nanomolar as well as micromolar concentrations of 11-keto steroids. Both isozymes contain an N-terminal membrane-insertion sequence, thus enabling anchoring in the endoplasmic reticulum (ER) (85). The catalytic moiety of 11β-HSD2 faces the cytoplasm, while 11β-HSD1 is directed into the ER lumen (86). This has significant implications for cofactor availability (NAD^+/NADPH ratio) and potential bi-directionality of

11β-HSD1. The co-localization of 11β-HSD1 in the lumenal surface of the ER membrane with hexose-6-phosphate dehydrogenase (H6PDH), which catalyzes the first two steps of the pentose-phosphate pathway generating NADPH, provides a supply of co-substrate to drive the predominant oxoreductase direction of 11β-HSD1 in intact cells. $H6PDH^{-/-}$ mice are unable to convert 11-dehydrocorticosterone to corticosterone, but the efficiency of the opposite dehydrogenase reaction is unaffected (87).

1.7.1.1. 11β-HSD1 in the liver, and regulatory effects on factors affecting insulin sensitivity

11β-HSD1 immunoreactivity is seen in hepatocytes, being particularly intense around the central vein (88). In humans the activity of this enzyme activates orally administered cortisone to its biologically potent form. Primary cultures of human and rat hepatocytes and the 2S FAZA cell line indicate exclusive 11-oxoreductase activity (89). In rat liver, but not mouse liver, there is a sexually dimorphic pattern of 11β-HSD1 activity and expression, with expression in males being higher than females.

In clinical studies venous blood draining the liver had increased cortisone to cortisol ratios relative to systemic blood indicating the conversion of cortisone to cortisol *in vivo.* These studies are further supported by studies that used isolated perfused livers where activity was predominantly reductase (89).

There is currently intense research in the role of 11β-HSD1 in insulin resistance. The regulatory role of 11β-HSD1 can occur at the level of adipose tissue (central and visceral obesity), liver (hepatic gluconeogenesis) and muscle. The work presented in this thesis focuses on the role of hepatic 11β-HSD1 in this process. An overview of the effect of glucocorticoids on hepatic carbohydrate metabolism has been detailed earlier in this introduction (1.6.1.6).

1. 7. 2. Inhibition of 11β-HSD1 as a therapeutic target

With its pivotal role in hepatic energy cycling and homeostasis, inhibition of the metabolic effects of this enzyme has been of interest to research groups since the early reports in the 1980s. A brief review of the development of enzyme inhibitors is given below.

1.7.2.1. Natural 11β-HSD1 inhibitors

Derivatives of the liquorice root (*Glycyrrhiza glabra*), including glycyrrhetinic acid and its synthetic hemisuccinyl ester, carbenoxolone, are potent (IC_{50} nM *in vitro*), but non-specific 11β-HSD inhibitors (93). A variety of endogenous steroids and their metabolites, as well as bile acids such as chenodeoxycholic acid, have been reported to have 11β-HSD inhibitory properties.

Studies using the prototypic drug, carbenoxolone, showed hepatic insulin sensitization in lean healthy subjects (94). The insulin sensitization appears due reduced hepatic glucose production and glycogenolysis rather than any effect on peripheral glucose uptake, perhaps because carbenoxolone fails to inhibit 11β-HSD1 in adipose tissue in rats or humans. Such non-selective liquorice-based compounds also potently inhibit 11β-HSD2 causing renal sodium retention, hypertension and hypokalaemia. They also have effects on other short-chain dehydrogenases, such as 15-prostaglandin dehydrogenase and on gap junctions, though these effects occur at higher concentrations than 11β-HSD inhibition.

Interestingly, while concurrent infusion of carbenoxolone, a non-selective inhibitor, made little difference; seven days' pre-treatment with carbenoxolone significantly reduced oxoreductase activity along with decreased expression of both G6Pase and PEPCK (89). Studies on healthy humans have supported animal data with a reduction in hepatic glucose production with non-selective inhibitor (carbenoxolone) administration (91). Similar studies in

type 2 diabetic patients (93) showed that the decrease in hepatic glucose production may be due to decreased glycogenolysis rather than a change in hepatic gluconeogenesis. However, in one study, carbenoxolone did not improve insulin sensitivity in Zucker obese rats (94); in these animals, hepatic 11β-HSD1 was downregulated so that additional inhibition by carbenoxolone may have been less effective, and carbenoxolone had no measurable effect on 11β-HSD1 in adipose tissue.

1.7.2.2. Specific 11β-HSD1 inhibitors

1.7.2.2.1. Specific inhibitors and animal studies.

Several selective 11β-HSD1 inhibitors are being developed with the aim of lowering intracellular cortisol concentrations in adipose and liver in patients with type 2 diabetes and obesity with promising results (81, 94-96). Biovitrium BVT2733, in several hyperglycaemic rodent models, has been shown to reduce fasting blood glucose (with decreased hepatic PEPCK and G6Pase expression) and insulin levels and lower cholesterol, FFA, and triglyceride levels (95, 96) and was the first specific inhibitor described to have a metabolic effect. The Pfizer compound, PF-915275, is selective for primate and human 11β-HSD1, and short-term administration in primates was found to inhibit 11β-HSD1 effectively, as assessed by conversion of prednisone to prednisolone and also reduced fasting insulin levels. Merck compound 544 has similarly been shown to improve insulin sensitivity (94). The specific 11β-HSD1 inhibitor UE2316 was developed and patented by a team at University of Edinburgh. UE2316 has been shown to reverse the metabolic syndrome phenotype in high-fat fed C56BL mice and reduce post-myocardial infarction injury size after acute administration (122).

1.7.2.2.1. Specific inhibitors and clinical studies.

1.7.2.2.1.1. Incyte—INCB013739.

The Incyte selective 11β-HSD1 inhibitor, INCB013739, when administered to patients with type 2 diabetes twice daily for 2 weeks, completely abolished all conversion of oral cortisone to cortisol (97). Metabolically, hepatic glucose production rates decreased without alteration in glucose disposal. Interestingly, the decrease in fasting glucose was most marked in the most hyperglycaemic patients. In addition, total and low-density lipoprotein (LDL) cholesterol decreased, with no change in high-density lipoprotein (HDL)-cholesterol or triglyceride levels (313). INCB013739 has also been trialled in combination with metformin (MET) in patients with type 2 diabetes. This double-blind study included over 300 patients with inadequate glycaemic control (glycosylated haemoglobin [HbA1c], 7–11%) after MET treatment for more than 10 weeks. Patients were randomized to receive 5, 15, 50, 100, or 200 mg INCB13739 in addition to MET once daily for a 12-week period. Treatment was well tolerated, and the frequencies of adverse events were similar across all treatment groups. Importantly, no hypoglycaemic events were reported during the trial, and there were no differences between treatment groups in electrocardiograms, serum chemistry, haematology, or urine analysis. A potential limitation of therapeutic 11β-HSD1 inhibition is the compensatory activation of the HPA axis due to reduced cortisol regeneration. Morning plasma and evening salivary cortisol levels were unchanged across treatment groups. However, there was a dose-dependent increase in ACTH levels, although these remained within the reference range and plateaued after 4 weeks. This increase was paralleled by an increase in the ACTH-dependent androgen precursor, dehydroepiandrosterone sulfate, although this too remained within the normal reference range.

1.7.2.2.1.2. Merck—MK0916

The Merck Compound MK0916 was used in a double-blind, placebo-controlled study, where patients were given a daily dose of 0.5, 2, or 6 mg of MK0916 for a 12-week period

(98). MK0916 was well tolerated, with a similar frequency of adverse events reported across all treatment groups.

MK0916 had only very modest effects on metabolic parameters. There was a decrease in weight and waist-hip ratio in the 6 mg group, and in this group there was also a small reduction in HbA1c (0.3%); however, there was no change in fasting plasma glucose, 2 h postprandial glucose, or levels of fasting or postprandial serum insulin. MK0916 increased LDL and non-HDL cholesterol; these results were unexpected and they contrast with previous studies, and the investigators suggest that this effect may be compound-specific and not related to its inhibition of 11β-HSD1.

1.7.2.2.1.3. Pfizer PF-915275

Pfizer has developed compound PF-915275, which is an effective 11β-HSD1 inhibitor as measured by changes in urinary steroid metabolite ratios and prednisone to prednisolone conversion studies (99).

1.7.2.2.1.4. Salicylates

Inhibition of 11β-HSD1 also offers some potential mechanistic explanations for the actions of other drugs. One such example is the action of salicylates that improve glucose tolerance in patients with type 2 diabetes; this class of agent has been shown to inhibit 11β-HSD1 in sc adipose tissue (100).

1.7.2.2.1.5. UE2316

UE2316 has been shown to reduce post-myocardial infarction injury size after acute administration and to reduce obesity and inflammation in diabetic obese rats (109). This drug is not orally bioavailable and has to be given subcutaneously via implanted osmotic mini-pumps.

1.7.2.2.2. Transgenic mice

Studies on mice with targeted disruption of the 11β-HSD1 gene showed a relative failure to express glucocorticoid-inducible genes in the liver indicating reduced hepatic glucocorticoid generation in these animals. These mice do not display fasting hypoglycaemia, but fasting glucose levels after high fat feeding are significantly lower than in wild type controls. While they have no difference in baseline expression of G6P and PEPCK upon starvation these key enzymes of hepatic glucose induction fail to be induced (88). The animals also have a less atherogenic lipid profile then wild type animals which is thought to be due to increased expression of hepatic enzymes that are involved in fat catabolism (89) and provided strong evidence for the role of glucocorticoid metabolism underlying metabolic disease.

To explore the role of hepatic 11β-HSD1 in global metabolic homeostasis, mouse models with liver-specific overexpression (101) and knockdown (102) have been developed. Transgenic mice overexpressing 11β-HSD1 in the liver under the hepatocyte-specific apolipoprotein E promoter are hypertensive and dyslipidaemic and develop hepatic steatosis due to increased triglyceride accumulation and impaired lipid clearance. Interestingly, they do not develop steatohepatitis and have only modest levels of insulin resistance when compared to the adipose transgenic 11β-HSD1-AP2 mouse (discussed below).

Liver-specific 11β-HSD1 KO mice have a mild metabolic phenotype, with a slight improvement in glucose tolerance without significant improvement in insulin sensitivity and no changes in hepatic lipid homeostasis, triglyceride accumulation, or serum lipids (102). Although circulating corticosterone levels in these mice were unchanged, adrenal size was increased, suggesting increased HPA axis activation.

A mouse overexpressing 11β-HSD1 within adipocytes, under the control of the aP2 promoter, has allowed the exploration of tissue-specific glucocorticoid activation (103). The transgenic mice had a 15–30% increase in adipose corticosterone concentration (without any

change in serum levels), increased food intake, and a small increase in subcutaneous adipose tissue, and a dramatic increase in visceral adipose tissue mass. Metabolically, animals were hypertensive, hyperglycaemic, hyperinsulinaemic, glucose intolerant, and insulin resistant, with raised serum fatty acids and triglycerides (104). This model therefore implicates 11β-HSD1 as having a key role within adipose tissue in regulating global metabolic homeostasis.

In a comparative study, a mouse overexpressing 11β-HSD2 in adipose tissue caused adipose tissue-specific glucocorticoid deficiency (105). These mice had reduced fat mass and were resistant to weight gain on a high-fat diet. Unexpectedly, the reduction in fat mass was predominantly due to a decrease in the subcutaneous depot, with a less dramatic impact upon the visceral adipose tissue. Globally, the mice had improved glucose tolerance and insulin sensitivity.

1.8. 11β-HSD1 & Uraemic insulin resistance

There is a large body of data linking 11β-HSD1 to metabolic syndrome in laboratory models and in human studies in diabetic and non-diabetic populations. However, the role of 11β-HSD1 in uraemia and its relation to uraemic insulin resistance has not been well described. We aim to assess the expression and activity of hepatic 11β-HSD1 and its relationship to uraemic insulin resistance, hepatic gluconeogenesis, and the effect of CBX as well as novel 11βHSD1 inhibitors on uraemic insulin resistance using rodent and transgenic murine models of uraemia.

On the background presented in the preceding sections, the general aim of the work carried out for this thesis was to investigate the impact of hepatic pre receptor glucocorticoid metabolism upon hepatic glucose homeostasis in the uraemic rat and mouse models and hence hepatic and whole body insulin sensitivity in uraemia. The overall hypothesis was that aberrant hepatic pre receptor glucocorticoid metabolism is implicated in the pathophysiology of the metabolic syndrome and insulin resistance seen in uraemia. Investigations were planned *in*

vivo, to characterise the expression and activity expression of hepatic 11β-HSD1 in normal rodent liver and how this compared with uraemic liver from rodents with either surgical or adenine-induced models of renal failure.

A number of experimental investigations were planned in rodent and murine models of uraemia, with the overall aim being to detect any *in vivo* differences in glucocorticoid metabolism between the normal and uraemic groups and correlating these differences with makers of metabolic phenotype and hepatic glucose production by gluconeogenesis. These studies are described in the following chapters with specific aims and hypotheses detailed in relevant sections.

2. Materials and Methods

2.1. Models of Uraemia

2.1.1. Animals

The rat is the most commonly used animal to create animal models for the study of renal and cardiovascular disease (Table 2.1.) (106). Types include Wistar, Sprague-Dawley, Fawn-hooded, Fisher and Lewis. The advantages of using rat models are that they are inexpensive and have short gestation periods (59-72 days), meaning large sample sizes can be achieved in a short space of time. The disadvantages are predominantly due to the anatomical, physiological and pathological differences between rat and man. However, the chief drawback of rat models is the lack of transgenic models

2.1.1.1. Animal Husbandry

Experiments were performed on male Wistar rats purchased from Harlan Ltd, Bicester, Oxfordshire (Bicester, Oxfordshire OX25 1TP), UK. All animals were kept in accordance with the Animals Scientific Procedures act 1986. Mice were housed 6 to a cage at a fixed temperature of 21±2^{o}C with 40% humidity and 12 h light /dark cycle. All animals had free access to drinking water and rodent chow.

2.1.2. Rodent models of Uraemia

A variety of rodent models of uraemia have been described. The differences in models are due to differences in the establishment of renal failure, whether an acute impairment (via temporary renal artery clamping) or established chronic renal impairment models. While models such as Unilateral Ureteric Obstruction (UUO) are more useful for assessment of tissue response to obstruction, injury and fibrosis, we selected the Subtotal Nephrectomy (SNx) and Adenine-induced diet (Ad) as established models of moderate to severe renal failure.

2.1.2.1. SNx

The 4-week SNx model is the most widely used model of chronic uraemia and displays many of the common characteristics that define the uraemic phenotype. The model leads to

animals that are growth restricted, hypertensive, anaemic, dyslipidaemic, proteinuric, and polyuric with a high fractional excretion of sodium and histological evidence of left ventricular hypertrophy in the heart. In addition, it has also been shown to lead to hypocalcaemia, hyperphosphatemia, and hyperparathyroidism, bioenergetic failure and reduced capillary density and myocardial fibrosis (107).

Uraemia was induced surgically in male Wistar rats using an established two-stage 5/6 nephrectomy procedure for a period of 4 weeks (108). Alternatively, rats were sham operated by removing the renal capsule and replacing the intact kidney. After 10 weeks, carbenoxolone (50mg/kg/day; 2 week) was administered to SNx rats by oral gavage, giving 3 groups. (1) SNx (uraemic, U), (2) SNx plus carbenoxolone (U+CBX), (3) sham operated (sham, S). After 12 weeks, animals were killed and blood was centrifuged to obtain plasma whilst the liver was snap frozen in liquid nitrogen for protein and mRNA analysis.

The SNx procedure established renal failure reliably within two weeks, but severe renal failure was induced within four weeks of uraemia (Table 2.2.). CBX was administered initially for one week with variable results in dynamic physiological testing: the treatment duration was increased to two weeks with reliable and reproducible results at baseline and dynamic testing. Overall food intake and body weight was not different between the groups (Table 2.3).

2.1.2.2. Adenine-induced Uraemia

The rodent adenine diet (Ad) model of CKD is well established (109). All mammals with the exemption of rodents produce adenine as a metabolite of the polyamine pathway. Unlike rodents, in other mammals, adenine is salvaged by adenine phosphoribosyltransferase (APRT). When functional APRT is absent adenine becomes a substrate for xanthine dehydrogenase which oxidises adenine into 2, 8-dihydroxyadenine (DHA) and because DHA has very low solubility it precipitates in the renal tubules. Rodents lack APRT and AD treated

Species	Number of References (No Date Limits)
Rat	1830
Mouse	416
Pig	325
Dog	275
Rabbit	173
Cat	28
Baboon	15
Cattle	15
Guinea pig	12
Hamster	10

Table 2.1. Publications on Animal Models of Renal and Cardiovascular Disease on PubMed (106).

Laboratory parameters	Sham (n=8)	SNx (n=8)	
		2 wk	4 wk
Serum Sodium (mmol/l)	135.9 ± 5.2	136.3±2.3	138.1 ± 3.1
Serum Potasssium(mmol/l)	4.9 ± 0.9	5.1±3.9	4.8 ± 0.5
Serum Urea (mM)	5.5 ± 0.3	24.1±6.9**	30.7 ± 3.6 **
Serum Creatinine (mM)	38.1 ± 0.9	98.5±8**	139.3 ± 10.9 **
Proteinuria (g/l)	0.27 ± 0.04	3.4±1.2 **	3.6 ± 0.2 **

Table 2.2. Serum and urine parameters at two weeks and four weeks after SNX.
**** *P*< 0.001significant versus control (2 or 4 weeks SNx).**

	Sham	SNx (n=8) 2 wk	SNx (n=8) 4 wks
Body weight (g)	307±92	309±60	303±48
Food intake (g)	27 ± 1	25±3	24± 2
Mean HR (pm)	403 ± 2	401±50	416 ±36
MBP (mm Hg)	119 ± 26	125±14	152± 13

Table 2.3. Body weight and food intake at two and four weeks after SNX.

animals demonstrate nephrolithiasis with extensive tubular dilatation, inflammation, necrosis and fibrosis with accompanying renal failure.

Wistar 7 week old rats, which are fed a 0.75% AD over 4 weeks, have been shown to demonstrate progressive macrophage and fibroblast infiltration into renal interstitium from 14 days as well as expression of chemokines and cytokines including Il-1β, Il-6, TNFα, MCP-1, CCR-2, and TGF-β (109). Tubular epithelial cells are physically stimulated by DHA crystals to produce the above cytokines and chemokines resulting in progressive peri-tubular fibrosis. The AD is therefore a model of progressive crystal nephropathy and interstitial fibrosis which is the final common pathway of most human chronic renal failure regardless of the original disease. APRT deficiency is an autosomal recessive disorder in humans who demonstrate DHA urolithiasis and can go on to develop chronic renal failure. We fed rats allocated to experiment groups a 0.75% Adenine diet obtained from Special Diets Service.™ All AD fed rats were otherwise kept in identical conditions as their sham littermates The diet was identical to standard chow (SDS RM1) apart from being pelleted as opposed to expanded and containing Adenine. All food was kept within the expiry date of 3 months. The AD reliably produced impaired renal function as measured by plasma creatinine (Table 2.4.). The AD also produced weight loss reliably but non-significantly (Table 2.5.) and a criticism of the model is the potential confounding effect of weight loss. Against this is the acknowledged positive correlation between increasing weight and insulin resistance, a chronic anorexic/starvation state being hypoinsulinaemic as befitting its physiological role.

Male Wistar rats (7 wk old, eight per group) were fed a high-adenine (0.75%) diet for 2 weeks (Harlan Biotech). Following this, carbenoxolone (50mg/kg/day; 2 week) was administered by oral gavage along with adenine or sham diet giving 4 groups. (1) Ad (uraemic, U), (2) Adenine plus carbenoxolone (Ad+CBX), (3) sham operated (sham, S), (4) Sham plus carbenoxolone (S+CBX). After four weeks on each diet weeks, animals were killed and blood

harvested and centrifuged to obtain plasma whilst liver was snap frozen in liquid nitrogen for protein and mRNA analysis.

2.1.3. Dynamic Physiological testing

A variety of laboratory techniques have been developed to assess insulin secretion and dispersal and glucose homeostasis *in vivo*. A brief critique of the techniques is presented here followed by a description of the techniques chosen in the present study.

2.1.3.1 Measuring fasting glucose and insulin

2.1.3.1.1. Principle

Measurement of fasting glucose and insulin is a simple screening method for detecting alterations in glucose metabolism. Typically, a single blood sample is taken from an unrestrained mouse by cutting off the tip of the tail or via an arterial catheter (110).

There are many commercially available kits for measuring plasma insulin levels, either by radioimmunoassay or by ELISA. Plasma requirements for these assays range from 5- 25 ul. Investigators must be careful not to over-interpret findings from fasting measurements in mice. Fasting measurements in humans are used as a surrogate index of insulin sensitivity. Humans typically fast overnight and morning glucose and insulin concentrations represent a basal 'steady state'. Rats and mice consume food throughout the day and, as such, feeding patterns in mice do not mimic human feeding patterns. It is thus possible that fasting glucose and insulin levels do not represent a basal steady-state in mice.

2.1.3.1.2 Method: Accu-Chek™ glucometer for tail capillary glucose measurement.

Regular tail-prick capillary samples were taken from sedated animals at regular intervals according to dynamic physiological testing using Accu-Chek Aviva ® capillary Glucose measurement kits as per manufacturer's instructions.

Laboratory parameters	Sham	Adenine	
		2weeks	4 weeks
Serum Sodium (mmol/l)	136.5 ± 4	138.5±5	135.7 ± 0.2
Serum Potasssium (mmol/l)	4.4 ± 0.1	5.1±1.2	5.24 ± 0.0 *
Serum Urea (mmol/l)	7.2 ± 0.4	32±12.8	86.3±8.5 **
Serum Creatinine (µmol/l)	39.5± 2	160±24.9	324.5±20 **
Proteinuria (g/24 h)	0.06 ± 0	1.2±.8	3.23 ± 0.3**

Table 2.4. Serum and urine parameters at two weeks and four weeks after AD diet; ** *P*< 0.001significant versus control (2 or 4 weeks AD).

	Sham	Adenine	
		2 weeks	4 weeks
Body weight (g)	325.4 ±4	309.8±5	308.6 ±4
Food intake (g/24 h)	25.03 ± 2.1	22±.9	21.5 ± 3.1
Mean HR (pm)	436±1	425±2	445 ±3
MBP (mm Hg)	122 ± 27	137 ± 25	129 ± 2

Table 2.5. The mean body weight of AD rats was not significantly different compared to sham-operated group despite CBX gavage.

2.1.3.2. Glucose tolerance tests

oral or intra-gastric dosing (OGTT), intraperitoneal injection (IPGTT) or intravenous injection (IVGTT) (111). The results of a GTT are determined by insulin secretion, insulin action, and 'glucose effectiveness'.

The protocol for carrying out a GTT is simple. Following a fast, a glucose load is administered and blood glucose is measured over a span of 2 h. Typically, a blood sample (0.5 ml or less) is taken prior to the glucose load (for baseline measurements) and then at 15- to 30-min intervals following the glucose load for the duration of the experiment.

The standard approach for fasting mice prior to a GTT is an overnight fast (111-113). This is likely a procedural remnant from GTTs performed in humans, which are typically conducted in overnight-fasted subjects (111). The choice of the route of administration depends on a number of variables, including the specific hypothesis being tested and the level of expertise of the personnel performing the tests.

OGTTs represent the most physiological route of entry of glucose. Typically, the glucose load is gavaged directly into the stomach via a gavage catheter or administered with a feeding needle. Mice can also be trained to consume a small volume of glucose solution in a short window of time. Whether administered orally or intragastrically, the clearance of glucose during an OGTT is affected by several factors, including the rate of gastric emptying and the incretin effect, which is the effect seen in enteric versus non-enteric glucose load. If an investigator wishes to circumvent these processes, then an IPGTT or an IVGTT can be performed. We chose the IPGTT to avoid the bias introduced by variations in gastric feeding.

When administering a GTT to humans, a fixed (standard) dose of glucose is given, regardless of the weight of the patient. The standard approach in rats and mice is to base the dose of glucose on the weight of the animal, usually at 1 or 2 g/kg (111,112). This is reasonable as long as the weight and body composition for different cohorts are similar. However, in

models with increased weight, which is common in many diabetic models, the increased body weight is typically due to a higher fat mass, without a proportionately higher lean mass. This is an important consideration, as lean mass (muscle, brain and liver) is the principal site of glucose disposal. If a glucose dose is administered based on total body weight, then the dose given to an obese mouse will be biased by the increase in fat mass. Therefore, the amount of glucose to which the lean tissue is exposed to in an obese mouse will be disproportionately high compared with that in a non-obese mouse with a similar lean mass. Obese mice could be misdiagnosed as being glucose intolerant simply because they receive more glucose for the same lean body mass. Therefore, if body composition data are available, then it is more appropriate to base the dose of glucose for a GTT on the lean body mass. However, obesity or weight gain was not a consideration in our rodent and murine models.

The standard presentation of results from GTTs is a description of blood glucose levels over time after the glucose administration. Generally, a time course of absolute glucose concentrations is presented. This is valid as long as the groups being compared have equivalent fasting glucose levels. When fasting glucose levels differ, as is often the case with diabetic or insulin resistant models, a time course of absolute glucose levels should still be presented along with a calculation of the area under the curve above baseline glucose. Accurate interpretation of a GTT can also benefit greatly from presentation of a time course of insulin levels. This requires sampling of larger blood volumes than those used for the measurement of glucose. Depending on the assay, up to 0.5 ml of blood can be required to measure insulin levels. We chose an initial fasting insulin and glucose sample with an insulin profile over the early (insulin-secretory) phase of the glucose load.

The frequency of sample acquisition was influenced by the sampling method (tail vs arterial catheter, as arterial catheterization would be a terminal procedure in our models).

Typically, samples are obtained at baseline and every 15-30 min following administration of the glucose bolus.

A caveat of the glucose tolerance tests is that it cannot be used to assess insulin action, as glucose tolerance and insulin action are not equivalent.

2.1.3.2.2. Glucose Tolerance test: Method

On day 28 of adenine treatment or four weeks after stage 2 of SNx, after both groups had undergone 14 days of CBX treatment, rats were fasted overnight and injected i.p. with 2 g/kg body weight of 25% dextrose (Sigma, Poole, UK) prepared 24 h beforehand. Blood glucose (tail vein) was measured (Accu-Chek, Roche, UK) at 0, 15, 30, 45, 60, 90 and 120 min and additional blood was collected in a heparinized tube at 0,30 and 45 min. Blood was centrifuged at 16,000 *g* for 15 min and the plasma was stored at -80^{0}C for analysis of plasma insulin concentration.

2.1.3.3. Insulin tolerance tests

2.1.3.3.1. Insulin tolerance tests: Principle

Like GTTs, Insulin Tolerance Tests (ITTs) monitor glucose concentration over time, but in response to a bolus of insulin rather than of glucose. The convention is to conduct ITTs in mice following a short (5- to 6-h) fast. Glucose concentration is monitored every 15 to 30 min for 60 to 90 min following a bolus of insulin administered via intraperitoneal or intravenous injection. The degree to which glucose falls following the insulin bolus is indicative of whole-body insulin action (113-114).

Differences in body weight and composition influence the dose of the insulin bolus (99). An obese mouse (a mouse with increased fat mass) will receive a larger dose of insulin than a non-obese mouse even though the mass of insulin-sensitive tissue (lean mass) might not differ significantly, or at least proportionately, to the difference in total body mass. Thus, normalizing the insulin dose to lean body mass, if such information is available, is a more

accurate means of determining the dose of insulin to be given. However, this was not a consideration for our model; though fat loss was observed in uraemic rats and mice, total weight did not change significantly over the duration of uraemia (maximum four weeks). A longer duration of uraemia has previously been associated with high procedural mortality (unpublished data, own lab). ITTs are typically conducted following short fasts in order to avoid the hypoglycaemia that would likely occur in overnight-fasted animals. As with GTTs, results from ITTs should be presented as a time course of glucose levels. In addition, results can be expressed as the inverse of the area under the curve below baseline glucose. A common method for presenting glucose levels during an ITT is as a percentage of basal glucose. This is a valid means of presenting results if the groups being compared have equivalent fasting glucose levels. However, if fasting glucose differs among groups, interpretation of a relative fall in glucose can lead to an erroneous conclusion. For the same absolute decrease in blood glucose following an insulin bolus, a rodent with higher fasting glucose will exhibit a smaller percentage fall in glucose. Therefore, if blood glucose is expressed only as a percentage of basal, the conclusion would be that the rodent with higher fasting glucose is insulin resistant. Although this might be the case, drawing such a conclusion from the ITT results would be an over-interpretation of the data. It is also important to note that the half-life of insulin is ~10 min in rats and mice (99,100). Therefore, differences in the glucose concentration after the initial fall (i.e. beyond 30 min after the insulin bolus) might not reflect an effect on insulin action. If a particular model exhibits a defect in the counter-regulatory response, this could be misinterpreted as enhanced insulin action. We have therefore taken the initial response to insulin load to indicate insulin action.

2.1.3.3.2. Insulin tolerance test: Method

On day 28 of adenine treatment or 4 weeks after stage 2 of the S Nx, after both groups had undergone 14 days of CBX treatment, rats were fasted overnight and injected i.p. with 2 units/kg body weight of porcine Insulin (Intervet, Milton Keynes, UK) prepared immediately before the procedure. Blood glucose (tail vein) was measured (Accu-Chek, Roche, UK) at 0, 15, 30, 45, 60, 90 and 120 min and additional blood was collected in a heparinized tube before the insulin injection (time 0). These samples were centrifuged at 16,000 *g* for 5 min and the plasma was stored at -80^0 C for analysis of plasma insulin concentration.

2.1.3.4. The intraperitoneal Pyruvate Tolerance Test

2.1.3.4.1. The intraperitoneal Pyruvate Tolerance Test: Principle

The intraperitoneal Pyruvate Tolerance Test (iPTT, 1-2g/kg body weight) in 15 h fasted, awake or sedated mice is a variant of the intra-peritoneal glucose tolerance test (GTT) in which pyruvate is injected instead of glucose (114). The pyruvate bolus elicits a glycaemic response that reflects hepatic gluconeogenesis. Although the method can be useful in cases of severe alterations in hepatic gluconeogenesis, it is highly dependent on the variables that influence the outcome of a glucose tolerance test (GTT), including glucose-stimulated insulin secretion (GSIS) and insulin sensitivity. It is thus always necessary to analyse results from a pyruvate tolerance test in light of data obtained from a GTT, GSIS and ITT.

2.1.3.4.2. The intraperitoneal Pyruvate Tolerance Test: Method

On day 28 of adenine treatment or four weeks after stage 2 of the subtotal nephrectomy, after both groups had undergone 14 days of CBX treatment, rats were fasted overnight and injected intraperitoneally (i.p.) with 2 g/kg body weight of sodium pyruvate (Sigma, Poole, UK) prepared 24 hours beforehand. Blood glucose (tail vein) was measured at 0, 15, 30, 45, 60, 90 and 120 min and additional blood was collected in a heparinized tube at 0, 30 and 45

min. Blood was centrifuged at 16,000 *g* for 15 min and the plasma was stored at -80^0 C for analysis of plasma insulin concentration.

2.1.3.5. Hyperinsulinemic Euglycemic Glucose Clamp

The "gold-standard" in assessing insulin sensitivity is a hyperinsulinaemic-euglycaemic clamp or insulin clamp (100-114). In this procedure, insulin is infused at a constant rate resulting in a drop in blood glucose. To maintain blood glucose at a constant level, exogenous glucose (50% Dextrose) is infused into the venous circulation. The amount of glucose infused to maintain homeostasis is indicative of insulin sensitivity. Following the induction of anaesthesia, a midline incision is made over the neck, and the left common carotid artery and right jugular vein are catheterized. Inserted catheters are flushed with heparinized saline, then exteriorized and secured. Animals are allowed to recover for 4-5 days prior to experiments, with weight gain monitored daily. Only those animals who regain weight to pre-surgery levels are used for experiments. On the day of the experiment, rats are fasted and connected to pumps containing insulin and D50. Baseline glucose is assessed from the arterial line and used a benchmark throughout the experiment (euglycaemia). Following this, insulin is infused at a constant rate into the venous circulation. To match the drop in blood glucose, D50 is infused. If the rate of D50 infusion is greater than the rate of uptake, a rise in glucose will occur. Similarly, if the rate is insufficient to match whole body glucose uptake, a drop will occur. Titration of glucose continues until stable glucose readings are achieved. Glucose levels and glucose infusion rates during this stable period are recorded and reported. Results provide an index of whole body insulin sensitivity. It can be further enhanced by the use of radioactive tracers that can determine tissue specific insulin-stimulated glucose uptake as well as whole body glucose turnover and contribution of hepatic gluconeogenesis indirectly.

Logistic considerations precluded the use of this method in the current study.

2.1.4 11β-HSD1 $^{-/-}$ mice

We used an established model of 11b-Hydroxysteroid dehydrogenase type 1 knockout mice which demonstrate attenuated glucocorticoid-inducible responses and are resistant to hyperglycaemia on obesity or stress (88, 89,115).

2.1.4.1. Generation, transfer and breeding of 11β-HSD1 $^{-/-}$ mice

Mice bearing targeted disruption of the 11b-HSD-1 gene were developed by our collaborators in Edinburgh and breeding pairs transferred to the Biological Sciences Unit, at our institution.

Briefly, the replacement vector was based on plasmid pBS-βKnpA16 containing the neomycin resistance gene flanked by the human β-actin promoter and the simian virus 40 polyadenylation signal sequence. (88, 89). Cells from the targeted ES cell clone were injected into C57BL/6J blastocysts and transferred into C57BL/CBA foster mothers. In the original reports, chimeras were bred to MF1 females, and the progeny was genotyped by Southern analysis of BamHI-digested DNA (115). The targeted 11β-HSD-1 transgene was re-derived onto the C57BL/6J strain by embryo transfer and then backcrossed with C57BL/6J mice for 10 generations before the current studies (115). Two breeding pairs of 11β-HSD1 $^{-/-}$ mice were transported to our institution, back-crossed into C57BL/6J, re-genotyped by PCR and northern blot (performed by Ms Man, Department of molecular endocrinology, University of Edinburgh, Edinburgh) and then used in accordance with UK home office regulations.

Male progeny of mice with targeted global disruption of the 11β-HSD1$^{-/-}$ gene congenic on C57BL/6J were derived as described previously (103). Controls were wild type (WT) C57BL/6J, age-matched males. Adult 8-wk old WT and 11β-HSD1$^{-/-}$ (six to eight per group) were fed a control or 0.25% AD for 4 wk. Mice were fasted overnight and killed at approximately 9:00 am, within 1 min of disturbing each cage, or used in dynamic physiological studies.

2.1.4.2. 11β-HSD1 -/- murine model of adenine-induced Uraemia

Male progeny of mice with targeted global disruption of the 11βHSD1−/− gene congenic on C57BL/6J were derived as described. Controls were WT C57BL/6J, age-matched males. Adult 8-wk old WT and 11βHSD1$^{-/-}$ (six to eight per group) were fed a control or 0.25% AD for 4 wk. This diet was based on previous reports in the literature on adenine-induced uraemia in mice.

Mice were fasted overnight and killed at approximately 9:00 am within 1 min of disturbing each cage, or used in dynamic physiological studies.

	No. of groups	N	Excluded*	N
SNx IPGTT	4	32	3	29
SNxIPITT	4	32	2	30
SNx IPPTT	4	32	2	30
Ad IPGTT	4	32	4	28
Ad IPITT	4	32	3	29
Ad IPPTT	4	32	2	30
Murine IPGTT	4	32	3	29
Murine IPITT	4	32	3	29
Murine:UE2316	3	32	1	31

Table.2.6. Number of groups per experimental model, total number of animals used, and excluded in each group.

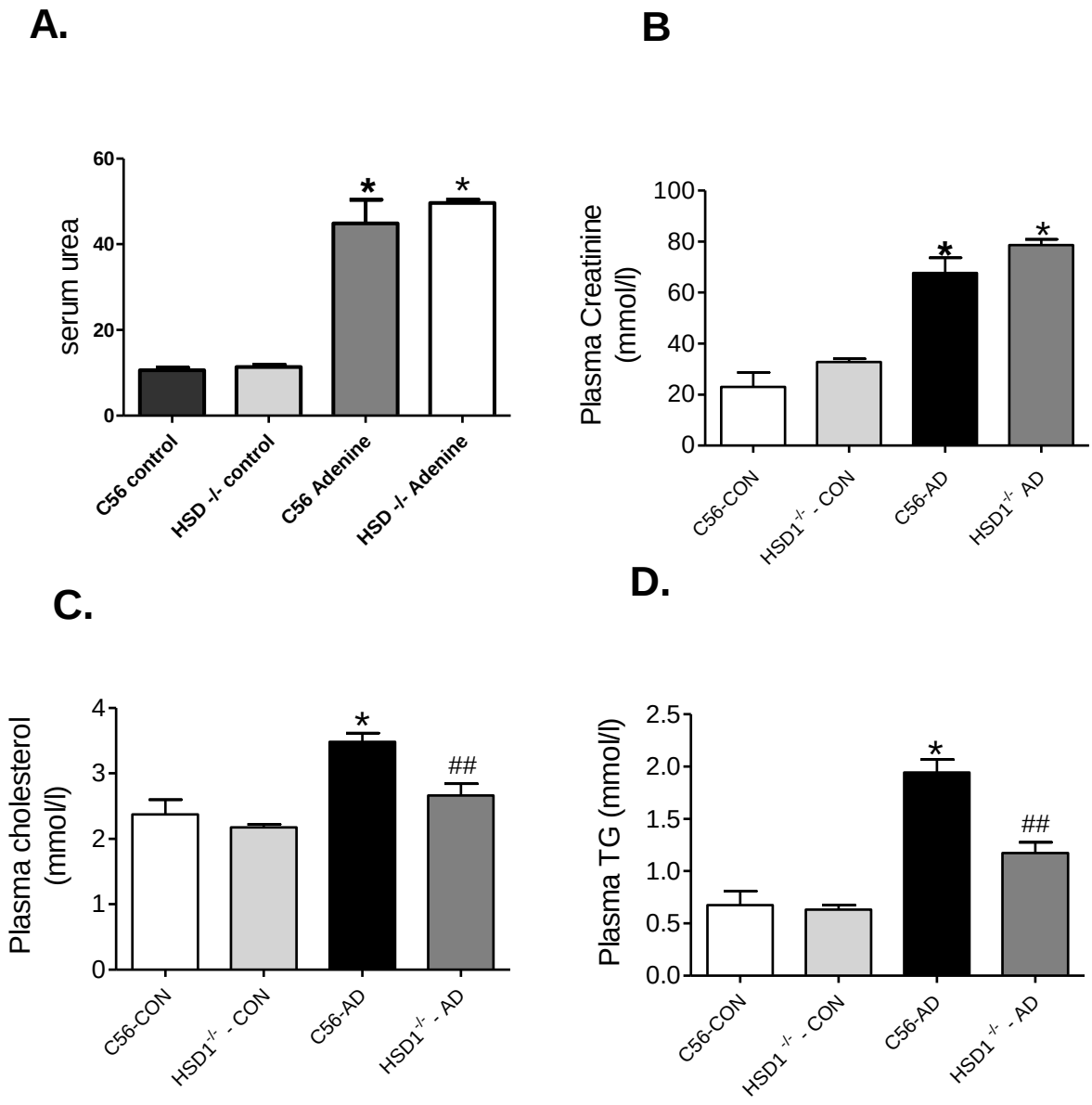

Fig. 2.1. A, B, C. D. Serum Parameters of Adenine-induced uraemia and control diet fed C57BL/6J and 11β-HSD1$^{-/-}$ mice. A: serum urea, B, plasma creatinine, C, Cholesterol and D. Triglycerides. Renal dysfunction was determined in adenine-fed (AD) mice (8 per group) by measurements of serum levels of creatinine, urea, sodium and potassium. Data are expressed as mean ± SEM. *P<0.05 vs. control, ##P<0.05 vs. c56 AD

2.2.5 Quantification of Renal Injury

Plasma sodium, potassium urea, creatinine and cholesterol were measured commercially using IDEXX laboratories.

2.3. Corticosterone measurements

Corticosterone concentrations in the media were measured by using a commercial EIA corticosterone kit (Cayman Chemicals, Cambridge Bioscience Ltd, Cambridge, UK). This assay is based on the competition between corticosterone and a corticosterone - acetylcholinesterase (AChE) conjugate (corticosterone tracer) for a limited number of corticosterone -specific rabbit antiserum binding sites. Because the concentration of the corticosterone tracer is held constant while the concentration of corticosterone varies, the amount of Corticosterone Tracer that is able to bind to the rabbit antiserum will be inversely proportional to the concentration of corticosterone in the well. This rabbit antiserum-corticosterone (either free or tracer) complex binds to the mouse monoclonal anti-rabbit IgG that has been previously attached to the well. The plate is washed to remove any unbound reagents and then Ellman's Reagent (which contains the substrate to AChE) is added to the well. The product of this enzymatic reaction has a distinct yellow colour and absorbs strongly at 412 nm. The intensity of this colour, determined spectrophotometrically, is proportional to the amount of corticosterone tracer bound to the well, which is inversely proportional to the amount of free corticosterone present in the well during the incubation. The assay was performed according to the procedure described in the kit (116). Media samples were diluted 1:500 for the values to fall within the standard curve of corticosterone (20-20000 pg/ml).

2.4.1 Colourimetric assay for Non-Esterified Fatty Acids

A commercially available ELISA (Cambridge Biosciences, Cambridge, UK) was used for NEFA assay in tissue homogenate and serum. Cell Biolabs' Free Fatty Acid Assay Kit measures non -esterified fatty acids (NEFA) in serum and plasma by a coupled enzymatic reaction system (ACS-ACOD Method). First, Acyl CoA Synthetase (ACS) catalyzes fatty acid acylation of coenzyme A. Next, the acyl-CoA product is oxidized by Acyl CoA Oxidase (ACOD), producing hydrogen peroxide which reacts with the kit's colourimetric probe (absorbance maxima of 570 nm). The Free Fatty Acid Assay Kit is a simple, colourimetric assay that quantitatively measures the free fatty acid concentration (non-esterified) in various samples using a 96-well microtiter plate format. The kit contains a palmitic acid standard and has a detection sensitivity limit of ~15 μM (117).

2.4.2. ELISA for IL-6, IL1β, & TNFα

R&D systems Rat IL-1beta ELISA kit, RLB00, R&D systems Rat IL-6 ELISA kit, and R&D systems Rat TNFα ELISA kit RTA00 were used according to manufacturer's instructions. In brief, the Quantikine Rat cytokine Immunoassay is a 4.5 hour solid phase ELISA designed to measure rat cytokine levels in cell culture supernates, serum, and plasma. It contains E. coli-expressed recombinant rat TNF-α, IL1β or IL6, and antibodies raised against the recombinant factor. This immunoassay has been shown to quantitate the recombinant rat cytokines accurately. Results obtained using natural rat cytokine standard showed dose response curves that were parallel to the standard curves obtained using the recombinant kit standards.

Before use, all reagents and samples are brought to room temperature before use. All samples, standards, and controls were assayed in triplicate.50 μL of Standard, Control, or sample was then added to each well of a 96 well plate. The plate was covered with a plate sealer, and

incubated at room temperature for 2 hours. Each well was aspirated and washed, repeating the process 4 times for a total of 5 washes. 100 µL of Conjugate was then added to each well. The microplate was then covered with a new plate sealer, and incubated at room temperature for 2 hours. This was then aspirated and washed five times, then 100 µL Substrate Solution added to each well. This was then incubated at room temperature for 30 minutes while protecting from light, then 100 µL of Stop Solution to each well added. The resultant intensity was read at 450 nm within 30 minutes, with wavelength correction set to 540 nm or 570 nm .

2.5. RNA extraction and PCR.

2.5.1. Isolation of cellular RNA

RNA is extracted from cultured cell monolayers or tissue explants using a single step procedure developed by Chomczynski (118). This is achieved by homogenizing tissue or lysis of cultured cells in TRI (Sigma-Aldrich) reagent. This solution contains phenol and guanidine thiocyanate, and immediately and effectively inhibits RNase activity. The addition of chloroform followed by centrifugation results in the formation of three phases. RNA is present exclusively in the aqueous phase, and is subsequently precipitated with isopropanol.

2.5.2. Method

For cultured cell monolayers: media was removed and cells washed in PBS before 1mL of TRI reagent was added per well (for a 12-well plate) and incubated at room temperature for 5 min using a mechanical homogeniser. For tissue ~20mg of tissue was homogenized in 1.5mL of TRI reagent under liquid nitrogen with mortar and pestle, having being stored according to instructions in RNAlater ICE (LifeTechnologies, UK), then homogenised using a mechanical ultrasonic homogeniser at 18,000 Hz. For both cultured cell monolayers and tissue explants, cell lysates in TRI reagent were transferred to eppendorf ® tubes. 200µL of chloroform was added and tubes were shaken vigorously for 30 s, before incubation at room temperature for 15 min. The mixture was centrifuged at 10,000 *g* for 15 min at 4˚C.

The Aqeuous phase solution containing the RNA was then purified used with RNAeasy mini Kit (Qiagen, Manchester, UK). The aqueous solution was mixed with buffer RLT (with β-mercaptoethanol for tissue homogenates). The resulting solution was then purified and RNA isolated in 1.5 or 2 ml eppendorf ® tubes and stored at -80^{0}C. Isolated RNA was further purified by removal of any contaminating genomic DNA by incubation at 30°C with DNase I enzyme (Ambion, Warrington, UK).

2.5.3. mRNA detection and quantification

The quantity of RNA was measured using NanoDrop ND-1000 UV-Vis Spectrophotometer (Thermo Scientific, Fisher Scientific, Loughborough, UK). The absorbance of 2µl of RNA at 260nm and 280nm was determined where 1 OD_{260} = 40µg/mL of RNA and the OD_{260}/OD_{280} ratio indicates the RNA purity. Only OD_{260}/OD_{280} ratios in the range of 1.8-2 were used. All measurements were made with respect to a blank consisting of the nuclease free water in which the RNA was suspended.

In addition, the integrity of the RNA was assessed by electrophoresis on a 1% agarose gel containing 0.15µg/mL ethidium bromide. The RNA separates down the gel according to its molecular mass and the resultant bands were visualized under UV light. Intact RNA shows two sharp bands corresponding to the highly abundant 28S and 18S rRNA.

2.5.4. Reverse transcription: Principles

Reverse transcription (RT) is the process of converting single stranded RNA to complementary DNA (cDNA), using RNA-dependent DNA polymerase. Initially the extracted RNA is heated to denature the secondary structure which allows the random hexamers to anneal to the RNA template. The reverse transcription process is initiated by increasing the temperature further, allowing the RNA-bound primers to be extended generating a

complementary DNA copy of the RNA template. Lastly, the reaction is heated to a high temperature to inactivate the enzyme and terminate the reaction.

2.5.5. RT: method

All RT reactions were carried out using Applied Biosystems Reverse Transcription Kit (Applied Biosystems, Warrington, UK). The reagents listed in the table below were combined in an eppendorf tube to generate a 2x RT master mix.

1µg of RNA was diluted with nuclease free water to a volume of 10µl before 10µl of 2x RT master mix was added giving a final volume of 20µl. Samples were loaded onto a thermal cycler (Applied Biosystems, Warrington, UK) and incubated at 25°C for 10 min followed by 48°C for 30 min and finally 95°C for 5 min to terminate the reaction.

Component	Vol per sample (ml)
10x RT Buffer	2
25x dNTP mix (100mM)	0.8
10x Random Hexemers	2
Reverse Transcriptase	1
RNase inhibitor	1
Nuclease-free H_2O	3.2
TOTAL VOLUME	10

Table 2.7. Components of RT buffer.

2.5.6. Real-time PCR: principles

Real-time PCR or relative quantitative PCR is a technique used to monitor the progress of a PCR reaction in real-time. Using oligonucleotide primers that are complementary to the 5' and 3' ends of a region of interest, cDNA can be amplified by PCR. The presence of an

oligonucleotide probe complementary to a sequence downstream of one of the primers allows quantification of the target transcript by fluorescence (Figure 2.2.). This probe is chemically synthesized with a fluorescent reporter dye at the 5' end and a quencher dye at the 3' end. Since the quencher dye is in close proximity to the fluorescent reporter dye it reduces the fluorescence emitted by the latter through a process called Fluorescence Resonance Energy Transfer (FRET). During the primer elongation step of the PCR reaction the probe bound downstream from one of the primers is cleaved due to the 5'- 3' exonuclease activity of taq DNA polymerase. Removal of the probe allows primer extension to continue and amplification of the sequence of interest but it does not inhibit the PCR process. Cleavage of the probe separates the quencher dye from the reporter dye, increasing the fluorescence emitted by the latter (Fig 2.2). Fluorescence intensity is proportional to the amount of PCR product produced. The point at which the target sequence is detected is called the cycle threshold (Ct). This threshold is set to the exponential phase of the amplification for the most accurate reading. The higher the target sequence copy number within the original cDNA sample the lower the cycle number at which fluorescence is observed. Real-time PCR is a relative measure of gene expression, therefore, the Ct of the target genes is compared to the Ct of a house keeping gene with constant expression levels. This is calculated by subtracting the Ct of the house keeping gene from the Ct of the target gene, the resultant value is known as the ΔCt. The greater the ΔCt, the greater the change in gene expression due to treatment.

2.5.7. RTPCR: method

Real-time PCR was carried out using Applied Biosystems reagents and expression assays unless otherwise stated. Target gene expression was normalised against the housekeeping gene and these measurements were carried out in separate wells from target gene expression measurements (singleplex). The 18s rRNA standard was used as housekeeping gene. All reactions were carried out in micro-tubes for Corbett Rotor Gene. For the 18S house

keeping gene, the following components were combined per well: 10µl of 2x MasterMix, 18S forward and reverse primers and vic labelled probe (final concentration 25nM each), 100ng of cDNA and nuclease free water to a final volume of 20µl. For the gene of interest, the following components were combined per well: 10µl of 2x MasterMix, 1µl of 20x expression assay, 100ng of cDNA and nuclease free water to a total volume of 20µl. Plates were sealed with clear adhesive film (Applied Biosystems, Warrington, UK) and run on a realtime PCR system (Corbett Rotor Gene 6000, Corbett Research, UK). Data was expressed and fold change was calculated using the delta-ct and comparative quantification methods.

2.6. Protein assay

Cells were washed with ice-cold phosphate-buffered saline (PBS) and lysed in ice-cold modified RIPA lysis buffer (B 50mM Tris HCl, pH 7.5, 150 nM NaCl, 50 mM NaF, 0.5% deoxycholic acid, 1% NP-40, 1mM sodium orthovanadate, 0.1% SDS) . Sodium Flouride (NaF) and sodium orthovanadate were used as inhibitor for protein phosposeryl-threonyl and phophotyrosyl phosphatases, respectively. Insoluble material was removed by centrifugation at 16,000 g for 15 min at 4^0C. The protein concentrations were measured using a bicinchoninic acid assay (Fisher Scientific) following the manufacturer's instructions. Lysates were matched for protein, loaded with Lithium dodecyl sulphate (LDS loading buffer, Invitrogen, UK) and separated by discontinuous sodium dodecyl sulphate-polyacrylamide gel electrophoresis (SDS-PAGE) and transferred to a polyvinylidene difluoride (PVDF) microporous membrane

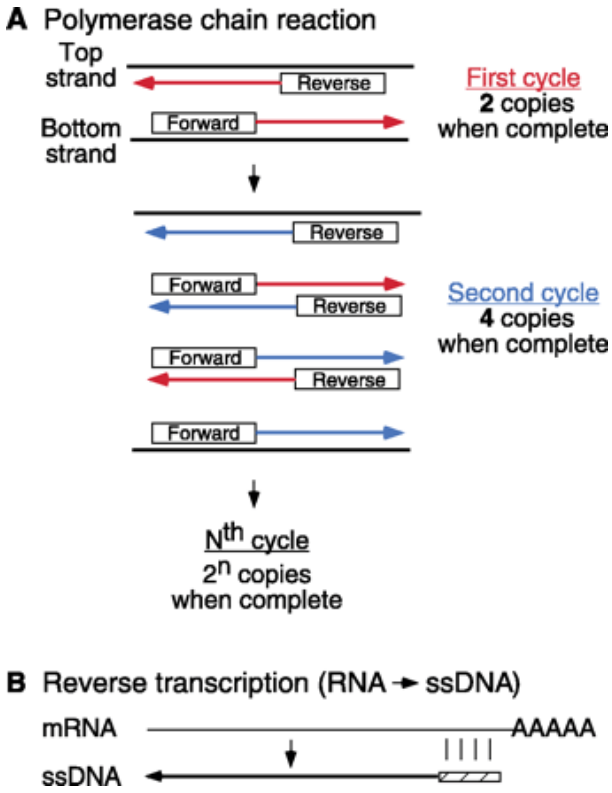

Fig 2.2. Enzyme reactions that make real-time PCR possible (119).

A: PCR is depicted. High temperatures are used to "melt" double-stranded (ds) DNA into its top and bottom strands. This mixture is cooled in the presence of sequence-specific primers (denoted as forward and reverse) that anneal to their targets, and an optimal temperature is then applied to allow elongation of complementary DNA (arrows) by the action of DNA polymerase to complete a cycle. This is repeated numerous times, and, if no reagents are limiting, 2n copies of the desired DNA fragment can be obtained.

B: because DNA polymerase does not utilize RNA as a template, the conversion of RNA to DNA can be achieved using the enzyme reverse transcriptase. ssDNA, single-stranded DNA.

(Millipore, Bedford, MA). The LDS maintains polypeptides in a denatured state once the protein sample has been heated at 100^0C for 5 min. SDS is an anionic surfactant and a detergent. The latter property is due to the amphiphilic nature of the molecule imparted by its tail containing 12 carbon atoms attached to a sulphate group. It denatures the protein by disrupting the non-covalent bonds (all intra- and intermolecular protein interactions). In addition, it also binds to the amino acids thereby, conferring a negative charge to the proteins that is significantly greater than the original charge of the protein a, and an identical charge: mass ratio. The resultant electrostatic repulsion causes unfolding of the proteins. The denatured proteins act like long rods instead of having a complex tertiary structure, the rate at which the resulting SDS coated proteins migrate in the polyacrylamide gel is relative only to its size and not its charge or shape. The membranes were blocked overnight in cold room (4^0C) in blocking buffer before being probed with the primary antibody. The primary antibodies were detected using horseradish peroxidase conjugated IgG (Santa Crux Biotechnology, Autogen Bioclear, Calne, UK) and visualised with enhanced chemiluminescence (ECL) system (GE Healthcare, Buchinghamshire, UK). All the primary antibodies were obtained from Cell Signalling Technology. The densitometric quantifications of relative band densities were performed using NIH Image J software.

2.7.1. Reversed phase extraction of steroids.

Whole rodent livers were snap-frozen and stored at −80 °C, then weighed and homogenized in RIPA buffer using a rotary-blade homogenizer. The homogenate was deproteinated immediately with 6% perchloric acid (1:1), then centrifuged at 10,000 ×*g* for 15 min. The supernatant was then collected separately and neutralized 1:1 with 1 M potassium hydroxide. The supernatant after centrifugation (10,000×*g*,10 min) was then passed through a Chromabond C18 column (Macherey-Nagel) using (i) two times 3 mL methanol, (ii)followed

by 3mL of H2O, (iii) 3 mL 50 mM HCl, (iv) 6 mL homogenate, (v) 3 mL 50mM HCl, and (vi) 13 mL H_2O. The steroids were collected using 6 mL 80% methanol (vol/vol), evaporated to dryness using a vacuum drier and reconstituted using 200 μL 80% methanol.

2.7.2. HPLC

Reconstituted hepatic steroids were quantified by HPLC using an apparatus consisting of a PU-2089 Quaternary Low Pressure Gradient Pump and MD-2010 Photometric Diode Array UV/Vis Detector (195–650 nm) from Jasco Instruments Ltd. The pump was connected to an AS-2055 Autosampler. Peak area was calculated by EZChrome Elite software (Agilent Technologies UK Ltd). Separations were performed using a reversed-phase ACE C18 column (0.46 cm × 15 cm; 5 μm-particle size) from Hichrom Ltd. The column was equilibrated with a solvent mixture consisting of 70:30 water: acetonitrile (CH_3CN). After injection, the solvent mix was adjusted so that at 7 min, the mixture was 60:40 water: CH_3CN.

Between 7 and 9 min the gradient was increased further so that 0:100 water: CH_3CN was reached. Between 9 and 10 min the solvent mix was maintained at 0:100 water: CH_3CN. Between 10 and 11 min the original solvent mix of 70:30 water: CH3CN was reapplied. UV chromatograms for 220 and 240 nm were analyzed and a 240:220 ratio was obtained and compared against steroid standard data. The AUC was analyzed on Prism 5.0 software to quantify unknown steroids against calibration curves. HPLC was performed by Dr Steve Harwood.

2.8.1. 11β-HSD1 activity measurement

11β-HSD1“reductase”activity was measured using methods as previously described by Hu *et al* (120). Snap-frozen rodent livers from the experimental groups were lysed with RIPA buffer, then treated with 1% Triton X-100 in assay buffer containing 100 mM NaCl, 1 mM EGTA, 1 mM EDTA, 1 mM MgCl 2, 250 mM sucrose, and 20 mM Tris ·HCl. Enzyme assays

were performed using 50 mg sample protein incubated for 1 h at 37 °C in 600 μL of assay buffer containing NADPH (500μM, Sigma Aldrich) and 11-dehydrocorticosterone (2,000 nM, Sigma Aldrich). Immediately following incubation, the samples were placed in a boiling water bath for 5 min. 11β-HSD1oxoreductase activity was then assessed by measuring corticosterone production using a corticosterone EIA kit, and enzyme activity was expressed in units of pg of corticosterone produced per milligram of protein per minute activity assay.

2.9 Specific 11β-HSD1 inhibitor

The specific 11βHSD1 inhibitor UE2316 is developed and patented by the University of Edinburgh. UE2316 has been shown to reduce post-myocardial infarction injury size after acute administration (122). To ensure delivery, subcutaneous mini-pumps were implanted in C5BL6 mice receiving a sham or AD and UE2316 or vehicle was infused subcutaneously.

The 2-wk adenine-fed rats were administered UE2316 (20 mg·kg−1·d−1) or vehicle (50:50 DMSO/PEG-400) equivalent for 2 wk to create three groups [(i) CON + vehicle, (ii) Ad + vehicle, and (iii) Ad + UE2316].

3. Characterization of hepatic gluconeogenesis, lipogenesis and 11β-HSD1 expression, content and activity in uraemic rodent liver and response to treatment with CBX.

3.1. Introduction

We investigated the possibility that 11β-HSD1 mediates abnormal elevation of gluconeogenesis and lipogenesis in uraemia, using two experimental rodent models with entirely distinct mechanisms of development of chronic renal failure. To investigate a potential causal role for 11βHSD1 in uraemia-induced insulin resistance, sham and uraemic rats were administered carbenoxolone (CBX), a derivative of glycyrrhetinic acid and a potent inhibitor of 11β-HSD1 activity which also lowers 11β-HSD1 mRNA and protein levels in rodents.

3.2. Rodent models

3.2.1. SNx

Uraemia was induced surgically in male Wistar rats (Charles River, London, UK) using an established two-stage Subtotal nephrectomy (SNx) procedure for a period of 4 weeks (43). Alternatively, rats were sham operated by removing the renal capsule and replacing the intact kidney. After 2 weeks, carbenoxolone (CBX, 50mg/kg/day; 2 weeks) or vehicle was administered to SNx rats by oral gavage, giving 4 groups. (1) SNx, (2) SNx plus carbenoxolone (SNx+CBX), (3) sham operated (sham) and (4) sham operated plus carbenoxolone (sham+CBX). After 4 weeks, animals were killed between 8.00 and 10.00, while minimizing animal handling and stimulation, blood obtained immediately via cardiac puncture and centrifuged (1600 *g*, 10 min) to obtain plasma whilst liver was snap frozen in liquid nitrogen for protein and mRNA analysis. Immunoblots in Fig 3.24 were performed by Dr P Caton.

3.2.2. Adenine-induced uraemia

Alternatively, uraemia was induced using dietary manipulation. Male Wistar rats were fed a high-adenine (0.75%) diet for 2 weeks (Lillico Biotechnology, Surrey, UK). Following this, carbenoxolone (50mg/kg/day; 2 week) or vehicle was administered by oral gavage along with adenine or sham diet giving 4 groups. (1) Adenine (Ad), (2) Ad plus CBX (Ad+CBX), (3) sham operated (sham), (4) sham plus carbenoxolone (sham+CBX). After four weeks on each

diet weeks, animals were killed between 08.00 and 10.00. Taking care to minimize stimulation, blood was obtained immediately via cardiac puncture and centrifuged to obtain plasma (1600 *g*, 10 min) whilst liver was snap frozen in liquid nitrogen for protein and mRNA analysis. Data for sham + CBX was statistically insignificant from the Sham groups in both the models and has not been reported in this study, with the exception of IPITT and IPGTT data.

3.3. Markers of uraemia

Plasma and urine levels of urea, creatinine, Na+ and K+ along with urinary protein were measured to determine levels of renal dysfunction (IDEXX Laboratories, Horsham, West Sussex, UK).

Serum creatinine was elevated 3.6 fold in SNx and 8.1 fold in Ad rats, while serum urea was elevated 5.5 fold and 11.8 fold respectively (Table.3.1). Further markers of chronic renal injury are shown in Table 3.1. Body weights, mean food intake and average heart rate were not significantly different between the uraemic and sham groups. Mean blood pressure, though numerically higher in CBX treated groups but were not significantly different because of wide variability (Table 3.2).

Laboratory parameters	Sham	SNx	Sham+CBX	SNx+CBX
Serum Sodium (mmol/l)	135.9 ± 5.27	136.1 ± 3.15	135.1 ± 2.6	138.4 ± 2.2
Serum Potassium (mmol/l)	4.9 ± 0.94	4.8 ± 0.50	4.38 ± 0.7	4.6 ± 0.2
Serum Urea (mmol/l)	5.5 ± 0.3	30.7 ± 3.69 *	8.72 ± 0.4	28.5 ± 1.44 *
Serum Creatinine (umol/l)	38.1 ± 0.97	139.3 ± 10.91 *	41.85 ± 2.03	133.01 ± 6.5 *
Proteinuria (g/24 h)	0.27 ± 0.04	3.6 ± 0.26 *	0.21 ± 0.36	3.24 ± 0.52 *
Laboratory parameters	**Sham**	**Adenine**	**Sham+CBX**	**Adenine +CBX**
Serum Sodium (mmol/l)	136.53 ± 4.46	135.7 ± 0.207	139.5 ± 1.4	140.94 ± 1.2
Serum Potassium (mmol/l)	4.46 ± 0.15	5.24 ± 0.098 *	4.75 ± 0.21	5.7 ± 0.1 *
Serum Urea (mmol/l)	7.26 ± 0.42	86.38±8.508 *	6.31 ± 0.68	92.06 ± 3.95 *
Serum Creatinine (umol/l)	39.58± 2.082	324.5±20.37 *	37.48 ± 0.65	314.2 ± 18.28 *
Proteinuria (g/24 h)	0.069 ± 0.03	3.23 ± 0.32 *	0.024 ± 0.05	3.68 ± 0.74 *

Table 3.1. Serum Markers of Renal Failure. Renal dysfunction was determined in SNx and Ad rats (8 per group) by measurements of serum levels of creatinine, urea, sodium and potassium and urine levels of protein at 4 weeks. Data are expressed as mean ±

	Sham	SNx	Sham+ CBX	SNx+ CBX
Body weight (g)	307.1±92.6	303.7±48.34	313.1 ± 19.62	302.1 ± 8.42
Food intake (g/24 h)	27.12 ± 1.6	24.7 ± 2.2	26.82 ± 1.43	24.64 ± 2.61
Mean HR (bpm)	403.8 ± 23.17	416.3 ±36.09	415.0 ± 26.30	423.8 ± 38.20
MBP (mm Hg)	112.0 ± 38.13	135.5 ± 12.01	119.7 ± 26.44	152.0 ± 13.87
	Sham	Adenine	Sham+ CBX	Adenine+CBX
Body weight (g)	325.4 ±40.99	308.6 ±40.99	312.6 ±10.67	299.7 ± 8.313
Food intake (g/24 h)	25.03 ± 2.1	21.5 ± 3.1	23.49 ± 2.54	20.51 ± 4.49
Mean HR (bpm)	436.5± 14.25	445.3 ±36.09	434.4 ± 16.85	440.6± 21.40
MBP (mm Hg)	122.0 ± 27.91	147.9 ± 25.51	129.5 ± 28.9	151.2 ± 15.92

Table 3.2. Measurements of body weight (g), Food Intake (g/24 h), heart rate (bpm) and blood pressure (mmHg) in experimental models of uraemia (8 per group) was measured on day 26 and 27 of treatment. Data are expressed as mean ± SEM.

3.4. Hepatic 11β-HSD1 is elevated in CKD

Hepatic 11β-HSD1 mRNA and protein levels were significantly elevated in SNx (Fig. 3.1, *A* and 1*B*) and Ad rats (Fig. 3.1, C and D) compared to sham animals. Similarly, intra-hepatic 11β-HSD1 activity was also markedly elevated in SNx and Ad (Fig. 3.2.1 and 3.2.2), as was hepatic corticosterone levels (3.3.A. and 3.3.B) when compared to sham animals.

However, consistent with the notion that 11β-HSD1 determines tissue-specific 'intracrine' glucocorticoid levels this occurred in the absence of elevated systemic serum glucocorticoid levels (Fig. 3.4.A. and 3.4.B.).

Administration of CBX (50 mg/kg/day; 2 weeks) normalized hepatic 11β-HSD1 mRNA and protein levels, suppressed 11β-HSD1 reductase activity and lowered hepatic corticosterone levels in SNx and Ad rats. In contrast, CBX had no effect on serum glucocorticoid levels, demonstrating that CBX selectively influences intra-hepatic glucocorticoid levels. Similar to observations in liver, white adipose tissue levels of 11β-HSD1 mRNA and protein were increased in uraemia, an effect that was reversed by CBX (Fig. 3.5). In contrast, 11β-HSD1 mRNA and protein levels in skeletal muscle were unchanged across all four experimental groups (Fig. 3.6).

Consistent with recent evidence demonstrating induction of 11β-HSD1 transcription by pro-inflammatory cytokines, serum levels of IL-1β TNF-α and IL-6 were elevated in the chronic-phase of SNx and adenine-induced uraemia (Fig. 3.7), but were unaffected by CBX, suggesting a possible uraemia-dependent mechanism upstream of 11β-HSD1 induction and hepatic glucocorticoid metabolism, involving elevated pro-inflammatory cytokine levels.

A

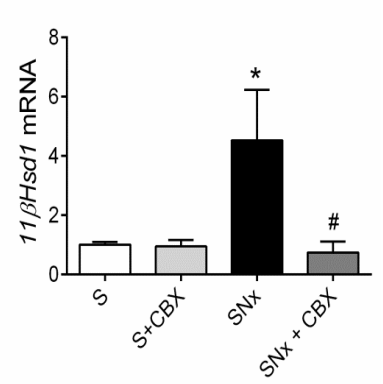

B

C

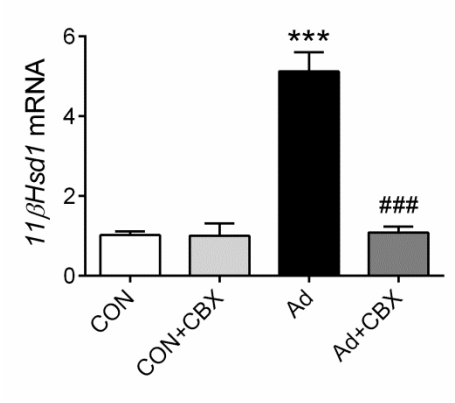

D

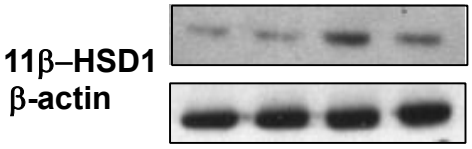

Fig 3.1 Hepatic 11β-HSD1 mRNA and protein are elevated in SNx (3.1 A, B) and Ad (3.1 C, D) rats. Data are expressed as mean ± SEM (8/group). Statistically significant differences between sham/control and Ad or SNx are indicated by * *P*<0.05, * *P<0.01*. Statistically significant effects of CBX treatment are indicated by # *P*<0.05, ### *P<0.01*.**

Fig 3.2.A.

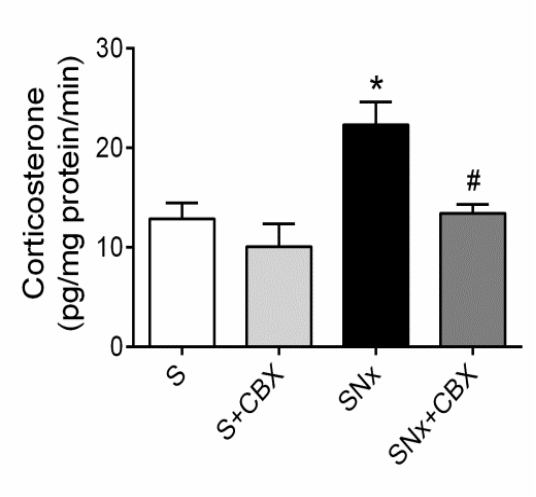

Fig 3.2.B.

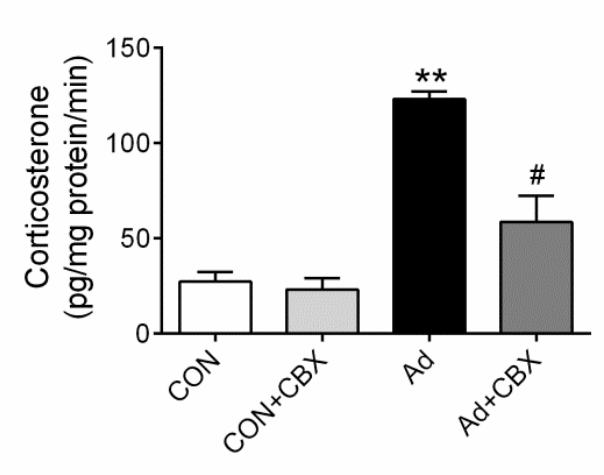

Fig 3.2. Hepatic corticosterone production (pg/min/mg liver protein), measured in hepatocyte homogenate in SNx (3.2.A. and Ad (3.2.B.) models reveal increased enzyme activity in Uraemic animals. This rise in activity is attenuated by two weeks of CBX gavage at 50 mg/kg /day. Data are expressed as mean ± SEM (8/group). Statistically significant differences between sham/control and Ad or SNx are indicated by * *P*<0.05, ** *P<0.01.* Statistically significant effects of CBX treatment are indicated by # *P*<0.05.

Fig 3.3.A.

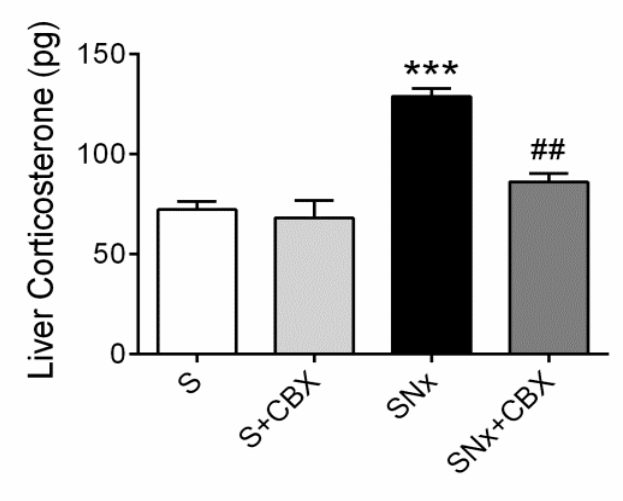

Fig 3.3.B.

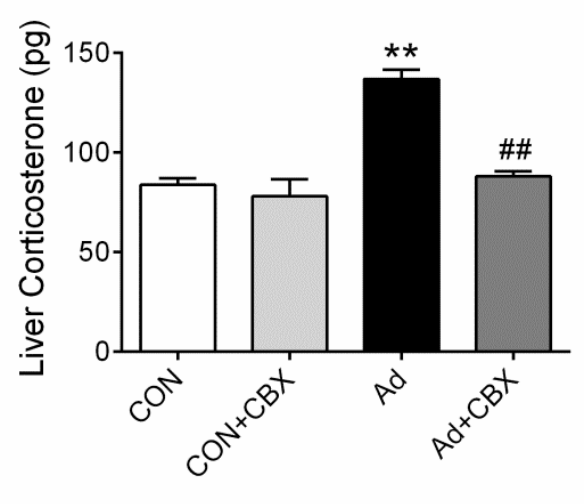

Fig 3.3. Hepatic corticosterone levels measured in hepatocyte homogenate in SNx (3.3.A. and Ad (3.3.B.) models reveal increased enzyme activity in Uraemic animals. This rise in activity is attenuated by two weeks of CBX gavage at 50 mg/kg /day. Data are expressed as mean ± SEM (8/group). Statistically significant differences between sham/control and Ad or SNx are indicated by * *P*<0.05. Statistically significant effects of CBX treatment are indicated by # *P*<0.05.

Fig 3.4.A.

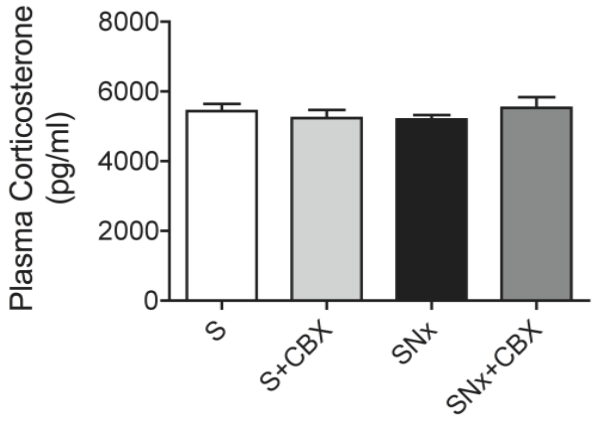

Fig 3.4.B.

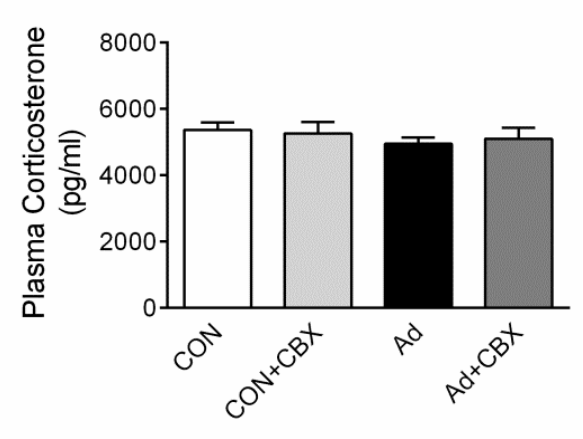

Fig 3.4. Circulating (plasma) corticosterone levels remain unchanged in SNx (3.4.A. and Ad (3.4.B.) Data are expressed as mean ± SEM (8/group).

Fig 3.5.A

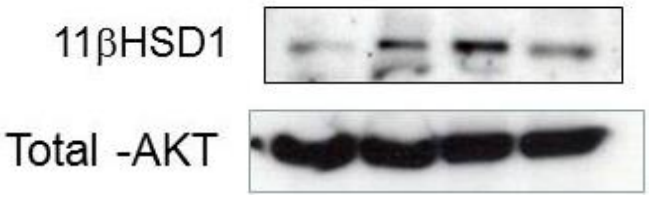

Fig 3.5.B

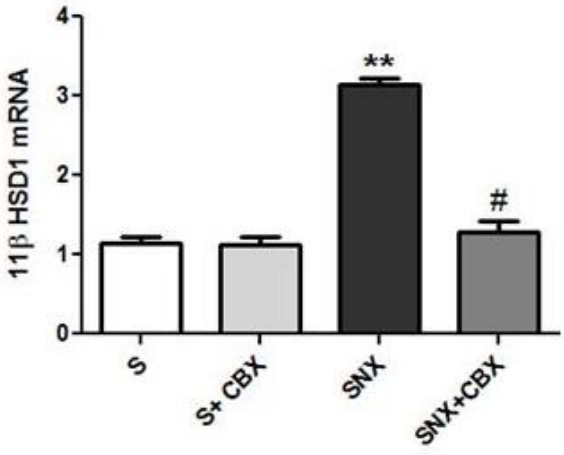

Fig 3.5. . White adipose tissue (WAT) HSD1 protein (3.5.A.), total AKt is loading control, and mRNA (3.5.B.) in SNx uraemia and the effect of CBX treatment. Sham/control and SNx are indicated by ** *P*<0.05. Statistically significant effects of CBX treatment are indicated by # *P*<0.05.

Fig 3.6.A

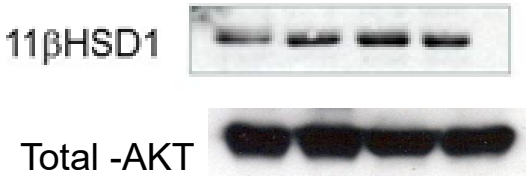

Fig 3.6.B

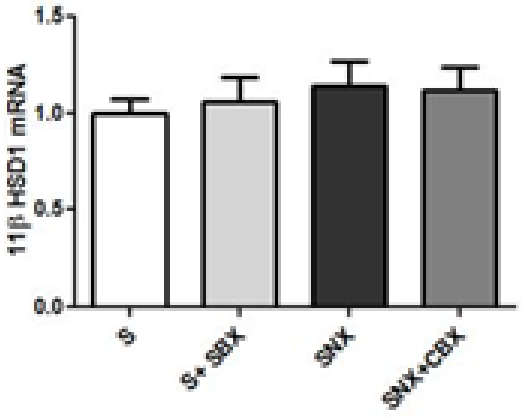

Fig 3.6. Muscle HSD1 protein (3.6.A.) and mRNA (3.6.B.) in SNx uraemia and the effect of CBX treatment. Data are expressed as mean ± SEM (8/group). There was no statistically significant difference between the groups.

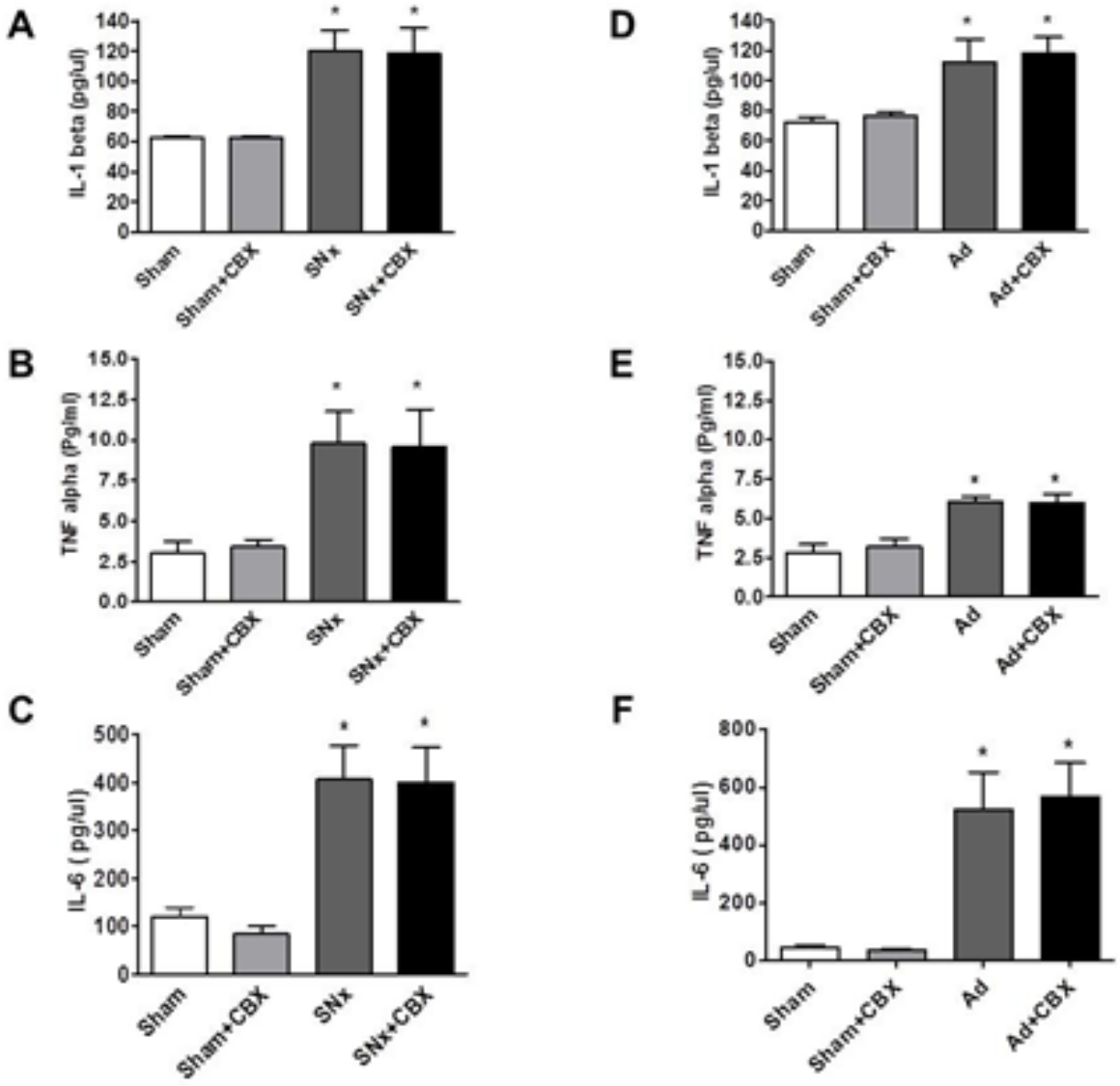

Fig 3.7. Plasma levels of IL-1β (A and D), TNFα (B and E) and IL-6 (C and F) were measured in SNx and Ad models using ELISA respectively. Statistically significant differences between sham/control and SNx are indicated by * *P*<0.05.

3.4. Uraemic rats develop impaired glucose tolerance and reduced insulin sensitivity.

After an overnight fast serum insulin levels were found to be markedly elevated in SNx (Fig. 3.8) and Ad rats (Fig. 3.9). However, fasting serum glucose concentrations in blood were unchanged (Fig. 3.10 and 3.11), suggestive of uraemia-induced insulin resistance.

To further analyse potential uraemia-induced changes in systemic glucose tolerance and insulin sensitivity, we conducted IPGTT tests. During the GTT, blood glucose concentrations were significantly higher in SNx and Ad rats compared to sham up to 60 min post-glucose administration (Fig. 3.12 and 3.13 respectively). In addition, serum insulin levels were elevated during a GTT, remaining elevated 45 min post-glucose administration in SNx and Ad rats compared to sham (3.14 and 3.15 respectively). Moreover, impairment in insulin's ability to lower blood glucose levels in an ITT was observed in SNx and Ad rats, with blood glucose levels remaining significantly elevated in both models 30 min-post insulin administration (Fig. 3.16 and 3.17 respectively) during an ITT.

Taken together, these data demonstrate the presence of insulin resistance in both of the models of uraemia used for this study. To determine whether uraemia-induced insulin resistance may be linked to elevated hepatic glucose production, we conducted a pyruvate tolerance test (PTT). Consistent with abnormally elevated hepatic glucose production, SNx and Ad rats displayed significantly increased blood glucose levels up to 90 min post-pyruvate administration (Fig. 3.18 and 3.19 respectively).

Collectively, these data demonstrate significant insulin resistance associated with abnormally elevated hepatic glucose production, in both SNx and adenine-feeding models of CKD.

Administration of CBX did not improve markers of renal failure in any group (Table 3.2). Despite this, CBX completely prevented uraemia-induced increases in serum insulin levels in both models (Fig. 3.12-3.19). Moreover, 11β-HSD1 inhibition with CBX resulted in

a significant improvement in insulin sensitivity and glucose tolerance, as well as reduced hepatic glucose production following a PTT. Taken together, these data demonstrate that abnormally elevated 11β-HSD1 plays a crucial role in mediating insulin resistance in uraemia.

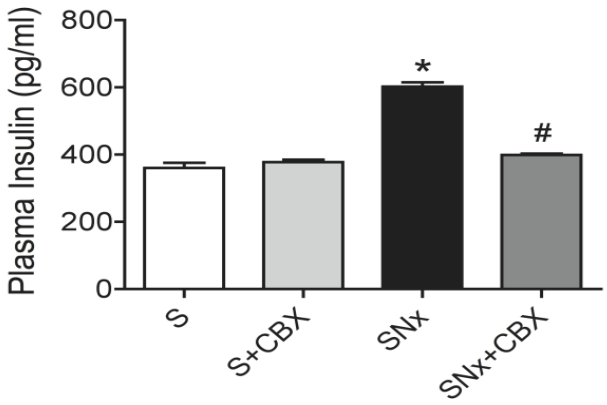

Fig 3.8. Circulating rat insulin was measured using ELISA in SNX and the effect of CBX treatment. Statistically significant differences between sham/control and SNx are indicated by * *P*<0.05. Statistically significant effects of CBX treatment are indicated by # *P*<0.05.

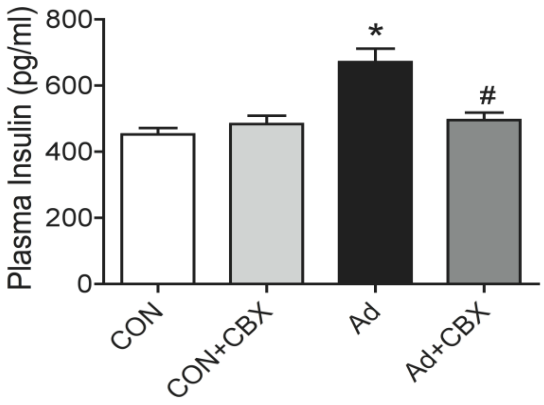

Fig 3.9. Circulating rat insulin was measured using ELISA in AD and the effect of CBX treatment. Data are expressed as mean ± SEM (8/group). Statistically significant differences between sham/control and SNx are indicated by * *P*<0.05. Statistically significant effects of CBX treatment are indicated by # *P*<0.05.

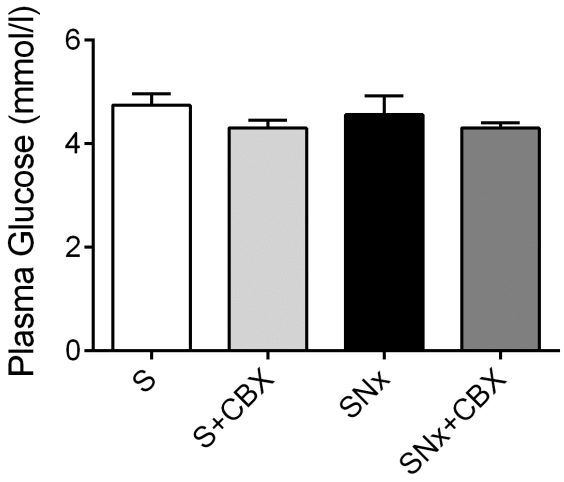

Fig 3.10. Fasting rodent glucose measured using Accu-Chek Aviva device in SNx and the effect of CBX treatment. Data are expressed as mean ± SEM (8/group). The means were not statistically different.

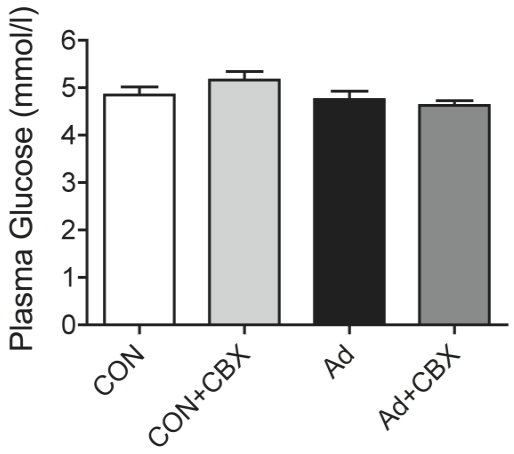

Fig 3.11. SNx Rodent glucose was measured using Accucheck Aviva device in AD and the effect of CBX treatment noted. Data are expressed as mean ± SEM (8/group). The means of the groups were not significantly different.

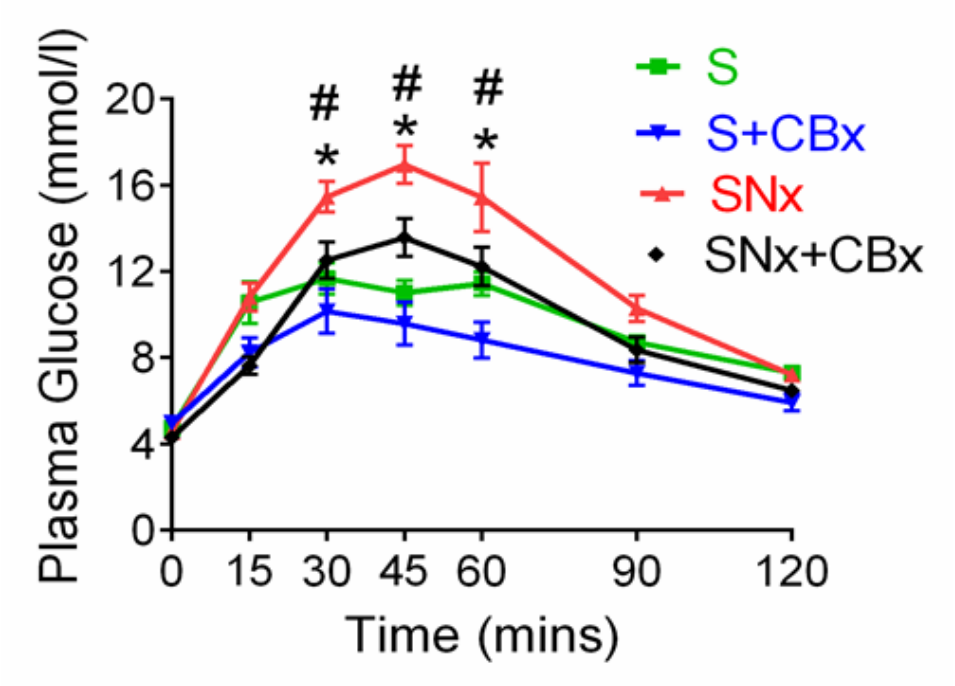

Fig 3.12. SNx IPGTT. Data are expressed as mean ± SEM (8/group). Statistically significant differences between sham and SNx are indicated by * *P*<0.05. Statistically significant effects of CBX treatment are indicated by # *P*<0.05.

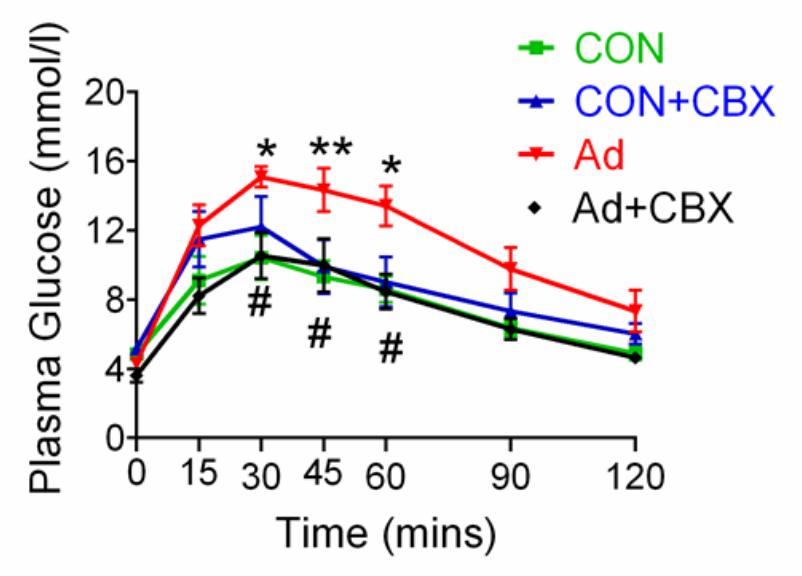

Fig 3.13. Ad IPGTT. Data are expressed as mean ± SEM. Statistically significant differences between control and Ad are indicated by * *P*<0.05; ** *P*<0.01. Statistically significant effects of CBX treatment are indicated by #*P*<0.05.

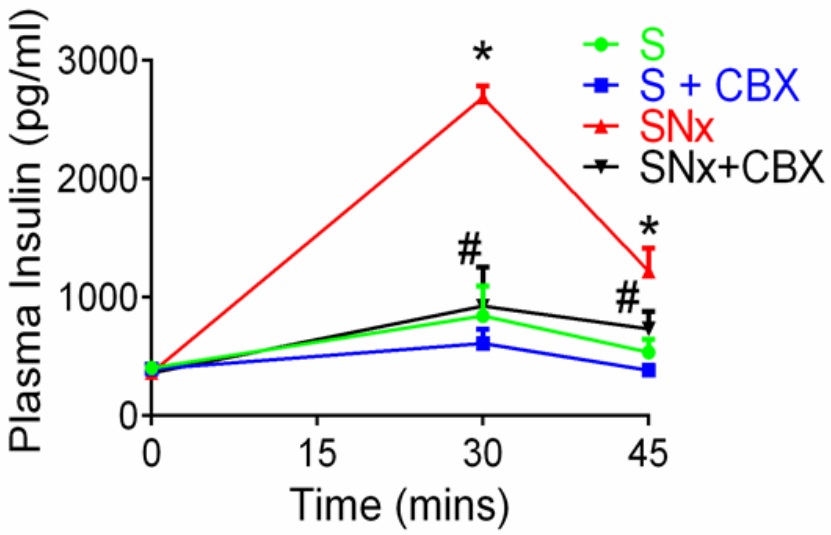

Fig 3.14. Plasma insulin during SNx IPGTT. Statistically significant differences between sham and SNx are indicated by * *P*<0.05. Statistically significant effects of CBX treatment are indicated by # *P*<0.05.

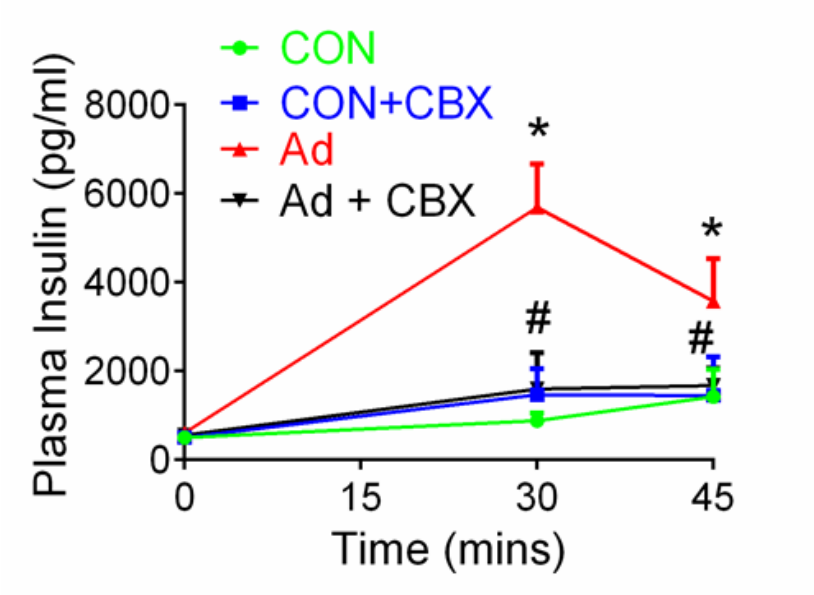

Fig 3.15. Plasma insulin during Ad IPGTT. Data are expressed as mean ± SEM. Statistically significant differences between control and Ad are indicated by * *P*<0.05. Statistically significant effects of CBX treatment are indicated by # *P*<0.05.

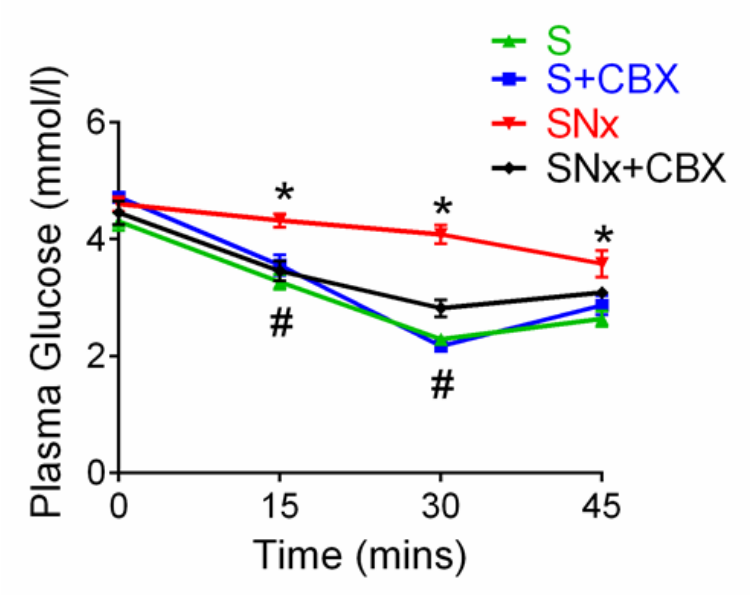

Fig 3.16. Plasma glucose response to SNx ITT. 1u/kg body weight Insulin was injected IP and plasma glucose measured. Data are expressed as mean ± SEM (8/group). Statistically significant differences between sham and SNx are indicated by * *P*<0.05; Statistically significant effects of CBX treatment are indicated by # *P*<0.05.

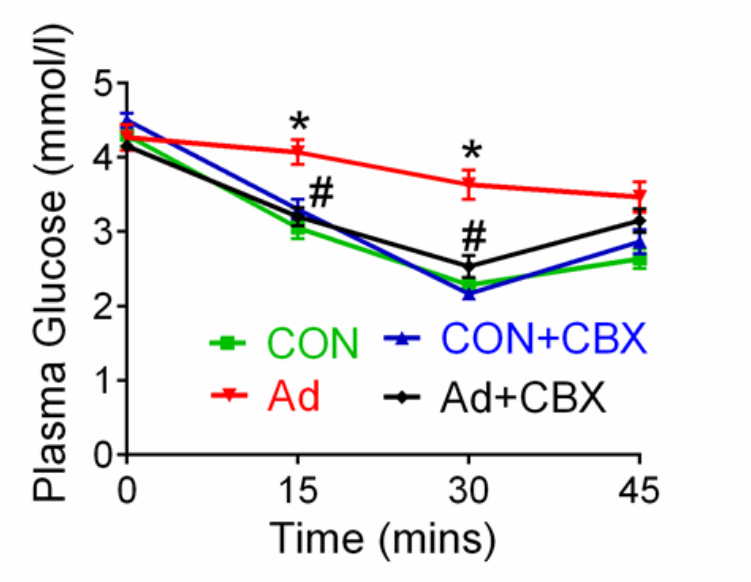

Fig 3.17. Plasma glucose response to Ad ITT. 1u/kg body weight Insulin was injected IP and plasma glucose measured. Data are expressed as mean ± SEM (8/group). Statistically significant differences between sham and Ad are indicated by * *P*<0.05. Statistically significant effects of CBX treatment are indicated by # *P*<0.05.

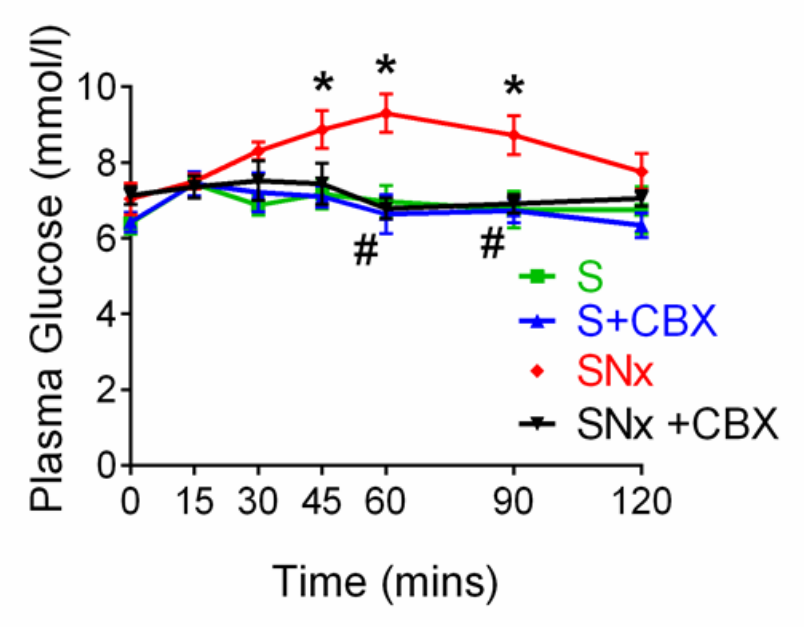

Fig 3.18. SNx Plasma glucose response to PTT. Statistically significant differences between sham and SNx are indicated by * *P*<0.05. Statistically significant effects of CBX treatment are indicated by # *P*<0.05.

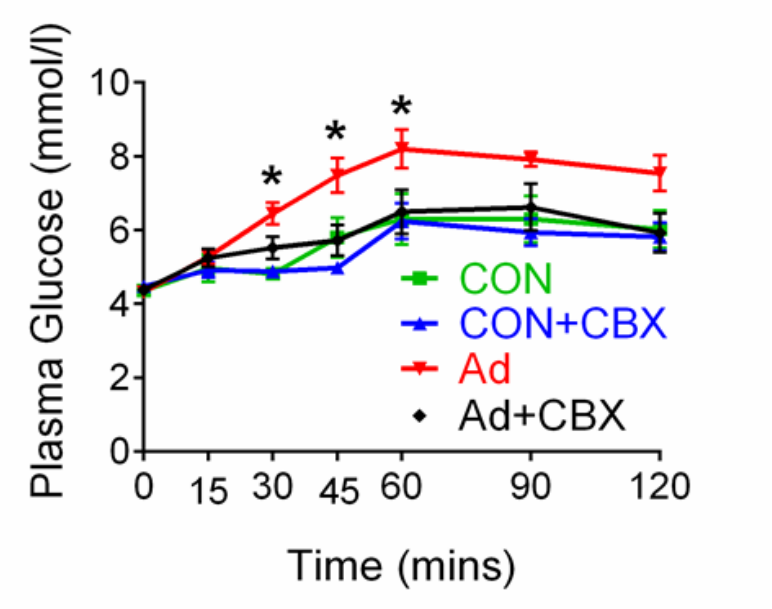

Fig 3.19. Ad plasma glucose response to ITT. Statistically significant differences between sham and Ad are indicated by * *P*<0.05.

3.5. 11β-HSD1 inhibition suppresses hepatic gluconeogenic gene expression and markers of impaired insulin signalling in uraemia.

Since uraemia-induced insulin resistance was associated with elevated blood glucose levels following a PTT, we examined for alterations in hepatic gluconeogenic enzymes.

Levels of PCK1 mRNA and protein and G6Pase protein were elevated in SNx (Fig 3.20.) and Ad rodent livers (Fig.3.21) compared to sham animals. PGC1-α mRNA and protein levels were also increased in SNx (Fig.3.22) and Ad rodent livers (Fig.3.23).

Similar to effects observed on systemic insulin resistance, CBX administration reversed these effects on gluconeogenic enzymes in both models of uraemia. To assess whether the changes that increased hepatic gluconeogenesis occur in association with impaired insulin signalling, we measured phosphorylation of AKT at serine 473. Protein levels of phospho-(Ser473)-AKT were reduced in liver and also in skeletal muscle and white adipose tissue of uraemic rats. In all three tissues, this effect was reversed by CBX administration (Fig. 3.24). Taken together, these data demonstrate that 11β-HSD1 mediates insulin resistance in uraemia through abnormal elevation of hepatic gluconeogenesis and dysregulation insulin signalling.

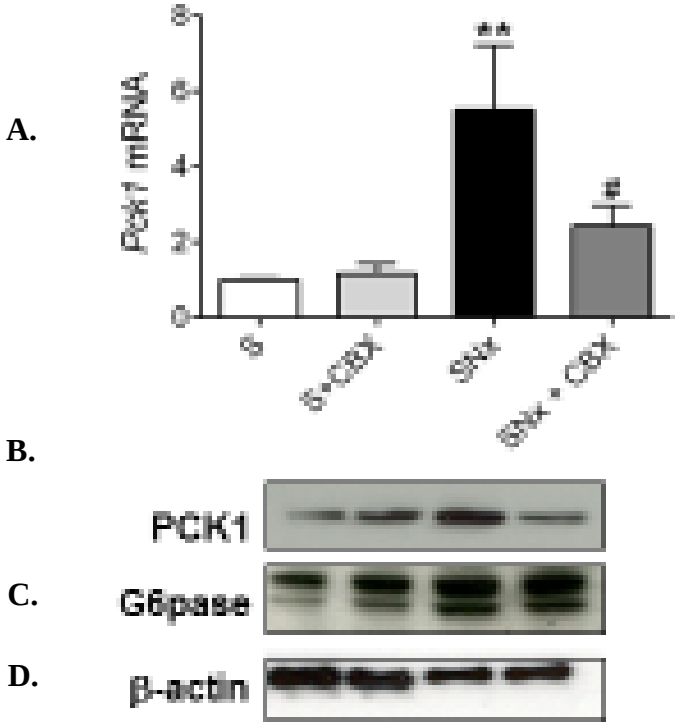

Fig 3.20. Gluconeogenic enzymes in SNx rodent liver. (A, B) SNx; PCK1 mRNA, and protein (C) SNX. Data are expressed as mean ± SEM. Statistically significant differences between sham and Ad or SNx are indicated by, ** *P*<0.01. Statistically significant effects of CBX treatment are indicated by # *P*<0.05

A.

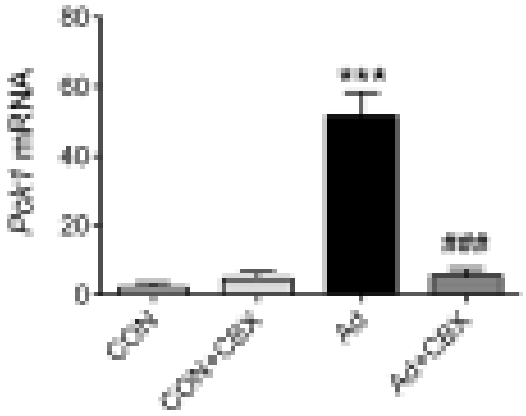

B.

C.

D.

Fig 3.21. Gluconeogenic enzymes in Ad rodent liver. (A, B) Ad; PCK1 mRNA and protein. (C) Ad; G6Pase protein. Data are expressed as mean ± SEM. Statistically significant differences between sham and Ad or SNx are indicated by * *P*<0.05. Statistically significant effects of CBX treatment are indicated by ### *P*<0.05**

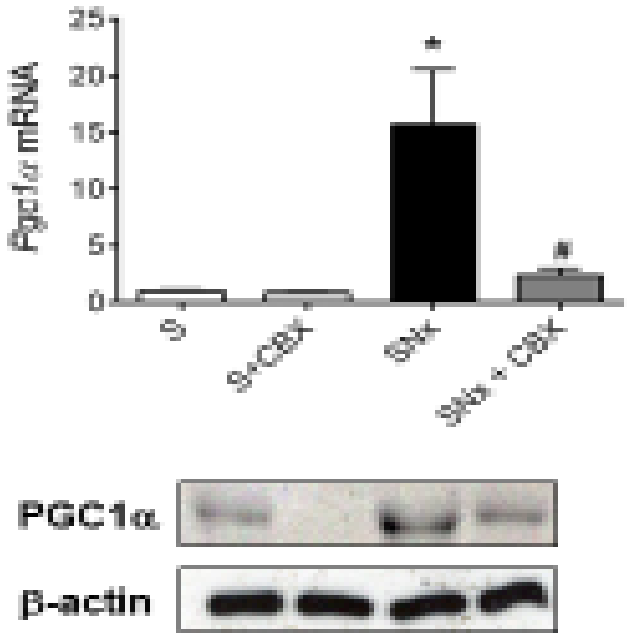

Fig 3.22. SNx; hepatic PGC1α mRNA and protein. Data are expressed as mean ± SEM. Statistically significant differences between sham and SNx are indicated by * *P*<0.05. Statistically significant effects of CBX treatment are indicated by # *P*<0.05

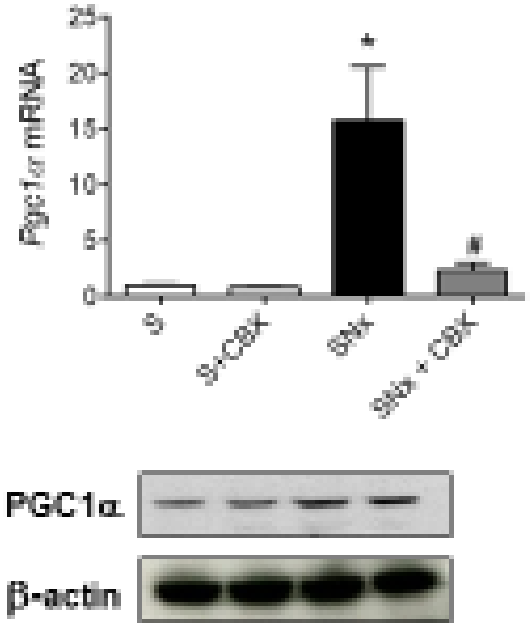

Fig 3.23. Ad hepatic PGC1α mRNA and protein. Data are expressed as mean ± SEM. Statistically significant differences between sham and Ad are indicated by * *P*<0.05, statistically significant effects of CBX treatment are indicated by # *P*<0.05

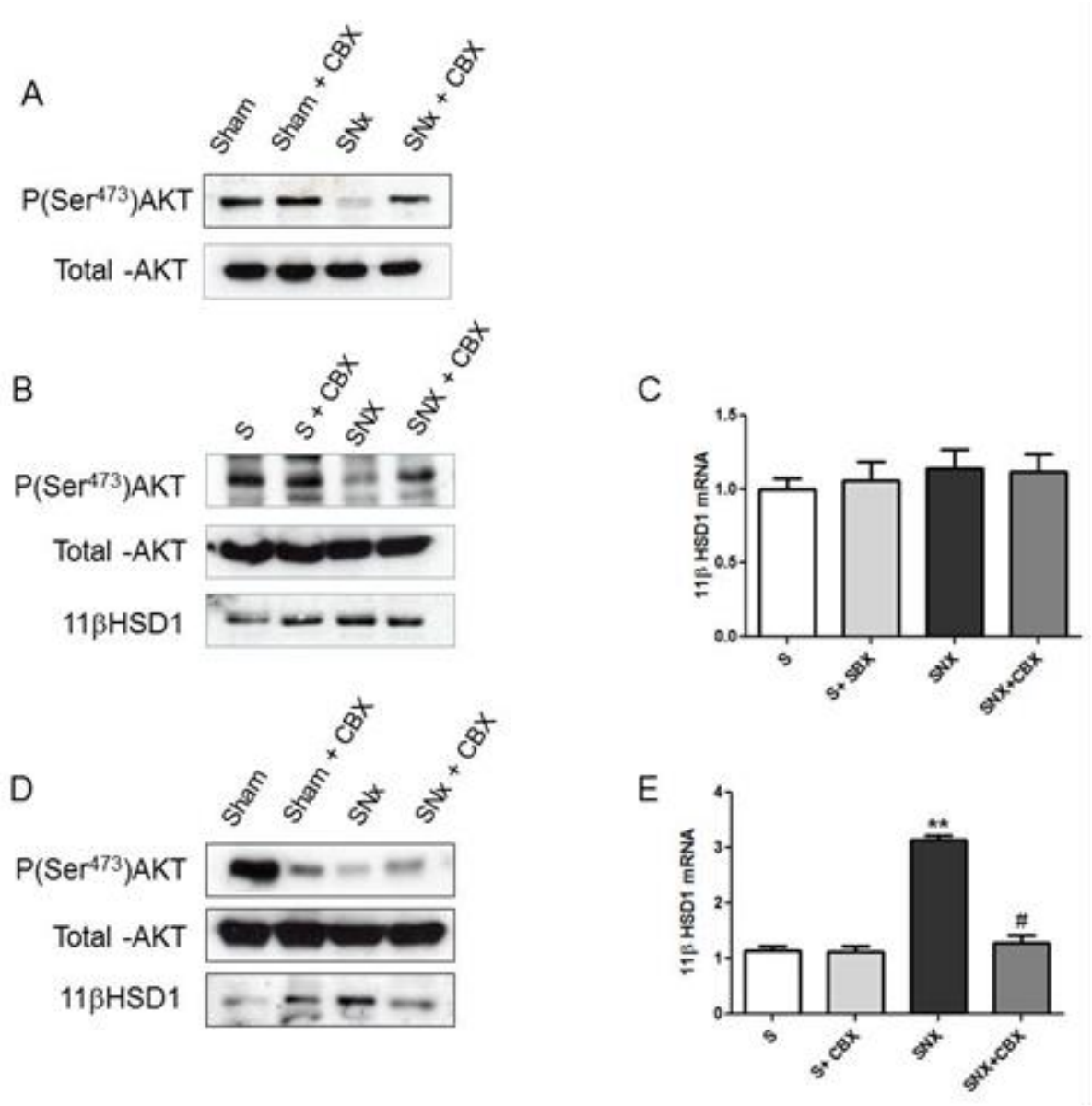

Fig 3.24 Uraemia induced changes in peripheral insulin signalling and 11β-HSD1 levels. (A) Hepatic phospho(Ser473)-AKT and total-AKT protein, (B) Skeletal muscle protein levels of phospho(Ser473)-AKT, total-AKT and 11β-HSD1, (C) skeletal muscle 11β-HSD1 mRNA, (D) Epididymal white adipose tissue protein levels of phospho(Ser473)-AKT, total-AKT and 11β-HSD1, (E) Epididymal white adipose tissue 11β-HSD1 mRNA. Western blots are representative (n=4). Data are expressed as mean ± SEM. Statistically significant differences between sham and SNX are indicated by ** *P*<0.01. Statistically significant effects of CBX treatment are indicated by # *P*<0.05

3.6. Uraemia-induced dyslipidaemia is corrected by 11β-HSD1 inhibition.

Consistent with previous reports in experimental models of uraemia, SNx and Ad rats showed elevated serum levels of cholesterol, triglycerides and non-esterified fatty acids (NEFA), (Fig. 3.25 *A – C*; Fig. 3.26 *A – C*). Hepatic mRNA expression of HMGCR was elevated in both uremic models (Fig.3.27A, B) suggesting increased *de novo* hepatic cholesterol biosynthesis.

Moreover, mRNA and protein levels of ACC1 (Fig.3.28), FAS (Fig. 3.29) and mRNA levels of SREBP1c (Fig. 3.30) were markedly increased in SNx and Ad rats, indicative of increased hepatic *de novo* lipogenesis. Importantly, in both CKD models abnormally elevated serum levels of cholesterol, triglycerides and NEFA were ameliorated following administration of CBX, demonstrating that uraemia-induced dyslipidaemia, like gluconeogenesis, may occur in part through an 11β–HSD1-mediated mechanism (Fig. 3.1., Fig 3.2.). Consistent with this, mRNA and protein levels of ACC1, FASN, SREBP1C and HMGCR were also partially normalized by CBX in SNx and Ad rats (Fig.3.28. – 3.30.).

We also assessed liver and skeletal muscle lipid content by measuring triglyceride levels in SNx rats. Despite observed changes in lipogenic gene and protein levels, hepatic triglyceride content was unchanged between sham and uremic rats (Fig. 3.31.A), In contrast, uraemia did increase skeletal muscle triglyceride levels, but these increases were not reversed by CBX (Fig 3.31.B). Liver and muscle lipids were measured using a colourimetric TG assay by Dr Paul Caton.

Taken together, these data demonstrate that uraemia-induced dyslipidaemia occurs through a11β–HSD1-dependent mechanism and may contribute to insulin resistance in these models.

A

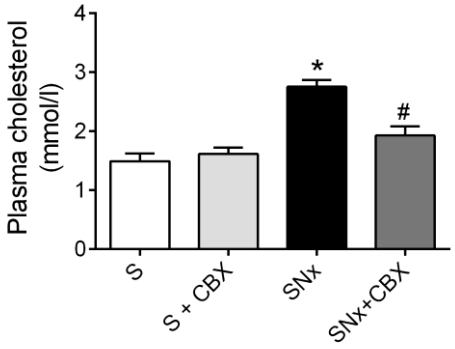

B

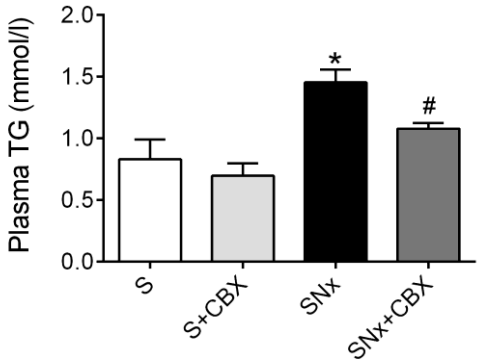

C

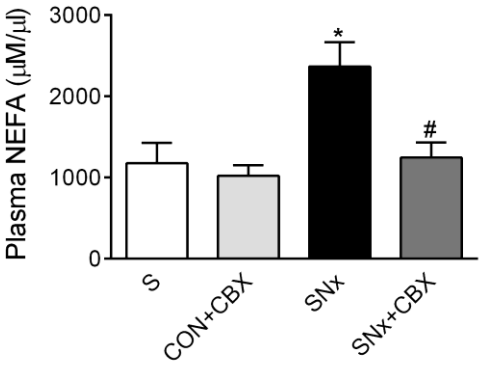

Fig 3.25. SNx. (A) Plasma cholesterol, (B) plasma triglycerides, (C) plasma NEFA, Data are expressed as mean ± SEM. Statistically significant differences between sham and SNx are indicated by * *P*<0.05, statistically significant effects of CBX treatment are indicated by # *P*<0.05

A

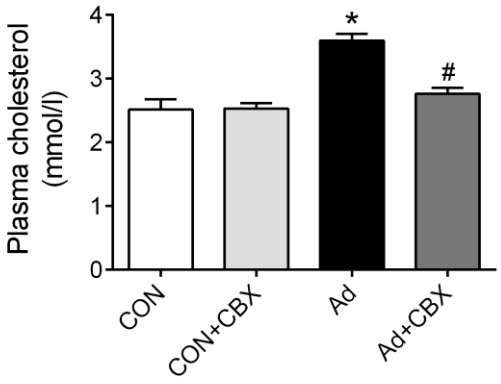

B

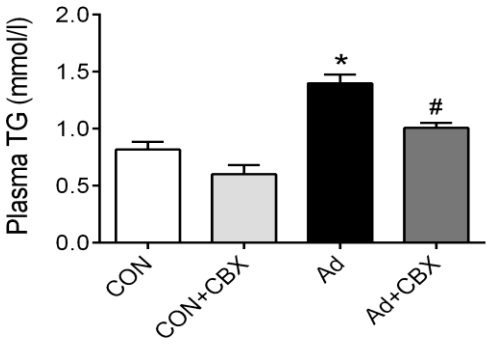

C

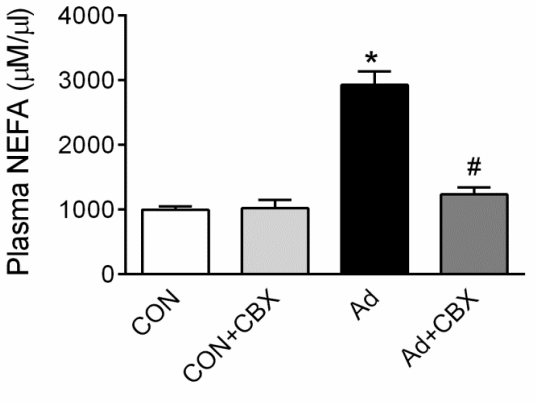

Fig 3.26. Ad (A) Plasma cholesterol, (B) plasma triglycerides, (C) plasma NEFA, Data are expressed as mean ± SEM. Statistically significant differences between sham and Ad are indicated by * *P*<0.05. Statistically significant effects of CBX treatment are indicated by # *P*<0.05

A

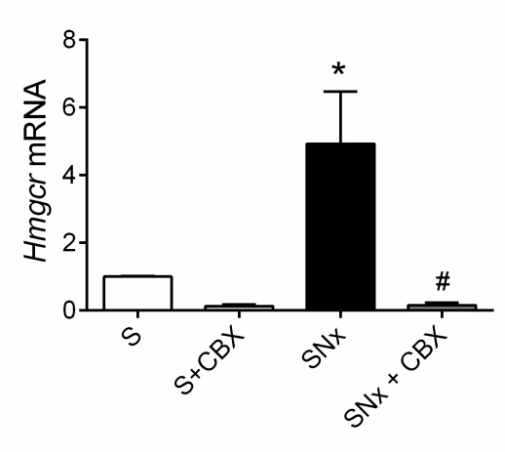

B

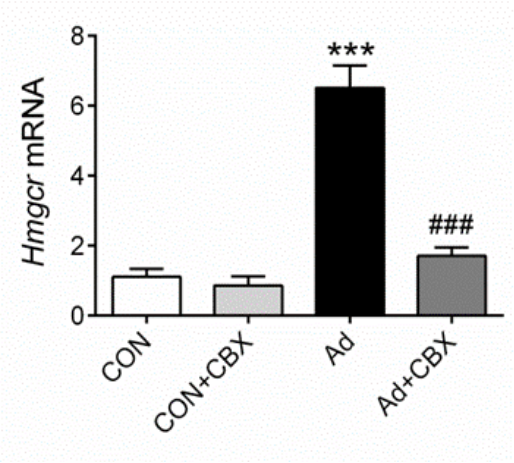

Fig 3.27. Hepatic HMGCR mRNA. Data are expressed as mean ± SEM. Statistically significant differences between sham and SNx are indicated by, * p< 0.001 * *P*<0.005. Statistically significant effects of CBX treatment are indicated by # *P<0.01,* ### *P*<0.05**

A

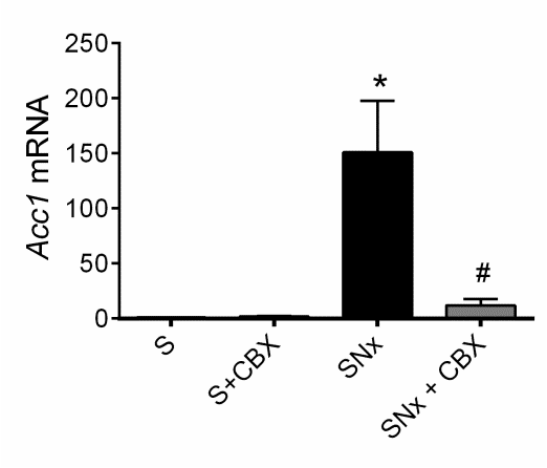

B

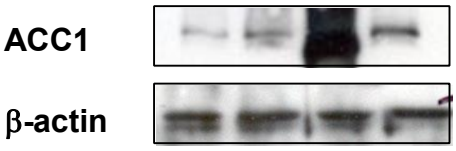

C

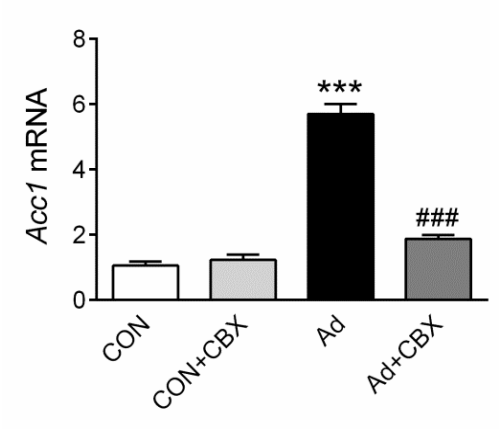

D

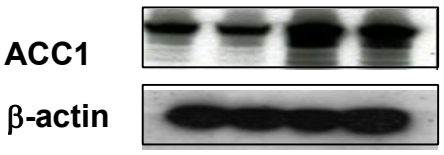

A B

Fig 3.28. SNx and Ad hepatic ACC1mRNA (A, C) and protein (B, D) Data are expressed as mean ± SEM. Statistically significant differences between sham and SNx are indicated by * *P*<0.05, * *P*<0.001. Statistically significant effects of CBX treatment are indicated by # *P*<0.01, ### *P*<0.05**

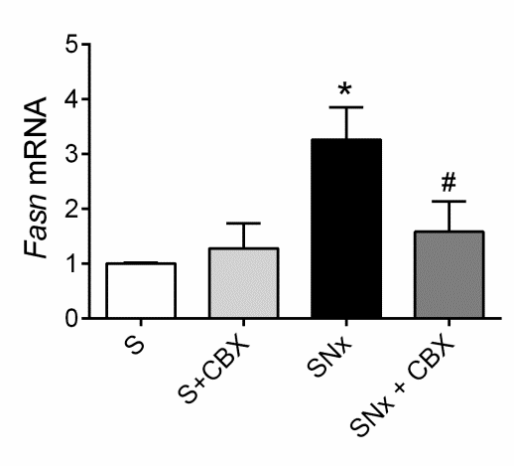

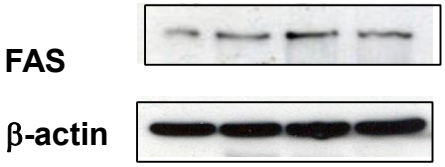

C

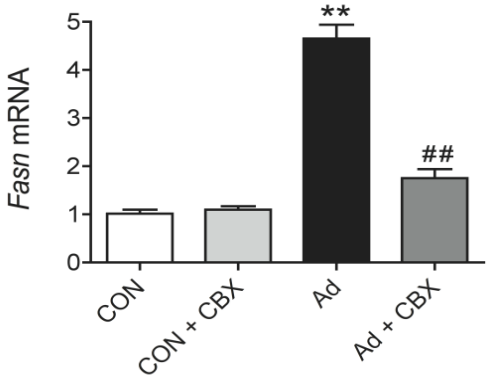

D

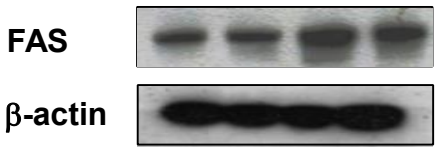

Fig 3.29. SNx and Ad hepatic FAS mRNA (A, C) and protein (B, D) Data are expressed as mean ± SEM. Statistically significant differences between sham and SNx are indicated by * *P*<0.05, * *P*<0.001. Statistically significant effects of CBX treatment are indicated by # *P*<0.01, ### *P*<0.05.**

A

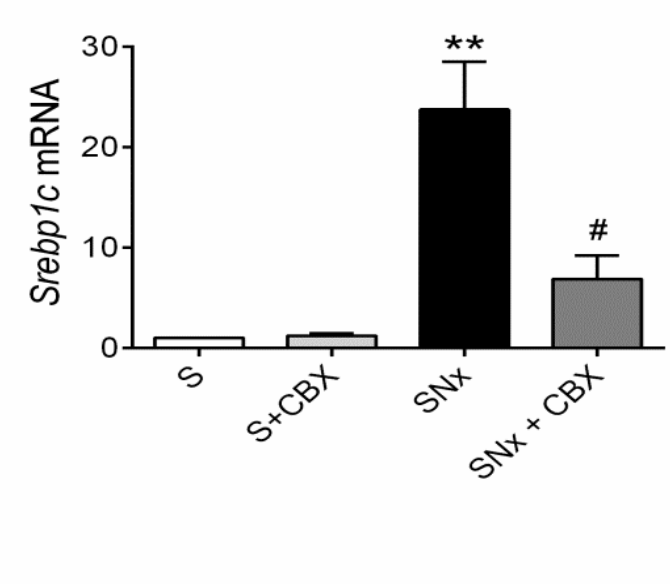

B

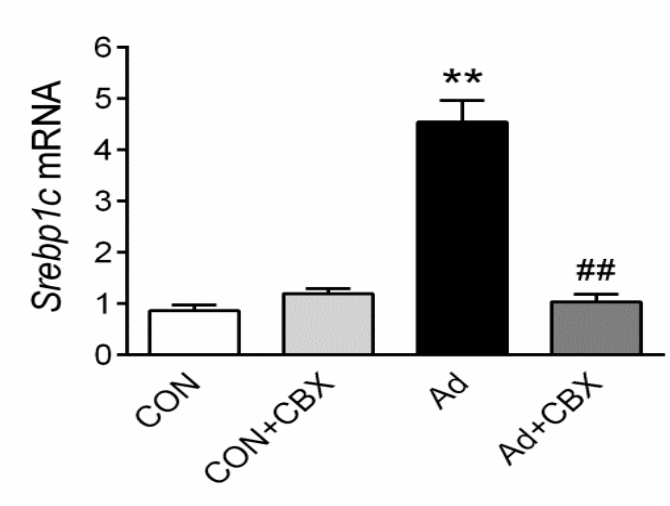

Fig 3.30. SNx and Ad hepatic Srebp1c mRNA (A, B). Data are expressed as mean ± SEM. Statistically significant differences between sham and SNx are indicated by ** *P*<0.01, Statistically significant effects of CBX treatment are indicated by #, ## *P*<0.05

A

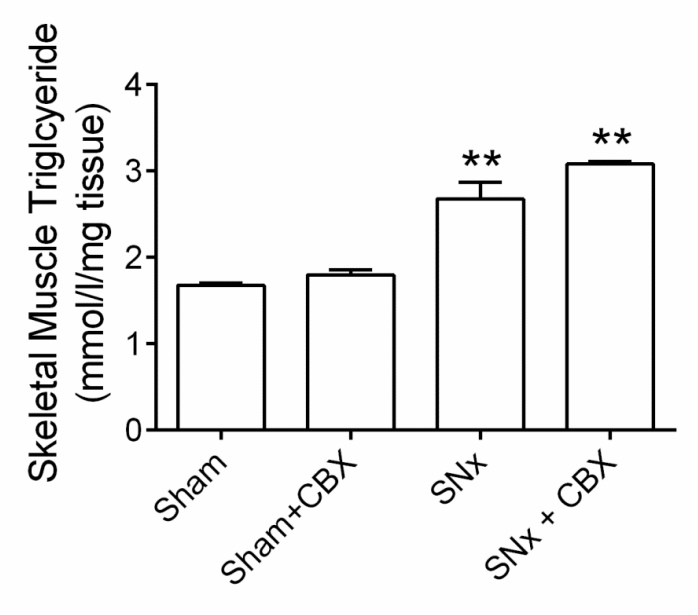

B

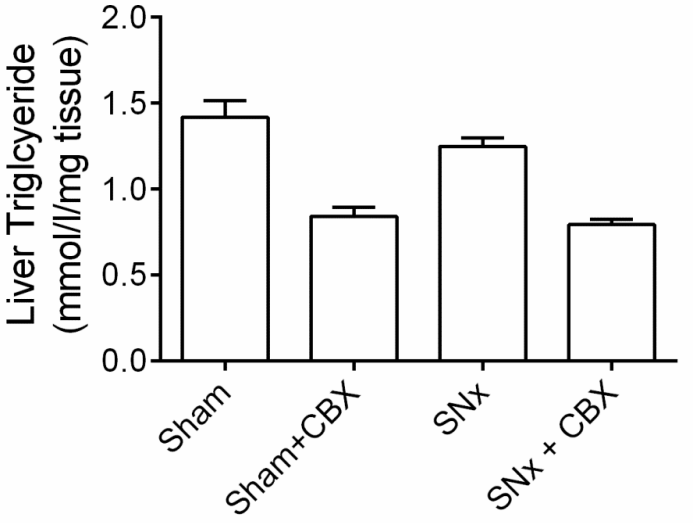

Fig 3.31. Uraemia induced changes in liver and skeletal muscle triglyceride levels. (A) Hepatic triglyceride levels, (B) Skeletal muscle triglyceride levels. Data are expressed as mean ± SEM. Statistically significant differences between sham and SNx are indicated by ** *P*<0.01.

3.7. Discussion

The data presented, in this chapter demonstrate that elevated hepatic 11β-HSD1 mediates impaired glucose tolerance, reduced insulin sensitivity, hyperinsulinaemia and dyslipidaemia in two distinct male rat models of CKD.

Importantly, increased hepatic 11β-HSD1 as measured by mRNA expression, protein amount, and activity, was associated with elevated hepatic corticosterone content without changes in systemic corticosterone. Rats rendered uraemic were glucose-intolerant, insulin-resistant and dyslipidaemic in accordance with previously published literature. This was associated with an up-regulation of PGC-1α associated gluconeogenic enzymes. Normally, the gluconeogenic pathway would be supressed in the presence of hyperglycaemia and/or hyperinsulinaemia, however, as demonstrated in the insulin-stimulation of hepatic insulin signalling, hepatocyte insulin signalling is also impaired in uraemia, leading to inappropriate gluconeogenesis with circulating hyperinsulinaemia. Use of CBX at the dose used in this study (50mg/kg for 2 weeks) has been reliably shown to reduce 11β-HSD1 mRNA as well as activity in the past. Treatment of uraemic rodents with CBX resulted in a reversal of changes in hepatocyte insulin signalling, reduction of hepatic gluconeogenesis (as measured by gluconeogenic pathway enzyme expression and dynamic physiological tests) and amelioration of insulin resistance and glucose intolerance, with a beneficial lipid profile. This suggests that impaired glucose tolerance and dyslipidaemia in CKD is closely associated with enhanced intrahepatic corticosterone production.

Whilst these studies require confirmation using female rats, improvements in metabolic profiles following 11β-HSD1 inhibition occurred without corrections in renal dysfunction, indicating that selective inhibitors of 11βHSD1 may be a plausible therapeutic approach to insulin resistance and its complications in CKD.

Previous studies have reported elevated hepatic glucose production in chronically uraemic patients (123). Furthermore, increased hepatic gluconeogenesis in acute experimental uraemia is reversed by the glucocorticoid receptor antagonist RU 38486 (124). Elevated hepatic gluconeogenesis can cause insulin resistance and hyperinsulinaemia (125), whilst knockdown of gluconeogenic genes and cofactors have resulted in the correction of insulin resistance and improvement in insulin sensitivity

in murine models (125,126,127,128) . This suggests that 11β-HSD1-mediated increases in hepatic gluconeogenesis via up-regulation of PCK1 and PGC1α may represent a likely cause of hyperinsulinaemia and insulin resistance in uraemia.

Dyslipidaemia is also a common complication of CKD. We observed abnormally elevated plasma lipids and cholesterol in uraemic rats, with parallel increases in lipogenic gene and protein expression. 11β-HSD1 inhibition corrected systemic dyslipidaemia, in association with reduced hepatic lipogenic gene and protein expression. These observations are consistent with glucocorticoid induction of triglyceride synthesis and fatty liver in rats, whilst mice over expressing hepatic 11β-HSD1 display increased hepatic lipogenesis (101). However, it is unclear in our model, whether increased hepatic lipogenic gene expression occurs via direct induction by glucocorticoids or through elevated insulin-mediated SREBP1c induction as would be anticipated because of undesirable metabolic consequence of hyperinsulinaemia (129,130).

The mechanism underlying elevated 11βHSD1 in uraemia have not been fully elucidated, but may involve inflammation. Consistent with observations in CKD patients, serum levels of IL-6, TNFα and IL1β were elevated in both models of uraemia, likely as a result of decreased renal cytokine clearance and increased systemic oxidative stress (131,132). TNFα and IL1β induce transcription of hepatic and adipose 11βHSD1, via a mechanism mediated by p38 and C/EBPα signalling, suggesting a potential mechanism for upregulation of 11βHSD1 in uraemia. Pro-inflammatory cytokines can also impair insulin signalling. However, since CBX corrects insulin resistance without changes in plasma cytokine levels, this rules out a direct role for pro-inflammatory cytokine induced insulin resistance.

Whilst our data point to a crucial role for hepatic 11β-HSD1 as a key mediator of insulin resistance in uraemia, we also observed increases in 11β-HSD1 expression and parallel impairment of insulin signalling in adipose tissue, changes which were reversed by CBX treatment. These changes may also contribute to uraemia-induced insulin resistance, for example via glucocorticoid mediated increases in circulating NEFA levels, as observed in our models, which may account for the impaired insulin signalling observed in uraemic liver, through ectopic lipid deposition in liver and skeletal muscle. This may be particularly plausible given the lack of increased triglyceride levels in the uraemic liver. Interestingly, studies have suggested that CBX may not act directly on adipose tissue, raising the

possibility that a secreted hepatokine produced during hepatic CBX metabolism may impact on adipose tissue 11β-HSD1. Similar to adipose tissue and liver, insulin signalling was also impaired in uraemic skeletal muscle, whilst skeletal muscle lipid levels are increased, suggesting a potential contributory role for muscle ectopic lipid deposition in uraemia-induced insulin resistance. However, uraemia-induced increases in skeletal muscle triglyceride were not reversed by CBX, whilst we did not observe changes in skeletal muscle 11β-HSD1 levels across all four experimental groups. Despite this, skeletal muscle insulin signalling was improved by CBX. This data suggest- that the insulin sensitising effects of CBX in skeletal muscle are indirect, and are not mediated through reversal of skeletal muscle triglyceride levels, instead occurring through direct CBX effects on liver and adipose tissue. Thus, both hepatic and adipose tissue 11β-HSD1 contribute to onset of insulin resistance in uraemia. However, without conducting longitudinal studies of uraemia, it is not possible to deduce in which tissue insulin resistance initially manifests.

4. Characterization of insulin resistance in uraemia, in 11β-HSD1 $^{-/-}$ mice and the response to treatment with the specific inhibitor UE2316 in Ad fed rodents.

4.1. Introduction

The liver is a key organ with respect to insulin resistance in that contributes to its pathogenesis through increasing glucose output, as well as being the primary metabolic target of glucocorticoid action. Specific inactivation of hepatic GRs has been shown to reduce elevated glucose output and ameliorate hyperglycaemia and hyperlipidaemia in streptozotocin (STZ)–induced diabetes (131) and in type 2 diabetic animal models (132,133). Glucocorticoid-induced alteration in hepatic glucose metabolism involves an increase in hepatic glucose output and reduction of glucose utilisation (134).

Treatment with dexamethasone (DEX) has been shown not to change insulin receptor and Insulin Receptor Substrate type 1 (IRS-1, 135), but decreases PI 3-kinase activity in the liver. Following glucose uptake and glycolysis, the PDH complex (PDC) facilitates entry of pyruvate into the mitochondria for subsequent oxidation. PDK inactivates PDC through phosphorylation of this enzyme (135). In cultured hepatoma cell lines, DEX treatment significantly increases PDK-4 gene and protein expression, which can be reversed by insulin. More recent studies have also demonstrated that PPARα coactivator (PGC-1α) might also be involved in the activation of PDK (136). However, unlike diabetes and fasting (where the GC-induced PDK-4 gene expression stimulation is through recruiting PGC-1α on the portion of the promoter), GCs stimulate PDK-4 gene via FOXO1. PDK inhibits glucose utilisation via inactivating PDC and switches the liver to synthesize glucose and store glycogen. This elevation in hepatic gluconeogenesis is associated with effects of glucocorticoids on the rate-limiting enzymes, like phosphoenolpyruvate carboxykinase (PEPCK) and glucose-6- phosphatase (G-6-Pase) (137). Glucocorticoids enhance the gene expression of PEPCK and G-6-Pase, resulting in increased glucose output from the liver, which contributes to whole body insulin resistance (137). Activation of PPARγ also plays a key role in glucocorticoid-regulated gluconeogenesis. Following DEX treatment, knockout of PPARγ shows unchanged hepatic PEPCK and G-6-

Pase, whereas reconstitution of PPARγ increased those enzymes (138). PGC-1α is another important regulator of gluconeogenesis, which is transcriptionally regulated by PPARα. Overexpressed PGC-1α in liver caused hyperglycaemia in mice with PPARα expression but not in PPARα null mice (138). Additionally, GCs promote hepatic TG storage. Normally, the TG levels reflect the balance between lipogenesis and lipolysis. While some early studies have suggested that hepatic stored TG undergoes lipolysis to release FA which is re-esterified to form TG in the ER. The role of TG storage in lipotoxic IR and on promotion of lipoprotein secretion is still controversial.

Carbenoxolone (CBX) is a derivative of the liquorice ingredient glycyrrhetinic acid and has been shown to be a potent inhibitor of both 11β-HSD1 and 11β-HSD2. The beneficial effect of 11β-HSD1 inhibition on insulin tolerance has been previously reported in both healthy men and type 2 diabetic patients using CBX treatment despite impaired cortisol inactivation within MR target tissues via inhibition of 11β-HSD2 as discussed in chapter 3. Similarly, CBX attenuated hepatic insulin tolerance and improved lipid metabolism in rodents, although it did not reduce insulin resistance in obese Zucker rats.

Work presented in Chapter 3 demonstrates that uraemic rodents are hyperinsulinaemic on fasting, are glucose intolerant, and insulin resistant. Both the SNX and Ad rodents demonstrated increased *in vivo* hepatic gluconeogenesis as measured via an IPPTT, and up-regulation of the key transcriptionally regulated hepatic gluconeogenic enzymes (PCK1, G-6-Pase) as well as upregulation of upstream PGC1α. These changes were ameliorated by CBX. A possible major criticism of the data presented so far in this thesis is that it does not address the question of specificity. The enzyme 11β-HSD1 has been previously reported as having bi-directional activity and CBX is a non-specific inhibitor. The presence of hepatic and adipose insulin resistance, along with hepatic gluconeogenesis and dyslipidaemia in the rodent models

of uraemia was therefore further investigated using a 11β-HSD1$^{-/-}$ murine model, as well as using UE2316, a specific inhibitor of 11β-HSD1 in the Ad fed uraemic rodent model.

4.2. Murine models

Male progeny of mice with targeted global disruption of the 11β-HSD1gene congenic on C57Bl/6J were derived as described previously (22). Controls were wild-type (WT), C57Bl/6J, age-matched, males. Adult 8-week old WT and 11β-HSD1$^{-/-}$ (6 – 8/group) were fed a control or 0.25% Ad for 4 weeks. Mice were fasted overnight and killed at ~9:00 a.m., within 1 min of disturbing each cage, or used in dynamic physiological studies.

For specific 11β-HSD1 inhibitor studies, 2-week Ad-fed rats were administered UE2316 (20mg/kg/day) or vehicle (50:50 DMSO/PEG-400) equivalent for 2 weeks by subcutaneous mini-pump (Alzet, CA, USA) to create three groups (1) CON + vehicle, (2) Ad + vehicle, (3) Ad + UE2316. Mini-pump insertion was performed by Mr J Kieswich,WHRI.

4.3. Adenine-induced murine uraemia

Serum creatinine was elevated 3.5 fold in Ad-fed 11β-HSD1$^{-/-}$ mice, while serum urea was elevated 4.5 fold, respectively (Table.4.1). Further markers of chronic renal injury are shown in Table 4.1. Body weights, mean food intake and average heart rate were not significantly different between the uraemic and sham groups.

Laboratory parameters	**WT - CON**	**WT - Ad**	**11β HSD1$^{-/-}$ CON**	**11βHSD1 $^{-/-}$ Ad**
Serum Sodium (mmol/l)	148.1 ± 3.2	147.2 ± 3.6	145.1 ± 4.1	142.8 ± 2.6
Serum Potassium (mmol/l)	5.6 ± 0.7	5.4 ± 1.2	5.6 ± 0.9	5.3 ± .09
Serum Urea (mmol/l)	11.4 ± 2.5	43.7 ± 1.5*	10.6 ± 3.3	44.86 ± 2.6*
Serum Creatinine (µmol/l)	22.2 ±2.2	68.6 ±4.3*	23.0 ± 3.1	67.74 ± 3.7*

Table 4.1. Serum markers of renal failure in Ad-fed 11β-HSD$^{-/-}$ mice. Renal dysfunction was determined in Ad mice (8 per group) by measurements of serum concentrations of creatinine, urea, sodium and potassium. Data are expressed as mean ± SEM. *p<0.05 vs. control diet.

4.4. Dynamic Physiological testing in 11β-HSD1 $^{-/-}$ mice

For GTT, animals were fasted overnight and injected i.p. with 2 g/kg body weight of 25% dextrose (Sigma, Poole, UK). Blood glucose (tail vein) was measured (Accu-Chek, UK) at 0 – 120 min and additional blood was collected in a heparinized tube at 0 – 45 min for measurement of insulin concentration. For ITT, animals were fasted overnight and injected i.p. with 2 units/kg body weight of porcine insulin (Intervet, Milton Keynes, UK). Blood glucose (tail vein) was measured (Accu-Chek, UK) at 0 – 45 min.

4.5. 11β-HSD1$^{-/-}$ mice are protected from uraemic insulin resistance.

Following consumption of an Ad both 11β-HSD1$^{-/-}$ and wild type (WT) mice developed similar levels of dyslipidaemia (raised systemic triglyceride levels) associated with renal dysfunction (Fig. 4.1). Similar to the phenotype observed in rats, uraemic WT mice developed dyslipidaemia, impaired glucose tolerance and reduced insulin sensitivity (Fig. 4.1 - 4.4). In marked contrast, 11β-HSD1$^{-/-}$ mice were protected against uraemia-induced insulin resistance and dyslipidaemia, displaying a lipid profile similar to control animals as well as improved glucose tolerance and insulin sensitivity comparable to that in WT controls.

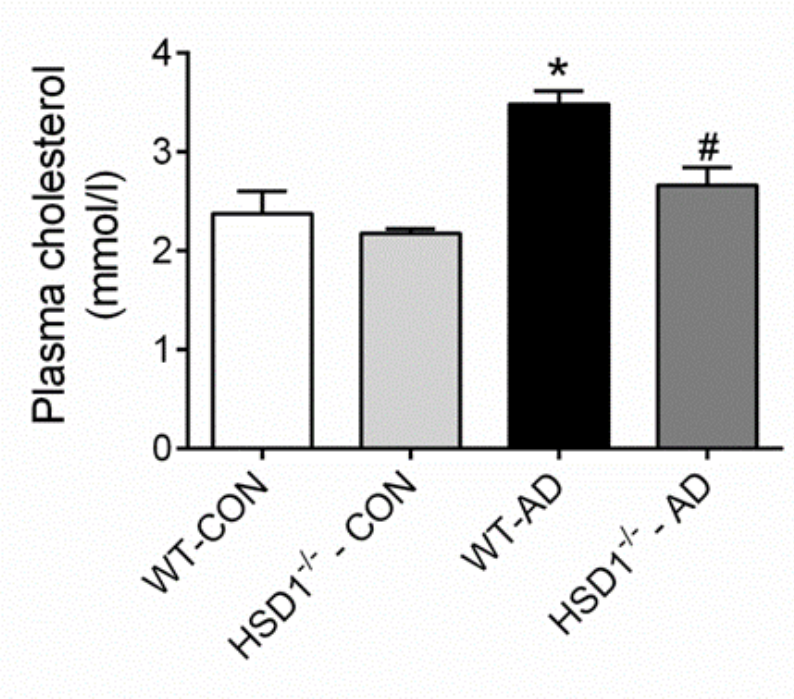

Fig. 4.1. Total plasma cholesterol. Experimental uraemia was induced in mice by the administration of a 0.25% Ad (8 per group). Data are expressed as mean ± SEM. Statistically significant differences between sham and Ad are indicated by, * p<0.01. #p<0.01,

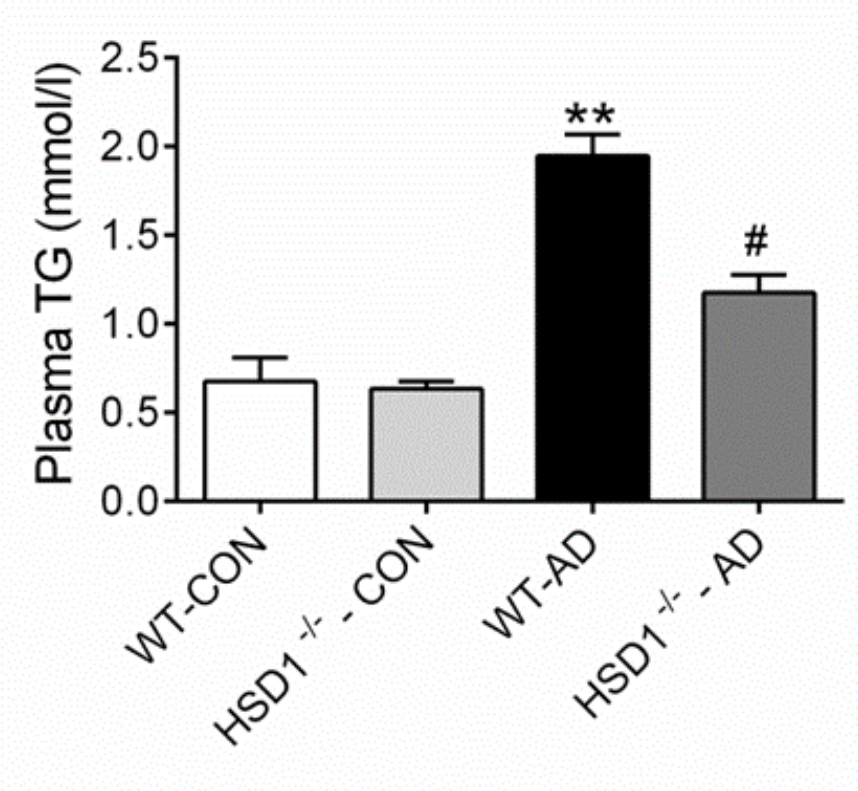

Fig. 4.2. Total plasma Triglyceride. Experimental uraemia was induced in mice by administration of 0.25% Ad (8 per group). Data are expressed as mean ± SEM. Statistically significant differences between sham and Adenine diets are indicated by # p<0.05, * * p<0.01.

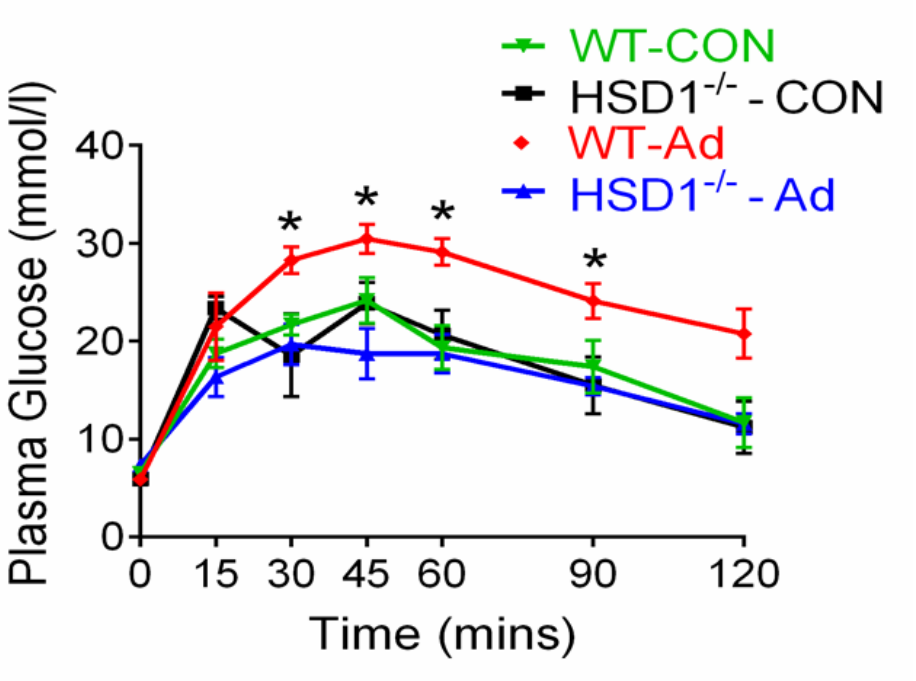

Fig. 4.3. Murine Intra-Peritoneal Glucose Tolerance Test (IPGTT). 25mg/kg of 25% dextrose was injected intraperitoneally as described. Experimental uraemia was induced in mice by administration of 0.25% Ad (8 per group). Data are expressed as mean ± SEM. Statistically significant differences between sham and Ad are indicated by * p<0.01.

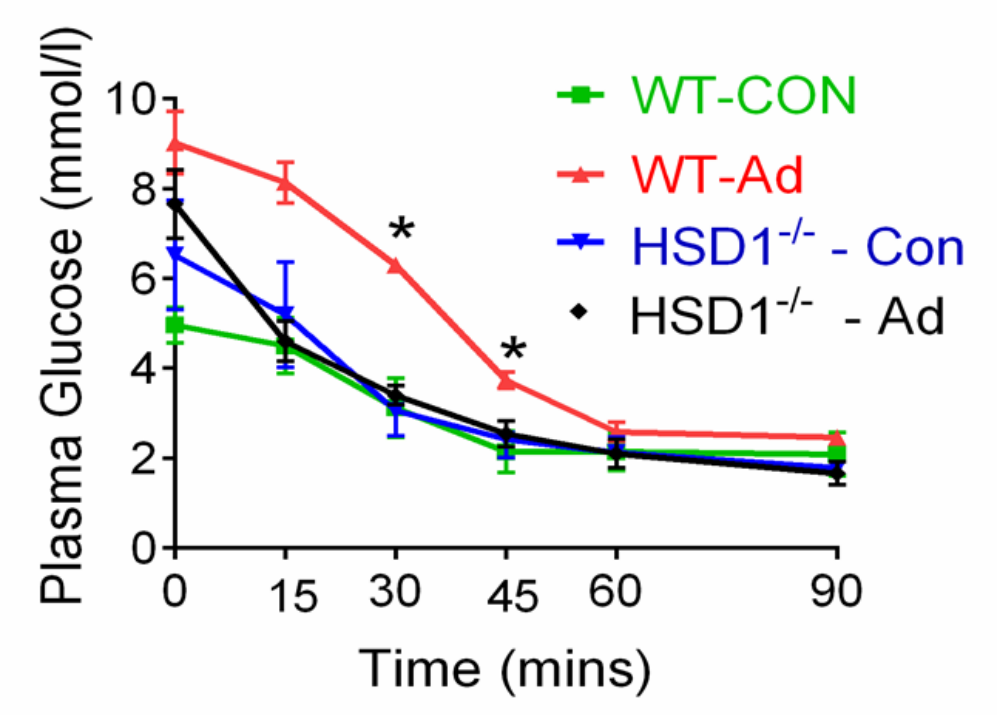

Fig. 4.4. Murine Intra-Peritoneal Insulin Tolerance Test (IPITT). 1 unit/kg of rapid-acting Insulin was injected intraperitoneally as described. Experimental uraemia was induced in mice by administration of 0.25% Ad (8 per group). Data are expressed as mean ± SEM. Statistically significant differences between sham and Ad are indicated by * p<0.01.

4.6 Specific inhibition of 11β–HSD1 with UE2316 protects uraemic mice from insulin resistance.

Finally, to confirm a specific role for 11β-HSD1 in uraemia-induced insulin resistance and to rule out potential non-specific CBX effects, we examined the effects of the specific 11βHSD1$^{-/-}$ inhibitor (UE2316) on insulin resistance in uraemic Ad fed mice. Briefly, mice were fed with either standard chow, or Adenine (0.75%), for four weeks. UE2316 was infused over the following two weeks, while adenine or standard chow was continued.

In agreement with data obtained from CBX treatment and 11β-HSD1$^{-/-}$ mice, UE2316 (20mg/kg/day) significantly improved glucose tolerance and insulin sensitivity in the Ad fed rats (Fig. 4.5-4.6), during dynamic physiological testing. However, the background parameters of renal failure were not different between the control and test diet groups (Table 4.2). These data demonstrate a clear role for 11β-HSD1 in mediating uraemia-induced insulin resistance.

Laboratory parameters	CON + Vehicle	Ad	Ad + Inhibitor
Serum Sodium (mmol/l)	145.2 ± 3.0	144.8 ± 3.4	142.2 ± 5.5
Serum Potassium (mmol/l)	5.3 ± 0.3	4.9 ± 0.7	4.9 ± 0.6
Serum Urea (mmol/l)	8 ± 2.4	73.6 ± 12.8 ***	72.6 ± 14.1 ***
Serum Creatinine (umol/l)	47.3 ± 11.6	301.7 ± 15.9 ***	291.1 ± 15.8 ***
Serum Albumin (g/L)	25.8 ± 2.8	24.6 ± 2.6	25.1 ± 2.1

Table 4.2. Serum Markers of Renal Failure in Adenine-fed rats treated with specific 11β-HSD1 inhibitor (UE2316). Renal dysfunction was determined in Ad fed mice (8 per group) by measurements of serum levels of creatinine, urea, sodium, potassium and albumin. Data are expressed as mean ± SEM. ***p<0.05 vs. CON diet

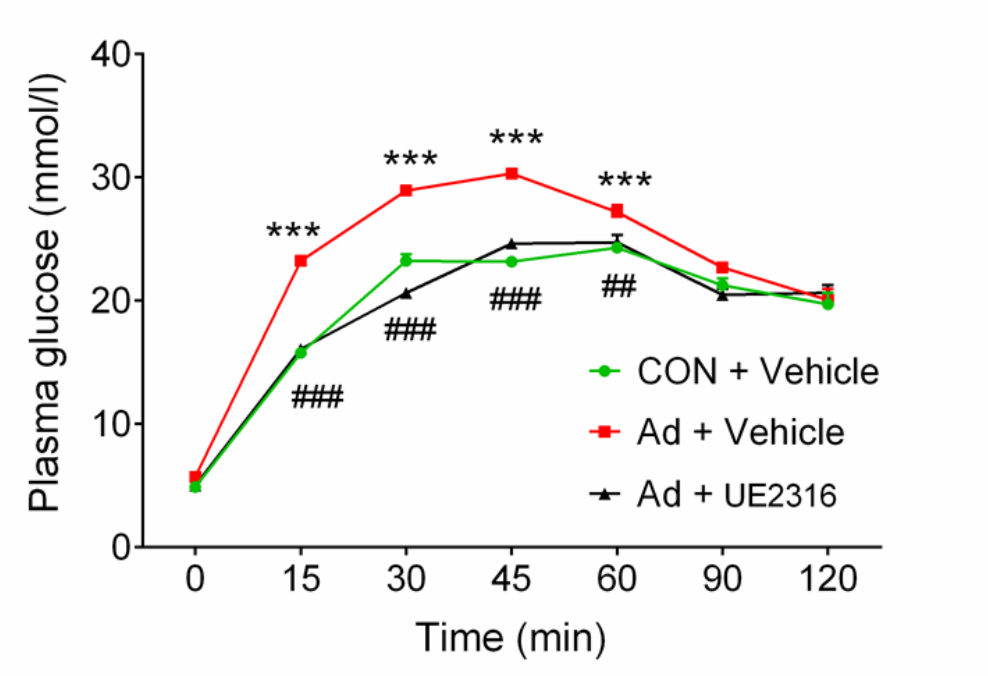

Fig. 4.5. Rodent IPGTT. 25mg/kg of 25% dextrose was injected intraperitoneally as described. Experimental uremia was induced in rats by Ad (8 per group). UE2316 (20 mg/kg/day) or vehicle was administered by an osmotic mini-pump for 2 weeks.). Data are expressed as mean ± SEM. Statistically significant differences between CON and Ad are indicated by *** p<0.001. Statistically significant effects of UE2316 treatment are indicated by # # p<0.05, ### p<0.001

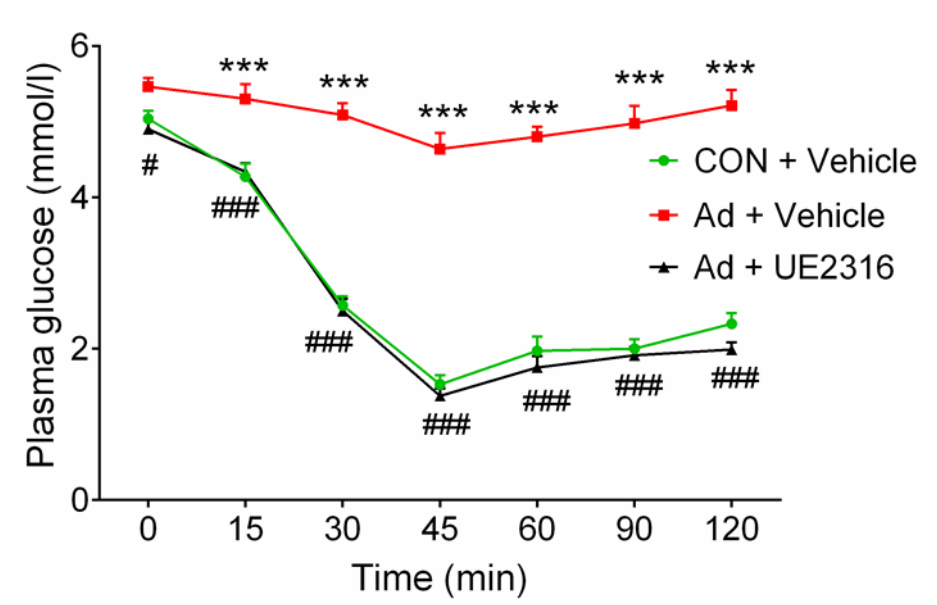

Fig. 4.6. Plasma glucose response to 2 units/kg/body weight porcine insulin injected intra-peritoneal (IPITT). Experimental uraemia was induced in rats by Ad (8 per group). UE2316 (20 mg/kg/day) or vehicle was administered by osmotic mini-pump for 2 weeks. Data are expressed as mean ± SEM. Statistically significant differences between CON and Ad are indicated by *** p<0.001. Statistically significant effects of treatment are indicated by # p<0.05, ### p<0.001

4.7. Conclusions.

The work presented here in this chapter demonstrates that Ad-induced murine and rodent non-diabetic CKD is associated with insulin resistance that can be ameliorated by specific inhibition of the enzyme 11β-HSD1 either with pharmacological inhibition, or with whole-body knock-outs. As discussed earlier in chapter 3, while the mechanisms underlying elevated 11β-HSD1 in uraemia have not been fully elucidated, it may involve upstream inflammation. While CBX has been demonstrated to have dose-dependent inhibition of activity and expression of 11β-HSD enzymes, a criticism of its use is the lack of specificity between 11β-HSD1 and 2, and its actions in gap-junction inhibition. However, 11β-HSD2 is not expressed in the liver, and its renal expression is confined to the distal nephron, which alone is unlikely to account for the substantial metabolic impacts observed. Importantly, a crucial specific role for 11β-HSD1 is underlined by the protective metabolic phenotype observed in the uraemic 11β-HSD1$^{-/-}$ mice and the fact that a specific 11β-HSD1 inhibitor (UE2316) also improved glucose tolerance and insulin sensitivity in uraemic rats.

Previous studies with conditional knockouts and reconstitution models concluded that the progression of insulin resistance to diabetes with fasting hyperglycaemia requires defects in tissues other than liver (139,140). However, results in liver insulin receptor knock-out and inducible liver insulin receptor knockout (iLIRKO) mice demonstrate (141) that liver-specific disruption of IR can impair both hepatic and extra-hepatic insulin signalling and that the severity of this resistance depends on the extent of IR deletion in the liver. iLIRKO mice display early insulin resistance as a primary defect related directly to the reduction or ablation of liver IR, but they also have impaired insulin signalling in other peripheral tissues, including skeletal muscle and brain. Thus, iLIRKO mice present systemic insulin resistance as a secondary effect.

Given that the deletion strategy did not alter IR expression in other tissues, this effect is likely the result of desensitization of the IR in extrahepatic tissues produced by prolonged hyperinsulinaemia. This is similar to the hepatic insulin resistance and circulating hyperinsulinaemia demonstrated in our current models.

Our results demonstrate that a primary defect, likely in the liver, triggers secondary insulin resistance in extrahepatic tissues and suggest that, similar to the data from iLIRKO mice, the progression to diabetes does not require defects other than liver IR deficiency. However, even though physiological data from dynamic testing (IPPTT) and gluconeogenic signalling is compelling, more work needs to be done before tissue-specific and temporal changes in insulin resistance in uraemia can be teased apart.

Specifically, while insulin resistance and glucose intolerance has been described in uraemia, the causes have been ascribed to increased hepatic gluconeogenesis, increased peripheral tissue resistance to insulin action, or to a combination of both. An obvious question is whether increased hepatic gluconeogenesis could be a compensatory mechanism for a decrease in renal cortical gluconeogenesis. Renal cortical gluconeogenesis has been described as accounting for 10-15% of total gluconeogenic flux. However, a compensatory increase in hepatic gluconeogenesis would not account for circulating hyperinsulinaemia and peripheral (and hepatic) insulin resistance, unless we hypothesise that the compensatory mechanism to gluconeogenesis is impaired. While the presented study supports the hypothesis that uraemic insulin resistance involves signalling downstream of the Insulin receptor, it does not provide either a temporal or a mechanistic model for this phenomenon.

Chapter 5. Conclusions and future studies

The work described in this thesis has established a pivotal role of hepatic glucocorticoid metabolism by 11β-HSD1 in uraemic insulin resistance in non-diabetic kidney disease, with particular relevance to hepatic and whole body insulin sensitivity.

In vivo studies in mouse and rat models characterized the expression of hepatic 11β-HSD1 mRNA and protein in detail, confirming excess expression and activity of the intra-hepatic enzyme. As suggested by the supporting changes in gluconeogenic enzymes, the impact of hepatic 11β-HSD1 on hepatic gluconeogenesis, and the resulting impact on whole body insulin sensitivity, a novel suggestion is presented of the physiological role of hepatic 11β-HSD1 in chronic kidney disease and corresponds with many of the observations from the clinical study comparing normal, obese and diabetic cohorts. This is in keeping with the intense focus of numerous published and ongoing studies on the importance and impact of 11β-HSD1 on hepatic glucose output via gluconeogenesis and represents an exciting new paradigm that warrants further investigation as a novel cardiovascular risk factor in uraemia.

Hepatic pre receptor glucocorticoid metabolism resulting in changes in hepatic glucocorticoid activation was found to be implicated and may thus be associated with the dysregulation of insulin sensitivity seen in CKD. In particular, hepatic glucocorticoid metabolism, specifically, cortisone to cortisol conversion, was found to be abnormal in tubular as well as glomerular models of non-diabetic CKD, whether murine or rodent. Furthermore, there was clear evidence of increased hepatic glucocorticoid activation and 11β-HSD1 gene expression, which may be important in defining the cause of the renal hepatic "pseudocushings" state. Hepatocellular gluconeogenic enzymes such as Glucose 6 phosphate and phosphenol carboxykinase 1 was defined as a direct link between glucose and glucocorticoid metabolism and was published in a peer-reviewed journal.

The results presented in the current thesis support the clinical studies comparing glucose and glucocorticoid metabolism in normal, obese and type 2 diabetic subjects and has, as discussed in individual chapters, revealed new data with relevance to the importance of insulin sensitivity and a strong association with hepatic 11β-HSD1 activity and hepatic gluconeogenesis. In addition, the association of hepatic lipid accumulation with activation of hepatic 11β-HSD1 and stimulation of lipogenesis in CKD was confirmed. Collectively, the data presented in this thesis provide support for the role of selective 11β-HSD1 inhibition for the treatment of insulin resistance in non-diabetic CKD, similar to that described in insulin resistant states and type 2 diabetes in previously published literature.

However, important questions arise with regard to the use of these agents in the presence of chronic kidney disease, in particular where increased glucocorticoid activation, and, possibly, decreased glucocorticoid clearance serve as a protective response to limit worsening inflammation and injury. In addition, the predicted impact of these inhibitors upon hepatic glycolysis and adipose and skeletal muscle insulin resistance warrants further investigation, as does the short and long-term effects of this inhibition.

In addition to the above, this work has led to the possibility of a number of future studies. It would be of great importance to fully define the physiological role of the distribution of 11β-HSD1 in CKD and its relevance upon glycolytic, gluconeogenic and lipogenic pathways and the resulting impact upon whole body and in particular adipose tissue and skeletal muscle insulin sensitivity. An initial study would include the comparison of the activity and expression of 11β-HSD1 in progressive uraemia in murine, rodent, and human tissue. It would be of significant interest to characterise expression of 11β-HSD1 in progressive stages of CKD, as well as other models of chronic kidney diseases (such as autoimmune and transplantation), that

are strongly associated with Insulin resistance and bear close resemblance with current models of CKD. This would be allied with studies to define the localisation of 11β-HSD1 within inflammatory cells in the liver and the factors involved in the activation of this process.

In addition, clinical studies to define hepatic glucocorticoid metabolism *in vivo*, in progressive stages of CKD would be important. Animal models of CKD would mimic stages of the disease, while samples from omental (and mesenteric) fat could be obtained during peritoneal dialysis catheter insertion in near-end stage pre-dialysis patients to compare with control specimens. On the basis of the results of the human study, a novel role for selective inhibition would be as a therapy specifically for insulin resistance and dyslipidaemia associated with CKD. Its aim would be to reduce hepatic glucocorticoid activation, and hence reduce endogenous hepatic glucocorticoid to limit the increase in hepatic glucose production. Its role, if proven, would be very significant in its ability to exert a decrease in hepatic glucocorticoid without the multiple undesirable effects of systemic glucocorticoid blockade. Further clinical studies in CKD, both rodent and human, are warranted to examine hepatic, adipose, muscle, and whole body glucocorticoid metabolism in progressive disease.

This study specifically chose those models with advanced CKD. It would be important to extend these investigations to subjects with earlier stages of disease, as well as in dialysis-dependent renal failure to characterise increased states of insulin resistance and to look for evidence of beta cell failure. Technically these studies would be more challenging but would provide important information of the detrimental or beneficial effect of 11β-HSD1 driven glucocorticoid activation and the role of hepatic glucocorticoids in renal impairment.

The results described in this thesis form key data with clear clinical importance and relevance in the application of 11β-HSD1 inhibition. Further studies will follow that will provide a greater depth of understanding and offer new possibilities for the treatment of patients with the metabolic syndrome, a serious global public health concern.

References:

1. Khwaja A, Throssell D. A critique of the uk nice guidance for the detection and management of individuals with chronic kidney disease. *Nephron Clin Pract*. 2009;113:c207-213.

2. Kaysen G.A. Disorders in high-density metabolism with insulin resistance and chronic kidney disease. *J Ren Nutr*. 2007;17:4-8.

3. Stefanovic V, Nesic V, Stojimirovic B. Treatment of insulin resistance in uremia. *Int J Artif Organs*. 2003;26:100-104.

4. Fliser D, Pacini G, Engelleiter R, Kautzky-Willer A,et al Insulin resistance and hyperinsulinemia are already present in patients with incipient renal disease. *Kidney Int*. 1998;53:1343-1347.

5. Shinohara K, Shoji T, Emoto M, Tahara H, et al. Insulin resistance as an independent predictor of cardiovascular mortality in patients with end-stage renal disease. *J Am Soc Nephrol*. 2002;13:1894-1900.

6. Nishimura M, Murase M, Hashimoto T et al. Insulin resistance and impaired myocardial fatty acid metabolism in dialysis patients with normal coronary arteries. *Kidney Int*. 2006;69:553-559.

7. Bodlaj G, Berg J, Pichler R et al.Severity and predictors of homa-estimated insulin resistance in diabetic and nondiabetic patients with end-stage renal disease. *J Nephrol*. 2006;19:607-612.

8. R Bright. Cases and observations illustrative of renal disease accompanied with the secretion of albuminous urine.*Guy's Hospital Trans*.1836;338–379.

9. J Harlos, A Heidland. Hypertension as cause and consequence of renal disease in the 19th century.*Am J Nephrol,*1994;14:436–442

10. Matsushita K, van der Velde M, Astor BC, et al, for the CKD Prognosis Consortium. Association of estimated glomerular filtration rate and albuminuria with all-cause and cardiovascular mortality in general population cohorts: a collaborative meta-analysis. The *Lancet* 2010; 375: 2073–81.

11. Van Der Velde M, Matsushita K, Coresh J, et al, for the Chronic Kidney Disease Prognosis Consortium. Lower estimated glomerular filtration rate and higher albuminuria are associated with all-cause and cardiovascular mortality. A collaborative meta-analysis of high-risk population cohorts. *Kidney Int* 2011; 79: 1341–52
12. Gansevoort, Ron T et al. Chronic kidney disease and cardiovascular risk: epidemiology, mechanisms, and prevention. *The Lancet,2010;*382;339 - 352
13. Roden M, Bernroider E. Hepatic glucose metabolism in humans--its role in health and disease. *Best Pract Res Clin Endocrinol Metab*. 2003;17:365-383
14. Unwin N. The metabolic syndrome. *J R Soc Med.* 2006;99:457–462.
15. Reaven G. Role of insulin resistance in human disease. *Diabetes* 1988. ;37:1595 -607
16. Third report of the National Cholesterol Education Program (NCEP) expert panel on detection, evaluation, and treatment of high blood cholesterol in adults (Adult Treatment Panel III). Final report. *Circulation.* 2002; 106: 3143–3421.
17. Einhorn D, Reaven GM, Cobin RH, et al. American College of Endocrinology position statement on the insulin resistance syndrome. *Endocr Pract*. 2003; 9: 237–252.
18. Part 1: diagnosis and classification of diabetes mellitus. World Health Organization: Geneva, Switzerland; 1999. [Last accessed on 2011 Jun 03]. World Health Organization. Definition, diagnosis and classification of diabetes mellitus and its complications: Report of a WHO Consultation. Available from: http://www.whqlibdoc.who.int/hq/1999/WHO_NCD_NCS_99.2.pdf .
19. Balkau B, Charles MA. Comment on the provisional report from the WHO consultation. European Group for the Study of Insulin Resistance (EGIR) *Diabet Med*. 1999;16:442–3.
20. Sanger, F.Chemistry of insulin; determination of the structure of insulin opens the way to greater understanding of life processes. *Science,1959;* 129,1340-4.

21. Walter, P. & Johnson, A. E. Signal sequence recognition and protein targeting to the endoplasmic reticulum membrane. *Annu Rev Cell Biol* ,1994;10,87-119.

22. Patzelt, C., Labrecque, A. D., Duguid, et al. Detection and kinetic behaviour of preproinsulin in pancreatic islets. *Proc Natl Acad Sci U S A* ,1978;75, 1260-4.

23. Maske, H.[Blood sugar-induced insulin secretion.]. Acta Neuroveg (Wien) 9,1954; 307-9.

24. Floyd, J. C., Jr., Fajans, S. S., Conn,et al.Stimulation of insulin secretion by amino acids. *J Clin Invest* ,1966;45, 1487-502.

25. Chisholm, D. J., Young, J. D. & Lazarus, L.The gastrointestinal stimulus to insulin release. I. Secretin. *J Clin Invest,*1969; 48;1453-60.

26. Ma, Y. H., Wang, J., Rodd, G. G., et al Differences in insulin secretion between the rat and mouse: role of cAMP.*Eur J Endocrinol* 1995;132, 370-6.

27. Thorens, B., Sarkar, H. K., Kaback, et al.Cloning and functional expression in bacteria of a novel glucose transporter present in liver, intestine, kidney, and beta-pancreatic islet cells. *Cell* ,1988; 55, 281-90.

28. Theler, J. M., Mollard, P., Guerineau, N., et alVideo imaging of cytosolic Ca2+ in pancreatic beta-cells stimulated by glucose, carbachol, and ATP. *J Biol Chem,*1992; 267, 18110-7.

29. Bokvist, K., Eliasson, L., Ammala, C., et al.Colocalization of L-type Ca2+ channels and insulin-containing secretory granules and its significance for the initiation of exocytosis in mouse pancreatic B-cells. *Embo J,*1995; 14, 50-7.

30. Yamazaki, S., Katada, T. & Ui, M..Alpha 2-adrenergic inhibition of insulin secretion via interference with cyclic AMP generation in rat pancreatic islets. *Mol Pharmacol,*1982;21, 648-53.

31. Czech, M. P. & Corvera,.Signaling mechanisms that regulate glucose transport. *J Biol Chem,*1999; 274, 1865-8.

32. Chiasson, J. L., Dietz, M. R., Shikama, H., et al.Insulin regulation of skeletal muscle glycogen metabolism. *Am J Physiol,*1980; 239, E69-74.
33. Chiasson, J. L., Liljenquist, J. E., Finger, et al. Differential sensitivity of glycogenolysis and gluconeogenesis to insulin infusions in dogs. *Diabetes,*1976;25, 283-91.
34. Elsas, L. J., Albrecht, I. & Rosenberg, L. E. Insulin stimulation of amino acid uptake in rat diaphragm. Relationship to protein sythesis. *J Biol Chem,*1968; 243, 1846-53.
35. Proud, C. G. & Denton, R. M. Molecular mechanisms for the control of translation by insulin. *Biochem J,*1998; 328 (Pt 2), 329-41.
36. Tischler, M. E., Satarug, S., Aannestad, A, et al. Insulin attenuates atrophy of unweighted soleus muscle by amplified inhibition of protein degradation. *Metabolism,*1997;46, 673-9.
37. Wolfrum, C., Asilmaz, E., Luca, E., et al. Foxa2 regulates lipid metabolism and ketogenesis in the liver during fasting and in diabetes. *Nature,*2004;432, 1027-32.
38. Chabowski, A., Coort, S. L., Calles-Escandon, J., et al.Insulin stimulates fatty acid transport by regulating expression of FAT/CD36 but not FABPpm. *Am J Physiol Endocrinol Metab,*2004; 287, E781-9.
39. Dyck, D. J., Steinberg, G. & Bonen, A.Insulin increases FA uptake and esterification but reduces lipid utilization in isolated contracting muscle. *Am J Physiol Endocrinol Metab,*2001; 281, E600-7.
40. Degerman, E., Landstrom, T. R., Wijkander, J.,et al. Phosphorylation and activation of hormone-sensitive adipocyte phosphodiesterase type 3B. *Methods* 1998;14, 43-53.
41. Andersen, A. S., Kjeldsen, T., Wiberg, F. C., et al. Identification of determinants that confer ligand specificity on the insulin receptor. *J Biol Chem,* 1997;267, 13681-6.
42. Bajaj, M., Waterfield, M. D., Schlessinger, J., et al. On the tertiary structure of the extracellular domains of the epidermal growth factor and insulin receptors. *Biochim Biophys Acta,*1987, 916, 220-6.

43. Cann, A. D. & Kohanski, R. A. Cis-autophosphorylation of juxtamembrane tyrosines in the insulin receptor kinase domain. *Biochemistry*,1997;36, 7681-9.
44. Fantin, V. R., Wang, Q., Lienhard, G. E. et al. Mice lacking insulin receptor substrate 4 exhibit mild defects in growth, reproduction, and glucose homeostasis. *Am J Physiol Endocrinol Metab*,2000; 278, E127-33.
45. Cai, D., Dhe-Paganon, S., Melendez, P. A.,et al.Two new substrates in insulin signaling, IRS5/DOK4 and IRS6/DOK5. J Biol Chem,2003;278, 25323-30.
46. Sun, X. J., Rothenberg, P., Kahn, C. R., Backer et al. Structure of the insulin receptor substrate IRS-1 defines a unique signal transduction protein. *Nature*,1991; 352, 73-7.
47. White, M. F., Maron, R. & Kahn, C. R. Insulin rapidly stimulates tyrosine phosphorylation of a Mr-185,000 protein in intact cells. *Nature*,1985; 318, 183-6.
48. Esposito, D. L., Li, Y., Cama, A. & Quon, M. J. Tyr(612) and Tyr(632) in human insulin receptor substrate-1 are important for full activation of insulin-stimulated phosphatidylinositol 3-kinase activity and translocation of GLUT4 in adipose cells. *Endocrinology*,2001; 142, 2833-40.
49. Myers, M. G., Jr., Backer, J. M., Sun, X. J.,et al. IRS-1 activates phosphatidylinositol 3'-kinase by associating with src homology 2 domains of p85. *Proc Natl Acad Sci U S A*,1992; 89, 10350-4.
50. Copps, K. D., & White, M. F. Regulation of insulin sensitivity by serine/threonine phosphorylation of insulin receptor substrate proteins IRS1 and IRS2. Diabetologia, 2001;55(10), 2565–2582.
51. Whorwood CB, Sheppard MC, Stewart PM: Licorice inhibits 11 beta-hydroxysteroid dehydrogenase messenger ribonucleic acid levels and potentiates glucocorticoid hormone action. Endocrinology,1993;132:2287-2292.

52. Roden, M. & Bernroider, E. Hepatic glucose metabolism in humans--its role in health and disease. *Best.Pract.Res.Clin.Endocrinol.Metab,* 2003;17, (3) 365-383.

53. Frayn KN .Metabolic Regulation. A human Perspective Oxford, *Blackwell Publishing*. 2003.

54. Vanhorebeek, I., De, V.R., Mesotten, D., Wouters, P.J.,et al. Protection of hepatocyte mitochondrial ultrastructure and function by strict blood glucose control with insulin in critically ill patients. *Lancet*,2005; 365, (9453) 53-59.

55. Landau, B.R. Methods for measuring glycogen cycling. *Am.J.Physiol Endocrinol.Metab,* 2001,281, (3) E413-E419.

56. Dohm, G.L. & Newsholme, E.A. Metabolic control of hepatic gluconeogenesis during exercise.*Biochem.J.*,1983; 212, (3) 633-639.

57. McMahon, M., Marsh, H.M., & Rizza, R.A. Effects of basal insulin supplementation on disposition of mixed meal in obese patients with NIDDM. *Diabetes*,1989; 38, (3) 291-303

58. DeFronzo, R.A., Ferrannini, E., Hendler, R., Felig, P., & Wahren, J. Regulation of splanchnic and peripheral glucose uptake by insulin and hyperglycemia in man. *Diabetes,* 1983. ;32, (1) 35-45 available from: PM:6336701

59. Magnusson, I., Rothman, D.L., Gerard, D.P., Katz, L.D., et al. Contribution of hepatic glycogenolysis to glucose production in humans in response to a physiological increase in plasma glucagon concentration. *Diabetes,* 1995;44,(2) 185-189.

60. Jiang, G. & Zhang, B.B. Glucagon and regulation of glucose metabolism. *Am.J.Physiol Endocrinol.Metab,* 2003. ; 284, (4) E671-E678.

61. Linn, T., Geyer, R., Prassek, S., et al. Effect of dietary protein intake on insulin, secretion and glucose metabolism in insulin-dependent diabetes mellitus. *J.Clin.Endocrinol.Metab*,1996; 81, (11) 3938-3943.

62. Felig, P., Wahren, J., & Hendler, R. Influence of maturity-onset diabetes on splanchnic glucose balance after oral glucose ingestion. *Diabetes*, 1978; 27, (2) 121-126.

63. Krebs, M., Brehm, A., Krssak, M., et al.Direct and indirect effects of amino acids on hepatic glucose metabolism in humans. *Diabetologia*, 2003;46, (7) 917-925.

64. Bogardus, C., Lillioja, S., Howard, B.V, et al. Relationships between insulin secretion, insulin action, and fasting plasma glucose concentration in nondiabetic and noninsulindependent diabetic subjects. *J.Clin.Invest*,1984; 74, (4) 1238-1246.

65. Sapolsky, R. M., Romero, L. M. Munck, A. U. How do glucocorticoids influence stress responses? Integrating permissive, suppressive, stimulatory, and preparative actions. *Endocr Rev*,2000; 21, 55-89

66. Christ, M., Haseroth, K., Falkenstein, E., et al. Nongenomic steroid actions: fact or fantasy? *Vitam.Horm.1999;*, 57, 325-373.

67. Schaufele, F., Chang, C.Y., Liu, W., et al.Temporally distinct and ligand-specific recruitment of nuclear receptor-interacting peptides and cofactors to subnuclear domains containing the estrogen receptor. *Mol.Endocrinol*.,2000;14, (12) 2024-2039.

68. Arriza, J.L., Weinberger, C., Cerelli, G., et al. Cloning of human mineralocorticoid receptor complementary DNA: structural and functional kinship with the glucocorticoid receptor. *Science*,1987; 237, (4812) 268-275.

69. Marver, D., Schwartz, M.J., & Kokko, J.P. Multiple effects of corticoid hormones on the mammalian nephron. *Ann.N.Y.Acad.Sci.*, 1981;372, 39-55.

70. Arriza, J.L., Weinberger, C., Cerelli, G., et al. Cloning of human mineralocorticoid receptor complementary DNA: structural and functional kinship with the glucocorticoid receptor. *Science*,1987; 237, (4812) 268-275.

71. Edwards, C.R., Stewart, P.M., Burt, D., et al. Localisation of 11 beta-hydroxysteroid dehydrogenase--tissue specific protector of the mineralocorticoid receptor. *Lancet,*1988; 2, (8618) 986-989.
72. Beato, M., Candau, R., Chavez, S., Interaction of steroid hormone receptors with transcription factors involves chromatin remodelling. *J.Steroid Biochem.Mol.Biol.,*1996; 56,(1-6 Spec No) 47-59
73. Reichardt, H.M., Kaestner, K.H., Tuckermann, J et al. DNA binding of the glucocorticoid receptor is not essential for survival. *Cell*, 19998;93, (4) 531-541.
74. Meyer, T.E., Waeber, G., Lin, J., Beckmann, W, et al. The promoter of the gene encoding 3', 5'-cyclic adenosine monophosphate (cAMP) response element binding protein contains cAMP response elements: evidence for positive autoregulation of gene transcription. *Endocrinology,*1993;132, (2) 770-780.
75. Kolla, V. & Litwack, G. Transcriptional regulation of the human Na/K ATPase via the human mineralocorticoid receptor. *Mol.Cell Biochem.,* 2000; 204, (1-2) 35-40.
76. Cori, C. & Cori, G. Fate of sugar in animal body:carbohydrate metabolism of adrenalectomized rats and mice. *J.Biol.Chem.,* 1927;74, 473-494.
77. Stalmans, W. & Laloux, M. Glucocorticoids and hepatic glycogen metabolism. *Monogr Endocrinol.,* 1979;12, 517-533.
78. Magnuson, M.A., Quinn, P.G., & Granner, D.K. Multihormonal regulation of phosphoenolpyruvate carboxykinase-chloramphenicol acetyltransferase fusion genes. Insulin's effects oppose those of cAMP and dexamethasone. *J.Biol.Chem.,* 1987; 262, (31) 14917-14920.
79. Exton, J.H. Regulation of gluconeogenesis by glucocorticoids. *Monogr Endocrinol*., 1979; 12, 535-546.

80. Hauner, H., Entenmann, G., Wabitsch, M.,et al..Promoting effect of glucocorticoids on the differentiation of human adipocyte precursor cells cultured in a chemically defined medium. *J.Clin.Invest,*1989; 84, (5) 1663-1670 .

81. Bujalska, I.J.,Walker, E.A., Hewison, M.,et al.A switch in dehydrogenase to reductase activity of 11 beta-hydroxysteroid dehydrogenase type 1 upon differentiation of human omental adipose stromal cells. *J.Clin.Endocrinol.Metab,*2002; 87, (3) 1205-1210.

82. Costas, M., Trapp, T., Pereda, M.P., et al. Molecular and functional evidence for in vitro cytokine enhancement of human and murine target cell sensitivity to glucocorticoids: TNF-alpha priming increases glucocorticoid inhibition of TNF-alpha-induced cytotoxicity/apoptosis. *J.Clin.Invest,*1996; 98, (6) 1409-1416.

83. Carani, C., Qin, K., Simoni, M., et al. Effect of testosterone and estradiol in a man with aromatase deficiency. *N.Engl.J.Med*.,1997; 337,(2) 91-95.

84. Paterson, J. M. et al. *Am J Physiol Regul Integr Comp Physiol* 2005;289: R642-R652

85. Odermatt, A., Arnold, P., Stauffer, A., The N-terminal anchor sequences of 11beta-hydroxysteroid dehydrogenases determine their orientation in the endoplasmic reticulum membrane. *J.Biol.Chem.,*1999; 274, (40) 28762-28770.

86. Lavery, G.G., Walker, E.A., Draper, N., et al. Hexose-6-phosphate dehydrogenase knock-out mice lack 11 betahydroxysteroid dehydrogenase type 1-mediated glucocorticoid generation. *J.Biol.Chem*.,2006; 281, (10) 6546-6551

87. Ricketts, M.L. & Stewart, P.M. Regulation of 11beta-hydroxysteroid dehydrogenase type 2 by diuretics and the renin-angiotensin-aldosterone axis. *Clin.Sci.(Lond),* 1999; 96, (6) 669-675

88. Ricketts, M.L., Verhaeg, J.M., Bujalska, I.,et al. Immunohistochemical localization of type 1 11beta-hydroxysteroid dehydrogenase in human tissues. *J.Clin.Endocrinol.Metab,* 83, (4) 1325-1335.

89. Kotelevtsev, Y., Holmes, M.C., Burchell, A., et al. 11beta-hydroxysteroid dehydrogenase type 1 knockout mice show attenuated glucocorticoid-inducible responses and resist hyperglycemia on obesity or stress. *Proc.Natl.Acad.Sci*.U.S.A,1997; 94, (26) 14924-14929

90. Morton, N.M., Holmes, M.C., Fievet, C.,et al. .Improved lipid and lipoprotein profile, hepatic insulin sensitivity, and glucose tolerance in 11betahydroxysteroid dehydrogenase type 1 null mice. *J.Biol.Chem*.,2001; 276, (44) 41293-41300

91. Monder, C., Stewart, P. M., Lakshmi, V.,et al. Licorice inhibits corticosteroid 11 beta-dehydrogenase of rat kidney and liver: in vivo and in vitro studies. *Endocrinology,* 1989;125, 1046-53.

92. Walker, B. R., Connacher, A. A., Lindsay, R. M, et al. Carbenoxolone increases hepatic insulin sensitivity in man: a novel role for 11-oxosteroid reductase in enhancing glucocorticoid receptor activation. *J Clin Endocrinol Metab,*1995; 80, 3155-9

93. Andrews RC, Rooyackers O, Walker BR: Effects of the 11β-hydroxysteroid dehydrogenase inhibitor carbenoxolone on insulin sensitivity in men with type 2 diabetes. *J Clin Endocrinol Metab,* 2003;88:285 –291.

94. Livingstone DEW, Walker BR: Is 11β-hydroxysteroid dehydrogenase type 1 a therapeutic target? Effects of carbenoxolone in lean and obese Zucker rats. *J Pharmacol Exp Ther,* 2003;305:167 –172.

95. Hermanowski-Vosatka A, Balkovec JM, Cheng K et al. 11B-HSD1 inhibition ameliorates metabolic syndrome and prevents progression of atherosclerosis in mice. *Journal of Experimental Medicine,* 2005;202 517–527.

96. Alberts P, Engblom L, Edling N, Selective inhibition of 11β-hydroxysteroid dehydrogenase type 1 decreases blood glucose concentrations in hyperglycaemic mice. *Diabetologia.* 2002; 45:1528–1532.

97. Alberts P, Nilsson C, Selen G. Selective inhibition of 11 β-hydroxysteroid dehydrogenase type 1 improves hepatic insulin sensitivity in hyperglycemic mice strains. *Endocrinology.* 2003; 144:4755–4762.

98. Rosenstock J, Banarer S, Fonseca VA. The 11-β-hydroxysteroid dehydrogenase type 1 inhibitor INCB13739 improves hyperglycemia in patients with type 2 diabetes inadequately controlled by metformin monotherapy. Diabetes Care. *2010*; 33:1516–1522.

99. Feig PU, Shah S, Hermanowski-Vosatka A. Effects of an 11 β-hydroxysteroid dehydrogenase type 1 inhibitor, MK-0916, in patients with type 2 diabetes mellitus and metabolic syndrome. *Diabetes Obes Metab.* 2011; 13:498–504.

100. Courtney R, Stewart PM, Toh M, et al. Modulation of 11 β-hydroxysteroid dehydrogenase (11 β HSD) activity biomarkers and pharmacokinetics of PF-00915275, a selective 11 β HSD1 inhibitor. *J Clin Endocrinol Metab.* 2008; 93:550–556.

101. Nixon M, Wake DJ, Livingstone DE. Salicylate downregulates 11β-HSD1 expression in adipose tissue in obese mice and in humans, mediating insulin sensitization. *Diabetes.* 2012; 61:790–796.

102. Paterson JM, Morton NM, Fievet C. Metabolic syndrome without obesity: hepatic overexpression of 11β-hydroxysteroid dehydrogenase type 1 in transgenic mice. *Proc Natl Acad Sci USA.* 2004; 101:7088–7093.

103. Lavery GG, Zielinska AE, Gathercole LL. Lack of significant metabolic abnormalities in mice with liver-specific disruption of 11β-hydroxysteroid dehydrogenase type 1. *Endocrinology*. 2012; 153:3236–3248.

104. Maeda K, Cao H, Kono K. Adipocyte/macrophage fatty acid binding proteins control integrated metabolic responses in obesity and diabetes. *Cell Metab.* 2005; 1:107–119.

105. Masuzaki H, Paterson J, Shinyama H. A transgenic model of visceral obesity and the metabolic syndrome. *Science.* 2001; 294:2166–2170.

106. Kershaw EE, Morton NM, Dhillon H, Ramage L, Seckl JR, Flier JS. Adipocyte-specific glucocorticoid inactivation protects against diet-induced obesity. *Diabetes.* 2005; 54:1023–1031.

107. Grossman RC. Experimental Models of Renal Disease and the Cardiovascular System. *The Open Cardiovascular Medicine Journal.* 2010;4:257-264.

108. McCafferty K et al. Response to Letter Regarding Article, "Ischemic Conditioning Protects the Uremic Heart in a Rodent Model of Myocardial Infarction" *Circulation.* 2012;126:e213.

109. Harwood SM, et al. Calpain is activated in experimental uremia: Is calpain a mediator of uremia-induced myocardial injury? *Kidney Int*,2003; 63(3):866–877.

110. Tamura, M., et al., Progressive renal dysfunction and macrophage infiltration in interstitial fibrosis in an adenine-induced tubulointerstitial nephritis mouse model. *Histochem Cell Biol*, 2009. 131(4): p. 483-90.

111. J.E. Ayala, D.P. Bracy, O.P. McGuinness,et al. Considerations in the design of hyperinsulinemic-euglycemic clamps in the conscious mouse. *Diabetes*,2006;55; 390–397.

112. Hughey, C. C., Hittel, D. S., Johnsen, V. L et al. Hyperinsulinemic-Euglycemic Clamp in the Conscious Rat. *J. Vis. Exp*.2011; 48, e2432.

113. Muniyappa, R., Lee, S., Chen, H.et al.Current approaches for assessing insulin sensitivity and resistance in vivo: advantages, limitations, and appropriate usage. *Am. J. Physiol. Endocrinol. Metab*,2008; 294, E15-E26.

114. McGuinness, O. P., Ayala, J. E., Laughlin, M. R, et al. NIH experiment in centralized mouse phenotyping: the Vanderbilt experience and recommendations for evaluating glucose homeostasis in the mouse. *Am. J. Physiol. Endocrinol. Metab*. 2009;297, E849-E855.

115. Shaodong Guo. Insulin signaling, resistance, and metabolic syndrome: insights from mouse models into disease mechanisms *J Endocrinol*,2014;220 (2) T1-T23.

116. Morton NM, Paterson JM, Masuzaki H, et al. Novel adipose tissue-mediated resistance to diet-induced visceral obesity in 11 beta-hydroxysteroid dehydrogenase type 1-deficient mice. *Diabetes* 2004, 53(4):931-938.

117. Caton PW, Nayuni NK, Murch O, et al. Endotoxin induced hyperlactatemia and hypoglycemia is linked to decreased mitochondrial phosphoenolpyruvate carboxykinase. *Life Sciences*. 2009; 738–744doi:10.1016/j.lfs.2009.02.024.

118. https://www.caymanchem.com/pdfs/500651.pdf

119. http://www.cellbiolabs.com/sites/default/files/STA-618-free-fatty-acid-assay-kit-colorimetric.pdf

120. Chomczynski P, Sacchi N. Single-step method of RNA isolation by acid guanidinium thiocyanate-phenol-chloroform extraction. *Anal Biochem.* 1987 Apr;162(1):156-9.

121. Mark A. Valasek , Joyce J. Repa . The power of real-time PCR. *Advances in Physiology Education* 2005, 29; 151-159.

122. Hu A, et al. Th2 cytokine-induced upregulation of 11beta-hydroxysteroid dehydrogenase-1 facilitates glucocorticoid suppression of proasthmatic airway smooth muscle function.*Am J Physiol Lung Cell Mol Physiol*, 2009; 296(5):L790–L803.

123. Nakamura S et al. Palmitate Induces Insulin Resistance in H4IIEC3 Hepatocytes through Reactive Oxygen Species Produced by Mitochondria. *J Biol Chem.* 2009 May 29; 284(22): 14809–14818.

124. Rubenfeld S, Garber AJ: Abnormal carbohydrate metabolism in chronic renal failure. The potential role of accelerated glucose production, increased gluconeogenesis, and impaired glucose disposal. *J Clin Invest* , 1978; 62:20-28, 1978.

125. Schaefer RM, Riegel W, Stephan E, et al. Normalization of enhanced hepatic gluconeogenesis by the antiglucocorticoid RU 38486 in acutely uraemic rats. *Eur J Clin Inves,1990;* 20:35-40.

126. Gomez-Valades AG, Mendez-Lucas A, Vidal-Alabro A, et al. Pck1 gene silencing in the liver improves glycemia control, insulin sensitivity, and dyslipidemia in db/db mice. *Diabetes* ,2008;57:2199-2210.

127. Gomez-Valades AG, Vidal-Alabro A, Molas M, Boada J, et al. Overcoming diabetes-induced hyperglycemia through inhibition of hepatic phosphoenolpyruvate carboxykinase (GTP) with RNAi. *Mol Ther*,2006; 13:401-410.

128. Rodgers JT, Puigserver P: Fasting-dependent glucose and lipid metabolic response through hepatic sirtuin 1. *Proc Natl Acad Sci U S* A,2007; 104:12861-12866.

129. Wang Y, Inoue H, Ravnskjaer K, et al.Targeted disruption of the CREB coactivator Crtc2 increases insulin sensitivity. *Proc Natl Acad Sci U S A*,2010; 107:3087-3092.

130. Shimomura I, Bashmakov Y, Ikemoto S, et al. Insulin selectively increases SREBP-1c mRNA in the livers of rats with streptozotocin-induced diabetes. *Proc Natl Acad Sci U S A* ,1999; 96:13656-13661.

131. Horton JD, Goldstein JL, Brown MS. SREBPs: activators of the complete program of cholesterol and fatty acid synthesis in the liver. *J Clin Invest*,2002; 109:1125-1131.

132. Chen Y, Sood S, Biada J, et al.Increased workload fully activates the blunted IRS-1/PI3-kinase/Akt signaling pathway in atrophied uremic muscle. *Kidney Int*,2008; 73:848-855.

133. Shen Y, Peake PW, Kelly JJ: Should we quantify insulin resistance in patients with renal disease? *Nephrology (Carlton)* ,2005;10:599-605.

134. Opherk C, Tronche F, Kellendonk C,et al. Inactivation of the glucocorticoid receptor in hepatocytes leads to fasting hypoglycemia and ameliorates hyperglycemia in streptozotocin-induced diabetes mellitus. *Mol Endocrinol* 2004;18:1346–1353.

134. Jacobson PB, von Geldern TW, Ohman L, et al. Hepatic glucocorticoid receptor antagonism is sufficient to reduce elevated hepatic glucose output and improve glucose control in animal models of type 2 diabetes. *J Pharmacol Exp Ther*, 2005;314: 191–200.

135. Liang Y, Osborne MC, Monia BP, et al. Antisense oligonucleotides targeted against glucocorticoid receptor reduce hepatic glucose production and ameliorate hyperglycemia in diabetic mice. *Metabolism*,2005;54: 848–855.

136. Guillaume-Gentil C, Assimacopoulos-Jeannet F, Jeanrenaud B. Involvement of non-esterified fatty acid oxidation in glucocorticoid-induced peripheral insulin resistance in vivo in rats. *Diabetologia*,1993; 36: 899–906, 1993.

137. Corporeau C, Foll CL, Taouis M, et al..Adipose tissue compensates for defect of phosphatidylinositol 3-kinase induced in liver and muscle by dietary fish oil in fed rats. Am J Physiol Endocrinol Metab,2006; 290: E78–E86.

138. Ma K, Zhang Y, Elam MB, Cook GA, et al. Cloning of the rat pyruvate dehydrogenase kinase 4 gene promoter: activation of pyruvate dehydrogenase kinase 4 by the peroxisome proliferator-activated receptor gamma coactivator. *J Biol Chem, 2005;*280: 29525–29532.

139. Friedman JE, Yun JS, Patel YM, et al. Glucocorticoids regulate the induction of phosphoenolpyruvate carboxykinase (GTP) gene transcription during diabetes. *J Biol Chem ,1993;*268:12952–12957.

140. Bernal-Mizrachi C, Weng S, Feng C, Dexamethasone induction of hypertension and diabetes is PPAR-alpha dependent in LDL receptor-null mice. *Nat Med,2003;* 9: 1069–1075.

141. Okamoto H, Nakae J, Kitamura T, Park BC, et al. Transgenic rescue of insulin receptor–deficient mice. *J Clin Invest*,2004; 114:214 –223.

142. Michael MD, Kulkarni RN, Postic C,et al. Loss of insulin signalling in hepatocytes leads to severe insulin resistance and progressive hepatic dysfunction. *Mol Cell*,2000; 6:87–97.

143. Escribano O, Guillén C, Nevado C,et al. Beta-Cell hyperplasia induced by hepatic insulin resistance: role of a liver-pancreas endocrine axis through insulin receptor A isoform. *Diabetes.* 2009;4; 58(4):820-8.

Conference presentations & journal publication arising from this thesis

Publication

Elevated hepatic 11β-hydroxysteroid dehydrogenase type 1 induces insulin resistance in uremia. Chapagain A, Caton PW, Kieswich J, Andrikopoulos P, Nayuni N, Long JH, Harwood SM, Webster SP, Raftery MJ, Thiemermann C, Walker BR, Seckl JR, Corder R, Yaqoob MM. Proc Natl Acad Sci U S A. 2014 Feb 25.

Oral presentations

- HSD1 null transgenic mice and uremic Insulin resistance. Ananda Chapagain, P Caton, Julius E Kieswich, Steven Michael Harwood, Martin J. Raftery, M Magdi Yaqoob. TranslationalMedicine and Therapeutics, WHRI, London, United Kingdom. Oral presentation, Renal association, Bournemouth, March 14, 2013

- Uraemia-Induced Increases in Rodent Hepatic 11bHSD1 activity and associated excessive gluconeogenesis contributes to Insulin Resistance in non-Diabetic Chronic Kidney Disease. Ananda Chapagain, P Caton, Julius E Kieswich,Steven Michael Harwood, Martin J. Raftery, M Magdi Yaqoob. TranslationalMedicine and Therapeutics, WHRI, London, United Kingdom.Oral presentation, Renal association, Gateshead, June, 2012

Poster Presentations

- A novel model of metabolic syndrome and Insulin resistance in experimental uraemia in rats and the effect of inhibition of the enzyme 11 beta hydroxyl-steroid dehydrogenase type 1 (11HSD1). Chapagain A, et al. poster presentation, Renal association, Manchester May 2010.
- Hepatic upregulation of 11-betaHSD1 and associated excessive gluconeogenesis: a likely mechanism of hyperinsulinemia in chronic kidney disease. Abstract, JASN and

poster presentation, ASN, San Diego, Nov 2009, Renal Association annual meeting, Liverpool, 2009.